

Development of SWAT Algorithms for Modeling Urban Best Management Practices

**Final Report submitted to
Watershed Protection Department,
City of Austin**

By

Jaehak Jeong, Narayanan Kannan, Raghavan Srinivasan

**Blackland Research and Extension Center
Texas AgriLife Research, Texas A&M System
720 East Blackland Road, Temple, TX 76502, USA**

**COA Report No. CN-##
October 2011**



Abstract

City of Austin (COA), Texas has experienced rapid urbanization in the last several decades and more development is expected in the upcoming years. Therefore, the land uses in Austin are characterized by increasing impervious cover like other urban areas in Texas. SWAT has been used for simulating hydrologic processes in Austin watersheds, but increasing urbanization has created challenges for accurately simulating flow and the structures built to reduce peak flows and capture pollutants. If not controlled, urbanization may cause flooding in downstream areas and, moreover, aquatic habitats can be vulnerable to either flash flows or untreated urban nonpoint sources pollutants. It is of great concern for COA watershed managers to accurately model Austin watersheds so they can proactively manage the effects of urbanization.

In this study, Soil and Water Assessment Tool (SWAT) was enhanced with modeling tools to describe and simulate sub-hourly scale processes of urban hydrologic systems and the cumulative effects of multiple Best Management Practices (BMP) systems on water quality at the watershed-scale.

The specific goals of the project are (1) to develop a sub-hourly rainfall runoff model to simulate urban watersheds and (2) to develop algorithms to model stormwater best management practices (such as detention basins, wet ponds, sedimentation filtration ponds, retention irrigation systems, etc.) that alter the quantity and quality of water entering the creeks in Austin. The model development is based on a widely used physically based watershed scale model Soil and Water Assessment Tool (SWAT) developed by the United States Department of Agriculture-Agricultural Research Service, Temple, TX. Algorithms are developed for sub-hourly rainfall runoff modeling and stormwater best management practices and integrated with SWAT model, followed by testing.

Table of Contents

1. Introduction.....	1
1.1 Background	1
1.2 SWAT model	3
1.3 Objectives.....	4
2. Algorithms for Sub-hourly Flow	5
2.1 Introduction.....	5
2.2 Methods.....	6
2.3 Case study	12
2.4 Results	17
2.5 Summary and recommendations	26
2.6 Limitations	27
2.7 References	27
3. Sub-hourly Erosion and Sediment Transport	32
3.1 Introduction.....	32
3.2 Methods.....	32
3.3 Results and Discussion.....	40
3.4 Summary and conclusion	44
3.5 References	45
4. Urban BMPs: Sedimentation-Filtration Basins	46
4.1 Introduction.....	46
4.2 Water Quality Volulme	46
4.3 Model configuration in SWAT	47
4.4 Filtration basin (Describe sedimentation first).....	48
4.5 Sedimentation basin	47
4.6 Case Study.....	54
4.7 References	61
5. Urban BMPs: Retention-Irrigation Basins.....	62
5.1 Introduction.....	62
5.2 Methods.....	62

5.3 Case study	65
5.4 Conclusion	69
6. Urban BMPs: Detention Ponds.....	70
6.1 Introduction.....	70
6.2 Methods.....	70
6.3 Results and Discussion.....	74
7. Urban BMPs: Wet ponds.....	77
7.1 Introduction.....	77
7.2 Methods.....	79
7.3 Results and Discussion.....	84
7. Summary	85

List of Figures

Figure 1. Influence of surlag, t_c , and Δt on fraction of surface runoff released to the main channel	8
Figure 2. Surface runoff hydrograph generated by superimposing dimensionless triangular unit hydrographs.....	9
Figure 3. Surface runoff responses of the gamma distribution UH with varying alpha factors. ..	10
Figure 4. Schematic flow chart showing the stream of processes in the sub-hourly simulation model.....	12
Figure 5. LGA watershed in Austin, Texas	13
Figure 6. Stream flow hydrographs for $\Delta t= 15$ minute.....	20
Figure 7. Stream flow hydrographs for $\Delta t= 1$ hour.....	22
Figure 8. Stream flow hydrographs for $\Delta t= 1$ day	24
Figure 9. Flow duration curves for LGA watershed showing the impact of temporal resolution	25
Figure 10. Schematic of sub-daily erosion processes (right) compared to daily erosion processes in SWAT2005 (left)	33
Figure 11. Experimental watersheds and rain gauges at the USDA-ARS Grassland, Soil and Water Research Laboratory near Riesel, Texas.....	39
Figure 12. Calibrated sediment yield at the Y-2 outlet for events on: a) 8 Mar 2001, b) 16 Dec 2001, c) 21 Oct 2002, d) 20 Dec 2002.....	43
Figure 13. Exceedance probabilities for measured sediment yield data from watershed Y-2 and SWAT sub-daily predictions.....	44
Figure 14. Schematic view of sand filter processes (please insert yes/no in appropriate place) ..	49
Figure 15. Infiltration rate is a function of inflow rate when ponding is considered ($R=$ inflow rate, $K_{sat}=40\text{mm/hr}$, suction head = 50mm, porosity=0.4, $\Delta t=15\text{min}$). Baseline (no ponding) is estimated with the original Green & Ampt equation.	51
Figure 16. Infiltration rate ($K=40\text{mm/hr}$, $R=80\text{mm/hr}$) with constant inflow to the filter.	52
Figure 17. Jollyville Sedimentation-filtration basin and its drainage area	55
Figure 18. Original DEM for Jollyville site showing the details (left) and a hypothetical DEM generated for watershed delineation (right)	56
Figure 19. Through-flow at the outlet during the calibration period (top) and validation period (bottom).....	58

Figure 20. Sediment concentration at the outlet during the calibration period (top) and validation period (bottom)	59
Figure 21. Water balance components during the calibration period	60
Figure 22. Flow chart of the retention-irrigation system in SWAT.....	63
Figure 23. LGA watershed.....	66
Figure 24. Influences of the two simulated RI systems are apparent in the amount of runoffs that actually reach the channel.....	67
Figure 25. Profile of water volume in the retention pond.....	68
Figure 26. A regional detention pond in Austin	71
Figure 27. Parabolic Wedge (Shape of water backup)	72
Figure 28. Flow through stormwater detention pond.....	76
Figure 29. A Wet Pond in Austin.....	78
Figure 30. Cumulative rainfall of the 1-year 3-hour design storm (City of Austin).....	80
Figure 31. Annual runoff coefficient used to estimate the permanent pool volume (City of Austin)	80
Figure 32. Simplified trapezoidal shape of wet ponds.....	81

List of Tables

Table 1. SWAT parameters used in the sensitivity analysis	15
Table 2. Sensitivity of SWAT parameters for different operational time intervals ($\Delta t= 15\text{min}$, 1hr, and 1day).....	18
Table 3. Predicted water balance components	19
Table 4. Performance evaluation of different time intervals	21
Table 5. SWAT parameters used in the sensitivity analysis.....	40
Table 6. Sensitive sediment parameters for three routing methods as ranked by the LH-OAT method.....	41
Table 7. and simulated sediment yields for annual periods and storm events	42
Table 8. Property of urban land use types in the drainage area	56
Table 9. Annual water budget for retention ponds	68
Table 10. Annual water budget for retention ponds	74

Acknowledgements

The authors extend their sincere thanks to the following individuals or organizations:

1. Dr. Jeffrey G. Arnold at the United Department of Agriculture – Agricultural Research Service (USDA-ARS) for providing guidance in the SWAT source code development,
2. Dr. Michael E. Barrett of the Center for Research in Water Resources at the University of Texas at Austin for providing expertise in urban stormwater hydraulics and best management practices,
3. Mr. Lee Sherman at the City of Austin Watershed Protection Department for providing BMP design guidance recommended by Water Environment Research Foundation,
4. Dr. R. Daren Harmel of USDA-ARS for sharing field data collected at USDA’s Riesel Experimental Watershed.

1. Introduction

1.1 Background

Urban planners consider the impacts on various factors such as transportation, schools and economic development when evaluating different future growth scenarios but the hydrologic impacts are rarely considered. The City of Austin (COA) Watershed Protection Department (WPD) is responsible for protecting lives property and the environment of the community by reducing the impacts of flooding, erosion and water pollution. This is accomplished by a two pronged approach; first, by implementing various rules and regulation affecting any new development and second by constructing or modifying structural controls in areas that do not conform to current regulations. While these activities are informed by the best available science and data, it is often difficult to evaluate different options with respect to all three missions of WPD; flood, erosion and water quality.

WPD envisioned a paradigm to evaluate the impacts of different future scenarios on flooding, erosion and water quality. This paradigm would consist of modeling existing conditions in the watershed and then changing the land use portion of the model to reflect a future scenario. Running the model with the same climatic inputs will allow for a comparison of the impacts of change in land use only. Due to the rapid changes in urbanized streams, this modeling effort will require a model with a sub-daily time-step.

These changes in hydrology due to changes in land use can have a wide range of impacts on waterways especially on flooding and erosion potential. In most cases, flooding impacts are quantified by evaluating the impact on the stage height of a design storm such as the 100-yr storm. While this method does evaluate changes in existing floodplains for large events and may be used protect buildings, it does not take into account the possible increased frequency of the events or the change in the duration of those events. It also does not allow for an evaluation of increased erosion potential because many smaller events contribute to erosion without resulting in flooding. The Watershed Protection Department (WPD) of the City of Austin (COA) needed to develop a set of tools to allow planners to evaluate the impacts on flooding, erosion and aquatic communities of different development scenarios and also test different combinations of best management practices (BMPs) to mitigate those impacts.

Instantaneous hydrologic responses in small watersheds or urbanizing areas often convey multiple flow events in a day when combined with flash storms. Therefore, the simulation time interval should be as short as possible to properly capture these short duration storms. There are only a few watershed-scale simulation models that have both long-term continuous and event-based simulation capabilities. The US Environmental Protection Agency (EPA)'s Storm Water Management Model (SWMM) is a dynamic rainfall-runoff model used for single event or continuous simulation in urban areas (Rossman 2004). SWMM has been used worldwide including the United States for storm water and combined sewer simulation of urban watersheds. The wide use and popularity makes it a strong choice for field scale system drainage modeling. However, for large watersheds the input and output processes can be tedious and time consuming.

In addition, stability problems in the numerical modeling algorithms are a known issue. Some of these drawbacks discourage the use of SWMM especially in modeling large watersheds in which urban areas are only a sub-unit of the watershed. Kim et al. (2009) suggests integrating SWMM with SWAT to mitigate these drawbacks in simulating large scale watersheds.

Source Loading and Management Model (SLAMM) (Pitt and Voorhees 1995) is another urban watershed management tool capable of continuous and event-based simulation. Special emphasis has been placed on small storm hydrology and particulate wash-off. SLAMM has strength in simulating various urban land uses with conventional or innovative types of storm water BMPs to determine how effectively they mitigate flash runoff and remove pollutants associated with urban stormwater. SLAMM is strongly based on actual field observations, with minimal dependence on theoretical processes. However, there is a limitation on the number of land uses (six) and the source areas within each land use that the model can handle. As well, the model cannot simulate snowmelt, base flow and in-stream processes.

Hydrological Simulation Program – Fortran (HSPF) (Bicknell et al. 1995) is a part of US EPA's Better Assessment Science Integrating point & Nonpoint Sources (BASINS) modeling system for the analysis of Total Maximum Daily Loads (TMDL). HSPF runs at any time step from 1 minute to 1 day and, therefore, can simulate individual storm events. However, HSPF may not be adequate for simulating intense single-event storms because of its conceptualization of overland areas as detention storage and flow routing using storage-based equations (Borah and Bera 2003; Xiong and Melching 2005). CASCade 2 Dimensional (CASC2D), a hydrologic model to calculate surface runoff on a cascade of planes in 2-Dimension (Julien and Saghafian 1991) and MIKE SHE (Refsgaard and Storm 1995) are both physically-based models for which numerical approximation techniques solve multi-dimensional simplified (or full) Saint-Venant equations. As is inherent in the numerical solutions, these models require relatively intense computation compared to the models with analytical solutions when simulating long periods or large watersheds.

QUALity HYdrological MOdel (QUALHYMO) (<http://beta.waterbalance.ca/>) is a continuous simulation model capable of modeling runoff and pollutants for urban as well as rural watersheds. It is widely used as a management tool by agencies in Alberta and Ontario provinces in Canada. However, the model is not validated adequately in other parts of the world. Lack of significant improvement of the model over the past few years since its development could be a concern for its use.

Watershed models may be characterized as continuous or event-based depending on their time scale of simulation. Continuous models, which typically simulate long time periods up to several decades with sub-daily, daily, or larger time intervals, are efficient tools for predicting long-term catchment responses to land cover changes or soil management practices. Examples of such models include SWAT, Ann-Agricultural Nonpoint Source (AGNPS) model by Bingner and Theurer (2001), the Large Scale Catchment Model (LASCAM) by Sivapalan et al. (2002),

the Simulator for Water Resources in Rural Basins (SWRRB) model by Arnold et al. (1990), and the Water Erosion Prediction Project (WEPP) model by Laflen et al. (1991).

Event-based models simulate finer time periods with intervals as small as several seconds. These models are generally formulated with physically-based flow and sediment equations, and the solutions are numerically approximated. A generally recognized drawback of event-based models is the high computational cost. As a result, they are typically used only for small catchments. Examples of event-based models include ANSWERS (Park et al. 1982) and the European Soil Erosion Model (EUROSEM) by Morgan et al. (1998).

Hydrological processes in watersheds may be defined as a continuous circulation of water on the earth through the processes of rainfall, surface runoff, base flow, stream flow, and evapotranspiration. The natural circulation is however altered as watersheds experience urbanization. Permeable surfaces are overlain with impervious cover such as buildings, roads, and pavements that disconnect the surface processes from sub-surface processes during the urbanization process. Urban impervious cover makes stormwater runoff instantaneous and flashy by increasing surface runoff and reducing infiltration. The amount of base flow decreases as less water infiltrates to the soil profile. Hantush and Kalin (2006) found 31% reduction in the base flow as 60% of a forested watershed was converted to commercial and low density residential areas. In the same context, Corbett et al. (1997) suggests a linear relationship between percent impervious surface and runoff volumes. The increased surface runoff tends to make hydrographs flashy with higher peaks and shorter durations. In the aspect of long term analyses, the impact of urbanization may be more significant during individual storm events than in the mean annual runoff (Chang 2007). However, its long term impact can also be significant depending on human practices (Burns et al. 2007). Therefore, the capability of simulating individual storms is important for watershed models to adequately capture hydrologic processes between short intervals, while continuous simulation capability is also necessary for investigating long term impacts of urbanization in urbanizing watersheds.

1.2 SWAT model

Soil & Water Assessment Tool (SWAT) is a continuous, physically-based, and watershed-scale model developed by the USDA Agricultural Research Service (ARS) to simulate long-term impacts of varying land management practices, land uses, and agricultural chemical yields on downstream water bodies (Arnold et al., 1998). SWAT has been widely used in water quality modeling including TMDL analyses (Borah et al. 2004; Benham et al. 2006; Radcliffe et al. 2009), applications within the US Department of Agriculture's Conservation Effects Assessment Project (van Liew et al. 2007; Harmel et al. 2008; Richardson et al. 2008), and in nonpoint source pollution analyses (Borah and Bera 2003; Santhi et al. 2001). Recently, Bracmort et al. (2006) used SWAT to study long term impact of structural Best Management Practices (BMPs) on sediment and phosphorus loads. While SWAT is a widely used tool in watershed modeling, SWAT 2009 version has limited capability to simulate hydrological processes at subdaily time

scales: weather and infiltration processes are assessed at any sub-hourly time interval; channel routing is simulated at hourly time interval and all other processes at daily interval. However, these subdaily routines in SWAT have not been fully validated to date and require a fundamental restructuring in the model's framework to further expand subdaily simulation capabilities such as sediment and nutrients simulated at a sub-hourly time interval as small as 1 minute.

1.3 Objectives

In collaboration with the Watershed Protection and Development Review Department, City of Austin, Texas AgriLife Research Scientists enhanced sub-daily modelling capabilities of the SWAT model and developed algorithms for simulation of urban Best Management Practices (BMP) in SWAT to enable evaluation of both in-place and hypothetical scenarios of hydrologic and water quality controls . The specific goals of the project were to develop:

- sub-hourly flow modeling routines within SWAT so that peak flows, erosive flows, as well as appropriate capture volumes for BMPs are well simulated. The City as well as others have determined that flow regime changes in the Texas area are usually the dominant factor in stream aquatic life degradation in urban areas.
- sub-hourly erosion and sediment transport routines within SWAT,
- routines for simulating urban BMPs within SWAT, include the standard controls required by the City of Austin sedimentation/filtration, wet ponds, regional detention facilities, and retention/irrigation (required within the Barton Springs recharge zone).

2. Algorithms for Sub-hourly Flow

Increasing urbanization changes runoff patterns to be flashy with instantaneous response and decreased base flow. A model with the ability to simulate sub-daily rainfall-runoff processes and continuous simulation capability is required to realistically capture the long-term flow and water quality trends in watersheds that are experiencing urbanization. Soil and Water Assessment Tool (SWAT) has been widely used in hydrologic and nonpoint sources modeling. However, its subdaily modeling capability is limited to hourly flow simulation. This chapter presents the development and testing of a sub-hourly rainfall-runoff model in SWAT. SWAT algorithms for infiltration, surface runoff, flow routing, impoundments, and lagging of surface runoff have been modified to allow flow simulations with a sub-hourly time interval as small as one minute. Runoff and flow routing is simulated at the requested time step. The more representative hydrology results will provide better data to assess hydrologic regime impacts on aquatic benthic communities.

2.1 Introduction

The City of Austin, Texas has experienced rapid urbanization in the last several decades and more development is expected in the upcoming years. The preservation of water resources in the Edward aquifer and the Colorado River with the growing population is the main concern for the City. SWAT has been used for simulating hydrologic processes in Austin watersheds, but increasing urbanization has created challenges for accurately simulating flow, and flow regime characterization is important since hydrologic modification has been identified as a critical element in impacts on aquatic life. Thus, a sub-hourly simulation capability is needed to improve flow simulation relative to daily time intervals in areas with rapid flow response. Especially, the rainfall-runoff processes such as flooding and bank erosion in their creeks and rivers in response to short and intense rainfall events in urban areas or at the fringe of urban areas are of great concern. With sub-hourly simulation capability added, the SWAT model is suitable for simulating hydrological processes in watersheds with various land uses in Austin areas. Debele et al. (2009)'s recent work on the Enhanced Soil and Water Assessment Tool (ESWAT) support our theory. They found ESWAT performed better in hourly simulations as they added hourly evapotranspiration and overland flow routines to the model.

The first goal of this study was to develop sub-hourly algorithms for flow, erosion and stormwater BMPs modules within a continuous and distributed modeling framework. This section focuses on the development of sub-hourly surface runoff and stream flow modeling components. SWAT routines for weather, infiltration, overland flow, impoundments, and channel flow have been modified to accommodate the sub-hourly simulation capability. Impact of simulation time scale to flow prediction is investigated using 15minute, 1 hour, and 1day interval. Performance of the Green and Ampt model and the SCS Curve Number method is compared to measure improvement in the model output.

2.2 Methods

This section describes the methods used for sub-hourly rainfall-runoff modeling including model equations, source code changes, and the strategy for modifying the model structure that is necessary for the development of sub-hourly modeling capability in SWAT.

Estimation of infiltration and excess rainfall

SWAT provides two methods for estimating surface runoff: the SCS curve number (CN) method (SCS 1972) and the Green and Ampt Mein Larson (GAML) excess rainfall method (Mein and Larson 1973). The CN method is an empirical model that is based on more than 20 years of studies involving rainfall-runoff relationships from small rural watersheds with various land use and soil types across the United States. The Green and Ampt equation is a physically based model that allows continuous simulation of infiltration process assuming the soil profile is homogeneous and antecedent moisture is uniformly distributed in the profile. The GAML equation uses a direct relationship between infiltration and rainfall rate based on physical parameters allowing continuous surface runoff simulation. While the CN method is widely used, its usage in continuous simulation is controversial because it estimates direct runoff using empirical relationships between the total rainfall and watershed properties (Garen and Moor 2005); therefore, the CN method may be abused if used in sub-daily runoff simulation. A study conducted by King et al. (1999) suggests that the CN method under-simulates surface runoff while the GAML method has no pattern associated with storm events implying less bias to the model prediction with the GAML method. After simulating the response of the Green and Ampt equation for 47 storms collected at seven locations, King (2000) recommends that an operational time interval of 10 minute yields the best results for the Green and Ampt equation. Therefore, the GAML method is considered to be suitable for sub-hourly surface runoff simulation in SWAT. The GAML infiltration rate is expressed as

$$f(t) = K_e \left(1 + \frac{\Psi \Delta\theta}{F(t)} \right) \quad (2-1)$$

where $f(t)$ is the infiltration rate at time t (mm/hr), K_e is the effective hydraulic conductivity in which the impact of land cover is incorporated (Nearing et al. 1996), Ψ is the wetting front matric potential (mm), $\Delta\theta$ is the change in moisture content, and $F(t)$ is the cumulative infiltration (mm). The SWAT routine for the GAML infiltration is modified to accommodate the comprehensive reconstruction of SWAT structure for sub-hourly hydrologic processes.

Surface runoff lag

Once the total amount of excess rainfall is determined by the GAML equation, a fraction that lags in the HRU is estimated by a lag equation. The existing lag equation in SWAT (Neitsch et al. 2005a, equation 2:1.4.1, pp: 112) is developed for daily simulation and is not sufficient for subdaily runoff modeling. This equation relates the surface runoff lag with *surlag* coefficient and time of concentration but not with operational time interval because daily interval is implicitly assumed. As time interval narrows down to a fraction of an hour one would expect less portion of excess rainfall to reach the main channel. Therefore, a new lag equation that relates lag amount with the time interval as well as *surlag* coefficient and time of concentration is developed for the sub-hourly model. A first order equation that estimates the surface runoff lag during the time interval is defined by

$$Q_{surf,i} = (Q'_{surf,i} + Q_{stor,i-1}) \left(1 - \exp \left[\frac{-surlag}{t_c / \Delta t} \right] \right) \quad (2-2)$$

where $Q_{surf,i}$ is the amount of surface runoff discharged to the main channel at the end of time step i , $Q'_{surf,i}$ is the amount of surface runoff generated in the subbasin, $Q_{stor,i-1}$ is the surface runoff stored (or lagged) from the previous time step, *surlag* is the surface runoff lag coefficient, Δt is time interval, and t_c is the time of concentration for the subbasin. *surlag* is a user input parameter. As shown in Figure 1, equation (2-2) gives reasonable amount of surface runoff lag with respect to the operational time interval as well as a great flexibility in calibrating the output. For example, for $t_c = 60$ minute and $\Delta t = 15$ min $Q_{surf,i}$ ranges 0.2 to 0.95 as *surlag* varies 1~10.

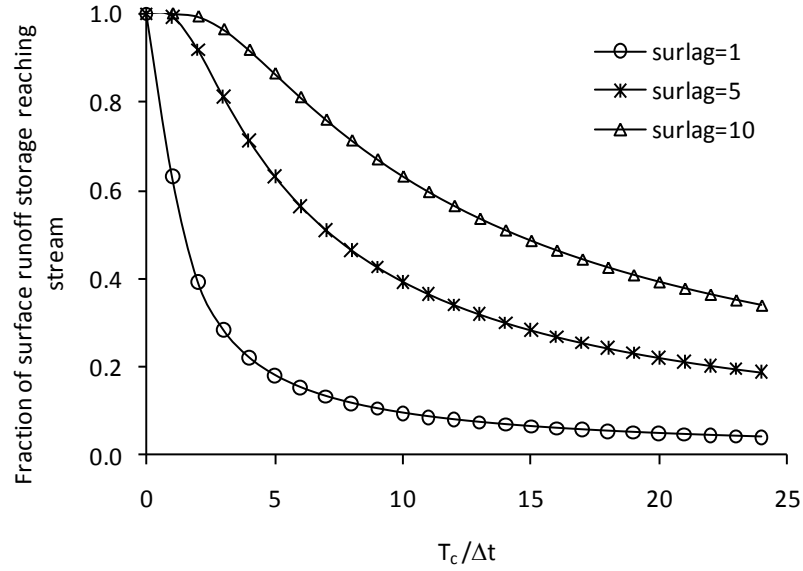


Figure 1. Influence of surlag, t_c , and Δt on fraction of surface runoff released to the main channel

Unit hydrograph

Surface runoff generated at each time step is routed using a dimensionless unit hydrograph (UH) method in which a hydrologic response to a pulse input (i.e. excess rainfall at a time step) is distributed in a triangular shape (retained from SWAT2005) or newly developed gamma distribution function based on the hydrologic property of the watershed. The triangular UH is defined by

$$q_{uh} = t/t_p \quad \text{if } t \leq t_p \quad (2-3a)$$

$$q_{uh} = \frac{t_b - t}{t_b - t_p} \quad \text{if } t > t_p \quad (2-3b)$$

where q_{uh} is unit flow rate at time t , t_p is time to peak flow since the direct runoff started, and t_b is time of recession. The unit flow rate is then normalized by the total amount of unit flow under the triangle. The duration of a UH in response to a pulse input of excess rainfall is related to hydrologic characteristics of the watershed, represented by t_c .

$$t_b = 0.5 + 0.6 t_c + tb_adj \quad (2-4)$$

In this equation, tb_adj is a user input factor for adjusting subdaily unit hydrograph. Then, the time to peak flow is estimated based on the SCS dimensionless unit hydrograph (SCS 1972) method in which 37.5% of the total volume is assigned to the rising side.

$$t_p = 0.375 t_b \quad (2-5)$$

For example, the UH triangle in bold lines in Figure 2 shows the unit hydrograph during time steps 2 to 8, multiplied by the excess rainfall that occurred at time step 2. Similarly, unit hydrographs that are associated with the excess rainfalls during the time steps from 0 to 4 are plotted separately, and then all UHs are superimposed at each computation node to generate the runoff hydrograph shown on the top of the figure in a smooth curve. Because the computational nodes are regularly spaced in time, t_p and t_b take the nearest integer values.

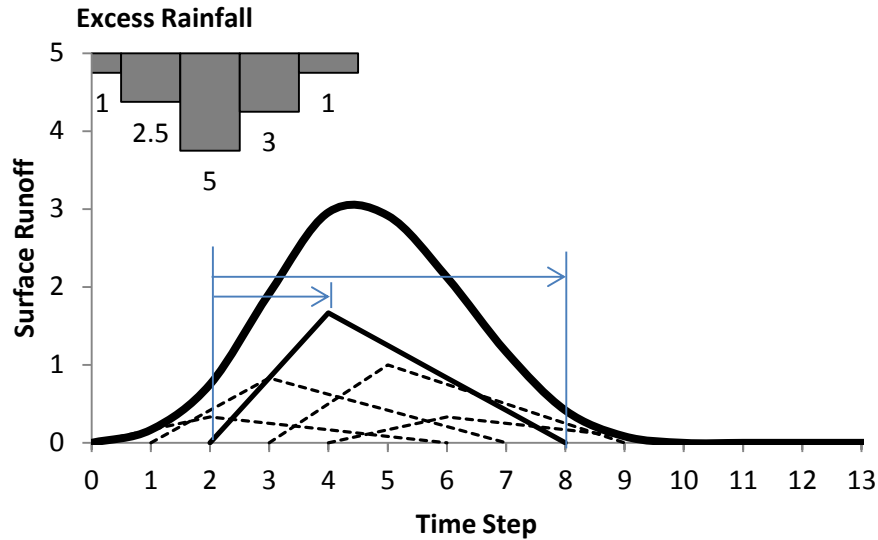


Figure 2. Surface runoff hydrograph generated by superimposing dimensionless triangular unit hydrographs.

The gamma distribution UH method adapted from Aron and White (1982) defines unit flow as follows:

$$q_{uh} = \left(\frac{t}{t_p} \right)^\alpha \cdot \exp \left(- \left(\frac{t}{t_p} \right)^\alpha \right) \quad (2-6)$$

where α is a dimensionless shape factor which is larger than zero. This method allows for calibration of peak flow and runoff lagging through the landscape (see Figure 3 for example).

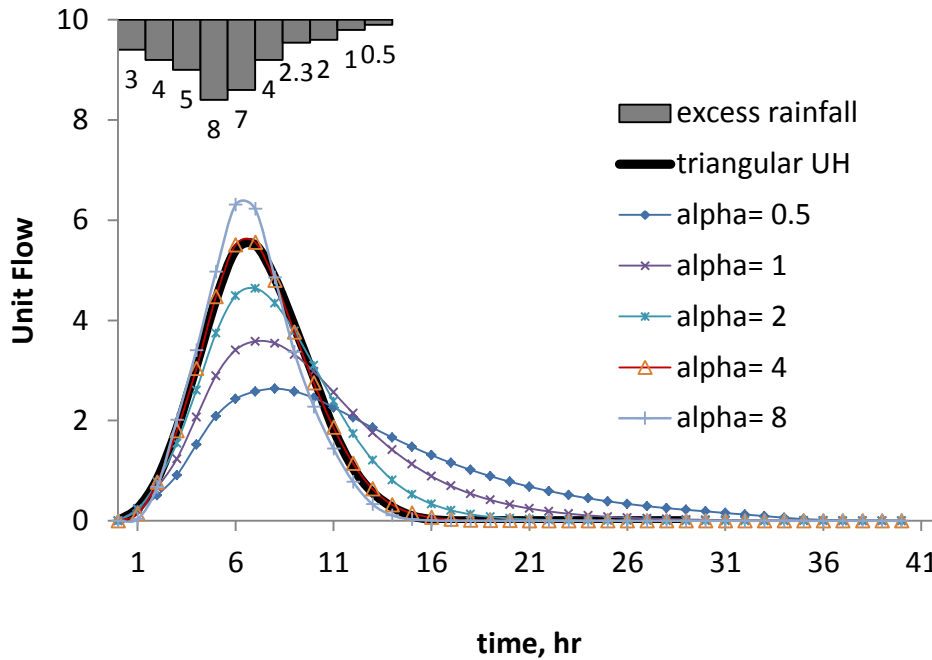


Figure 3. Surface runoff responses of the gamma distribution UH with varying alpha factors.

Channel, impoundment routing

In SWAT, stream flow is routed through the channel network using the variable storage routing method (Williams 1969) or the Muskingum routing method (Overton 1966). Both the variable storage routing method and the Muskingum routing method are variations of the kinematic wave (KW) model which predicts short duration storms better than the nonlinear reservoir model that is often used in hydrologic modeling (Xiong and Melching 2005). Impounded water bodies are assessed in four different types: ponds, wetlands, depressions/potholes, and reservoirs. Ponds, wetlands, and depressions/potholes are located within a subbasin off the main channel while reservoirs are located on the main channel. The routines for channel routing and impoundment routing were modified such that these routines run at sub-hourly time intervals as small as 1 minute to accommodate the capability of sub-hourly simulation.

Processes in sub-hourly simulation

The schematic of the sub-hourly model structure is presented in Figure 4. The GAML procedure simulates excess rainfall from each HRU in a subbasin at every time interval. The amount of water that lags at the end of time step is estimated by equation (2-2), and the lag

amount is added to the excess rainfall that occurs in the next time step. HRU output values are aggregated at subbasin scale for flow routing. Estimated values at the end of day are retained in temporary arrays for continuous simulation over midnight. There are 3 layers of iteration loops for temporal marching ($\Delta t \rightarrow \text{day} \rightarrow \text{year}$) of solution processes and one iteration loop for spatial discretization covering all HRUs. For upland processes, HRU results are aggregated for processing at larger spatial scales (HRUs \rightarrow Subbasins \rightarrow Watershed). Surface runoff, channel flow, and impoundment storage including ponds and reservoirs are routed at a subdaily time interval, but base flow and evapotranspiration are calculated on a daily basis and distributed for each time step.

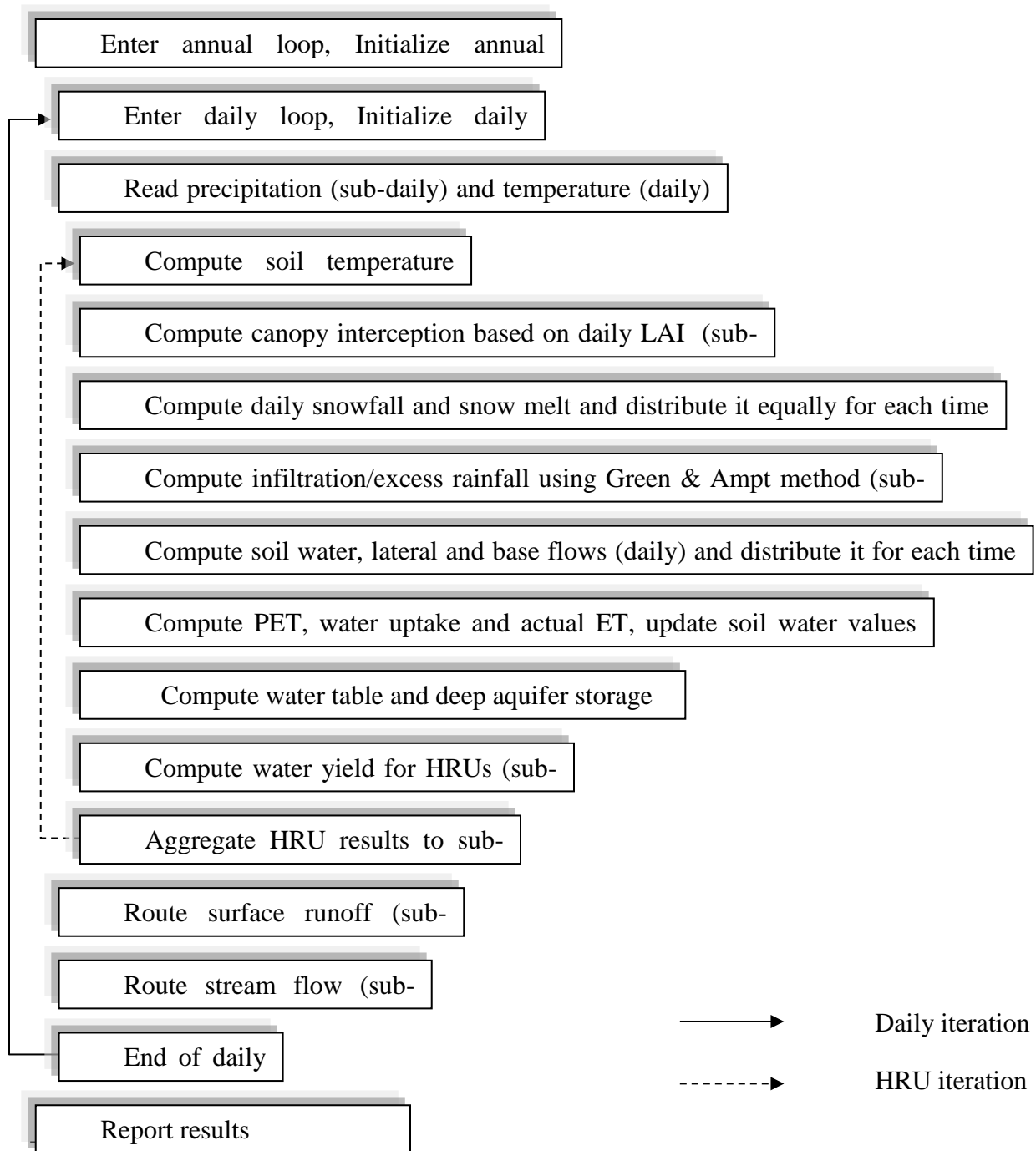


Figure 4. Schematic flow chart showing the stream of processes in the sub-hourly simulation model

2.3 Case study

A small, mostly pristine watershed in Austin, TX was selected for testing the sub-hourly model (Figure 5). The study area, Lost Creek Golf course Area (LGA) watershed (Area =1.94 Km²), is mostly undeveloped with no significant discharge or recharge of groundwater to deep

aquifer (City of Austin 2006). The GAML infiltration method with Hargreaves evapotranspiration (ET) estimation method (Hargreaves et al. 1985) is used for the sub-daily model runs. For the daily runs, CN method with Hargreaves ET is used.

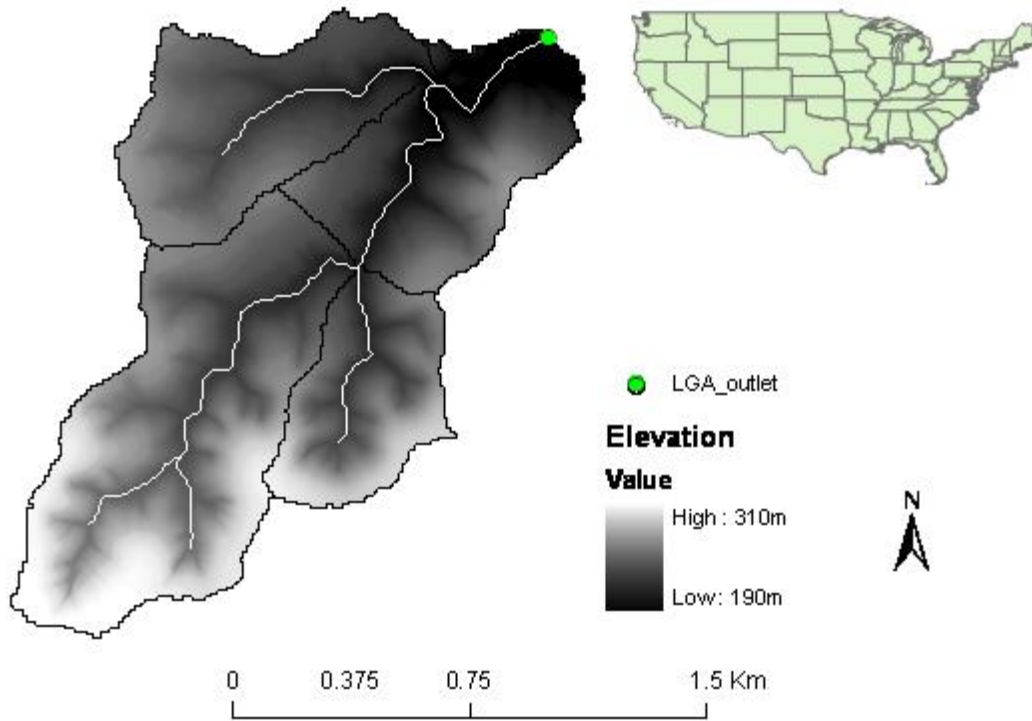


Figure 5. LGA watershed in Austin, Texas

The modeling time step always corresponds to the resolution of precipitation data (e.g., 15 min precipitation data is used in 15 min model runs). However, daily maximum and minimum temperature data is used for all the model runs irrespective of time step. Channel routing is carried out using the Muskingum method for all the model runs. Given the goals of the current project, applicability of the sub-hourly SWAT model, and short deadlines, the sub-daily soil water or evapotranspiration (ET) calculations are not attempted in the present study.

Description of the watershed and input data

A Digital Elevation Model (DEM) with 0.3 meter (1 foot) resolution was prepared by City of Austin for watershed delineation. Soil data was obtained from Natural Resources Conservation Service (NRCS) Soil SURvey GeOgraphic (SSURGO) database. A land cover map of the study area for the year 2003 was prepared by City of Austin through aerial survey. Rainfall data of 1 minute interval recorded at a weather station near the watershed outlet was collected,

and then aggregated to 15 minute interval. The watershed was divided into 4 subbasins and 36 HRUs based on the delineated stream network, land use, soil and slope combinations. The dominant soils are fine textured (proportion of clay+silt > 65 %) shallow soils underlain by karstic rocks. Most of the soils are classified as hydrologic soil groups C and D. The dominant land use is undeveloped (70 %), which includes small residential structures and roads. Golf course/pasture (18 %) and residential (12 %) are other dominant land uses in the watershed. The main channel in the LGA watershed is highly ephemeral, having no stream flow for more than 70% - 80% of time during the test period.

Sensitivity analysis

A sensitivity analysis was conducted to investigate the impact of model operational time step in the subdaily SWAT applications. The sensitivity of stream flow to SWAT was indexed for various time intervals and those highly ranked parameters were selected for the model calibration. Due to the importance of the relative influences between parameters, a global method - the Latin hypercube sampling method incorporated with One-factor-at-a-time analysis technique (LH-OAT) - was used in the study. LH-OAT is a highly efficient global method based on the Monte Carlo simulation but uses a stratified technique that reduces computational time (van Griensven et al. 2006). It subdivides each parameter into N intervals and assumes the parameter is uniformly distributed within each interval. Random values of the parameters are generated such that the parameter is sampled only once for each interval. The total number of model runs is $N \times (K+1)$, where N is the number of intervals and K is the number of parameters. Based on the literature review (Muleta and Nicklow 2005; Neitsch et al. 2005a, 2005b; Kannan et al. 2007; Di Luzio and Arnold 2004; Immerzeel and Droogers 2007; Santhi et al. 2001), 15 mostly used parameters in calibrating hydrologic processes were selected (Table 1) for the sensitivity test. The 15 parameters ($K=15$) were divided into 10 intervals ($N=10$) of equal probability. Therefore, a total of 160 model runs was made for the LHS-OAT sensitivity analysis. This compares well with the number of model runs that a local method requires in which every possible combination of parameters is simulated ($N^K = 1.0E+15$).

In the OAT analysis method, the derivatives of the model output are calculated for each parameter (x_i) as a small perturbation (Δx_i) is added while other parameters are fixed. The change in the model output is entirely attributed to Δx_i . A sensitivity index, defined as a normalized change in the model output divided by a normalized change in the input parameter, is useful to facilitate a direct comparison of parameters (Wang et al. 2005).

$$S_{ij} = \frac{|M(x_1, \dots, x_i + \Delta x_i, \dots, x_K) - M(x_1, \dots, x_i, \dots, x_K)|}{|M(x_1, \dots, x_i + \Delta x_i, \dots, x_K) + M(x_1, \dots, x_i, \dots, x_K)|} \frac{|\Delta x_i|}{x_i} \quad (2-7)$$

where S_{ij} is the relative partial effect of parameter x_i around the LH point j , K is the number of parameters, and M is the model output. In this study, M represents time series result of stream flow at every time step at the watershed outlet. The partial sensitivity index values for x_i are averaged to get the final sensitivity index (S_i).

Table 1. SWAT parameters used in the sensitivity analysis

Parameter	Definition	File name	Range of values	
			Min.	Max.
ALPHA_BF	Base flow recession constant (days)	.gw	0.001	1
SURLAG	Surface runoff lag coefficient (days)	.bsn	0.001	15
AWC	Available water capacity	.sol	-25%*	+25%*
CH_K 1,2	Effective hydraulic conductivity of channel (mm/hr)	.rte, .sub	0.025	150
CH_N 1,2	Manning's n value for the main and tributary channels	.rte, .sub	0.01	0.07
CN2	SCS runoff curve number for moisture condition II	.mgt	-4.0**	+4.0**
EPCO	Plant uptake compensation factor	.hru	0.001	1
ESCO	Soil evaporation compensation factor	.hru	0.001	1
GW_DELAY	Delay time for aquifer recharge (days)	.gw	0.001	100
GW_REVAP	Groundwater revap coefficient	.gw	0.02	0.2
GWQMN	Threshold water level in shallow aquifer for base flow (mm)	.gw	0.01	100
Ksat	Saturated hydraulic conductivity (mm/hr)	.sol	-50%*	+50%*
MUSK_CO1	Weighting factor for influence of normal flow on storage time constant value	.bsn	0.01	10
MUSK_CO2	Weighting factor for influence of low flow on storage time constant	.bsn	0.01	10
OVR_N	Manning's n value for overland flow	.hru	0.05	0.8

* Value varies with land use; changes by multiplying a ratio within the range

** Value varies with land use; changes by adding/subtracting a value within the range

A public domain FORTRAN code developed by van Griensven and Meixner (2003) was adapted for the analysis. Multiple analyses were conducted for flow in 2004 with a 2-year warm-up period using subdaily (15 minute and 1 hour interval) and daily intervals. In SWAT, many physically-based parameters vary at the HRU level and thus a significant number of parameters need to be assessed for the sensitivity analysis while each parameter has little influence on the model output. Therefore, these parameters were assessed in a clustered way by adding or

multiplying relative changes to the default values (e.g. -4 ~ +4 for CN2 or -25% ~ +25% for AWC).

Calibration of stream flow

A simple semi-automated procedure was developed for calibrating the subdaily SWAT model. Parameters for calibration were selected based on a sensitivity analysis. As there were many sensitive parameters included for calibration, it was decided to do the calibration in an efficient way, covering the whole parameterization process in a few steps. In this procedure, parameter values vary one at a time in an iterative loop covering all different possible combinations of parameters.

The calibration procedure is coupled with a statistical tool that evaluates model performance statistics. The model performance is evaluated at the end of iteration based on statistical measures and the breakdown of water balance components. The statistical criteria include Nash and Sutcliffe efficiency (NSE), Coefficient of Determination (R^2), Percent Bias (PBIAS), and Root Mean Square Error Standard Deviation Ratio (RSR) (Abulohom et al. 2001; Moriasi et al. 2007). NSE provides a normalized indicator of the model performance in relation to a benchmark. $NSE = 1$ is the optimal value. Values should be larger than 0.0 to indicate “minimally acceptable” performance and a value equal to or less than 0.0 indicates that the mean observed flow is a better predictor than the model value. Generally, a daily NSE of 0.65 or higher is considered good but the criteria may be lower for subdaily results and higher for monthly or annual outputs since performance improves as time interval increases. PBIAS measures the average tendency of the simulated component to be larger or smaller than their observed counterparts. With the optimal value of 0.0, positive values indicate model underestimation bias and negative values indicate model overestimation bias. As a general rule, a PBIAS of 10% or less is considered very good, 15% or less is good, and 25% or less is satisfactory (van Liew et al. 2007). RSR normalizes root mean standard error (RMSE) using the standard deviation of observation, incorporating the benefits of error index statistics with a normalization factor. RSR varies from 0 to a large positive value. $RSR = 0$ is the optimal value indicating a perfect model performance. Lower values of RSR indicate lower RMSE which means better model performance. A RSR value of 0.5 or less is considered very good, and 0.55 or less is good and 0.6 or less is considered satisfactory. R^2 describes the proportion of the variance in the residuals (the difference between observed flow and predicted flow) ranging from 0 to 1. A high value indicates less error with $R^2=1$ meaning the perfect match.

Strategy for calibration-validation

Subdaily simulation models are often calibrated for individual storm events rather than for a long continuous period (Zhang and Cundy 1989; Feng and Molz 1997; Tisdale and Yu 1999; Di Luzio and Arnold 2004; Jain and Singh 2005). However, the new sub-hourly SWAT

model is developed for long term continuous simulations and thus, the model is expected to yield good results not only for individual storm events but also for long term periods. Therefore, a one year period was selected for the model calibration, and another one year was used for model validation. In some of the previous studies, it is found that better results can be obtained if a model is calibrated with wet condition data than dry condition data (Kannan et al. 2007; van Liew and Garbrecht 2003). In Austin, TX where the LGA watershed is located, year 2004 is the wettest year in the simulation period; thus, the model was calibrated to the stream flow data in 2004 with two years of warm-up period (2002-2003). Because the LGA watershed has experienced urbanization since 2005, an earlier period (year 2002) was selected for validation to make sure that the results are not affected by the changes in land use.

An automated base flow separation technique (Arnold et al. 1995) was used to separate base flow from stream flow using 5 years of data (2002-2006). Estimates of base flow are important to understand low flow characteristics of the streams and to investigate water pollution assessment. For example, the sub-hourly model was able to adequately reproduce stream flow with different percent contributions of surface runoff varying from less than 2% (i.e. 98% base flow) to more than 50%. Since multiple percent surface runoff profiles guaranteed good fittings of model output to the stream flow observation, the uncertainty in the model output could easily overwhelm the model reliability when used in water quality modeling because some of instream water quality is highly dependent on surface runoff. The base flow filter estimated the contribution of base flow to the stream flow as 40% for LGA. In calibration and validation, however, the percentage of surface runoff was assumed slightly smaller than 60% because of the following reasons. The geomorphic characteristics of LGA is represented by thin soil layers (20cm to 40 cm) above fractured base rock and steep slopes (average slope=6.2%) which promotes high lateral flow. SWAT output confirms this theory with significant lateral flow contributing 30% to the stream flow (see Table 3). We concluded that a considerable amount of lateral flow was assigned to surface runoff by the base flow filter. Therefore, the average ratio was adjusted to around 55% surface runoff and 45% base flow during the calibration period.

Stream flow was calibrated at the watershed outlet through a combination of manual and automatic procedures. During the initial manual calibration, the range of parameter values are narrowed down based on the statistical measures and water balance. Then the semi-automatic calibration finds a set of parameters that gives the best efficiency values (NSE and R^2) and water balance. By repeating the manual and semi-automatic procedures, a set of parameters that yields the best efficiency values as well as realistic breakdown in water balance components can be found in relatively shorter time than a full manual calibration. The integration of automatic and manual calibration can substantially increase the calibration efficiency compared to a fully automatic procedure depending on modeler's experience and expertise (White 2009).

2.4 Results

Parameter sensitivity

The result of the sensitivity analysis is summarized in Table 2. The sensitivity of SWAT parameters was significantly influenced by the model operational time step. The parameters related to channel routing (*CH_N*, *CH_K*, *MSK_CO1*, and *MSK_CO2*) became very sensitive as time scale narrows down. On the other hand, the significance of groundwater flow parameters (*GWREVAP*, *GWQMN*, *ALPHA_BF*, and *GWDELAY*) was relatively higher with the daily time interval. Plant available water capacity parameter (*AWC*) was highly influential in all tests and no meaningful correlation was found between *AWC* and model operational time interval. Meanwhile, *KSAT*, *ESCO*, *CN2*, and *SURLAG* were marginally ranked for sensitivity in all tests.

Table 2. Sensitivity of SWAT parameters for different operational time intervals ($\Delta t = 15\text{min}$, 1hr, and 1day)

Rank	$\Delta t = 15\text{min}$		$\Delta t = 1\text{hr}$		$\Delta t = 1\text{day}$	
	Parameter	S_i	Parameter	S_i	Parameter	S_i
1	CH_N	116.7	ALPHA_BF	25.7	AWC	21.2
2	AWC	43.4	AWC	24.5	GWREVAP	10.7
3	SURLAG	19.5	GWQMN	9.5	GWQMN	7.8
4	MSK_CO2	9.2	ESCO	8.6	ESCO	7.4
5	KSAT	8.8	GWDELAY	7.0	ALPHA_BF	6.5
6	OVR_N	8.1	CN2	4.7	GWDELAY	5.8
7	ALPHA_BF	6.8	GWREVAP	3.4	CN2	4.5
8	ESCO	6.6	KSAT	2.4	SURLAG	3.4
9	CH_K	5.7	SURLAG	1.1	KSAT	1.8
10	CN2	4.9	CH_N	0.7	EPCO	0.5
11	GWDELAY	4.8	MSK_CO2	0.4	OVR_N	0.2
12	MSK_CO1	2.9	CH_K	0.4	MSK_CO2	0.1
13	GWQMN	1.2	EPCO	0.3	CH_N	0.1
14	GWREVAP	0.9	OVR_N	0.2	MSK_CO1	0.1
15	EPCO	0.6	MSK_CO1	0.1	CH_K	0.0

Water balance

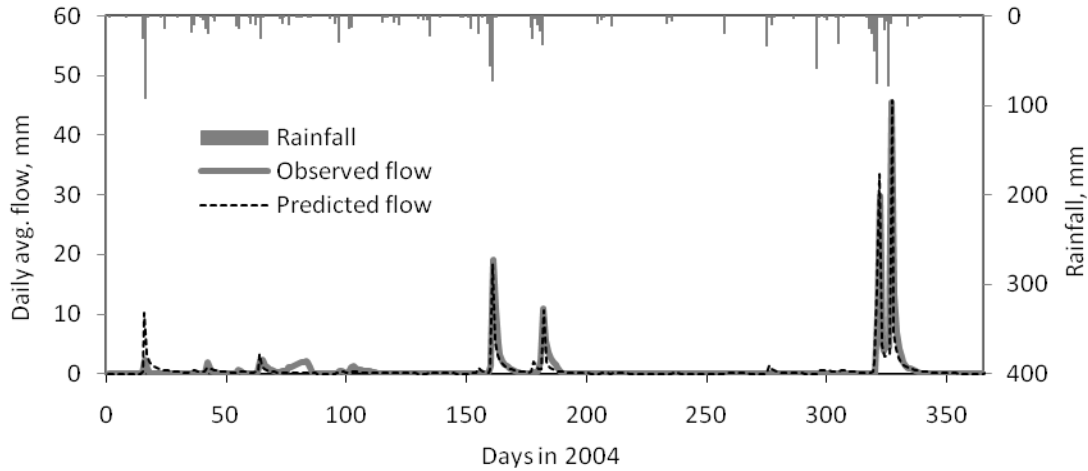
Shown in Table 3 is the predicted water balance in the upland processes scaled to the percent annual rainfall. There was more rainfall during the calibration period (1186mm/yr) than in the validation period (870mm/yr); therefore, it was reasonable that the predicted surface runoff was estimated higher in the calibration period than in the validation period and vice versa for the evapotranspiration. According to the Texas Irrigation Technology Center (2004), solar radiation recorded during the validation period was 34% higher than calibration period. The relatively higher amount of evapotranspiration in the validation period may be explained by the high amount of solar radiation during this period.

Table 3. Predicted water balance components

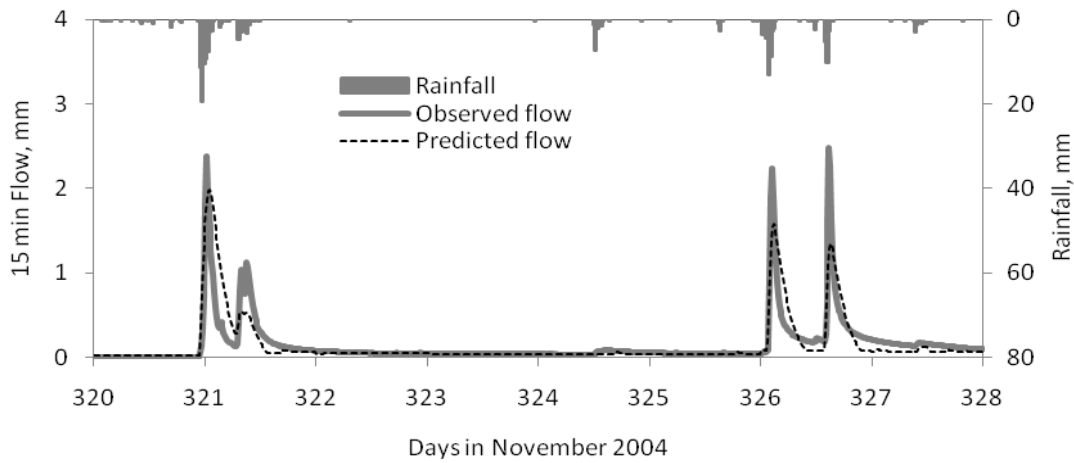
Time Interval	Period	Water balance components in terms of percent annual rainfall				
		surface runoff	lateral flow	groundwater flow	total water yield	evapotranspiration
15min	Calibration	12.1	8.8	2.0	22.9	59.0
	Validation	4.0	8.6	6.0	18.4	70.0
1hr	Calibration	12.5	5.8	5.2	23.5	59.0
	Validation	3.7	6.0	9.3	18.9	68.8
1day	Calibration	12.2	6.3	5.1	23.5	46.7
	Validation	6.1	6.8	2.8	15.6	54.9

Analysis of model performance

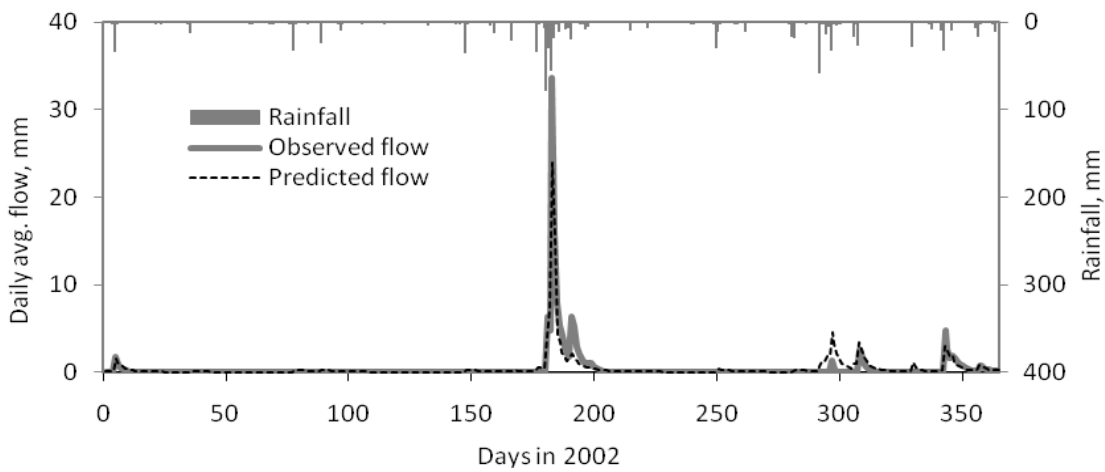
Stream flow hydrographs are presented in figures 6, 7 and 8 showing both model predictions and field observations for 15min, hourly and daily time step, respectively. Since one of the objectives of the study was to investigate the advantage of the new sub-hourly simulation model over existing daily model, sub-hourly results were aggregated to daily averages to directly compare the outputs from sub-hourly model to those from daily simulation model. Figure 5a shows the performance of sub-hourly model during the calibration period, where predicted 15min stream flow was aggregated to daily values. Due to the large number of data points in 15min output, the sub-hourly hydrograph with 15min interval was plotted for only one month period during the calibration period (Figure 5b). Figure 5c shows the predicted and observed stream flow during the validation period. In Figure 5c, 15min output is plotted in terms of daily averages same as Figure 5a. Similarly, 1hr and 1day results are presented in Figure 6 and Figure 7 respectively.



(a) Daily stream flow aggregated from 15min output (calibration)



(b) 15min stream flow (calibration). NSE_{15min} is estimated for the entire year



(c) Daily stream flow aggregated from 15 min output (validation)

Figure 6. Stream flow hydrographs for $\Delta t= 15$ minute

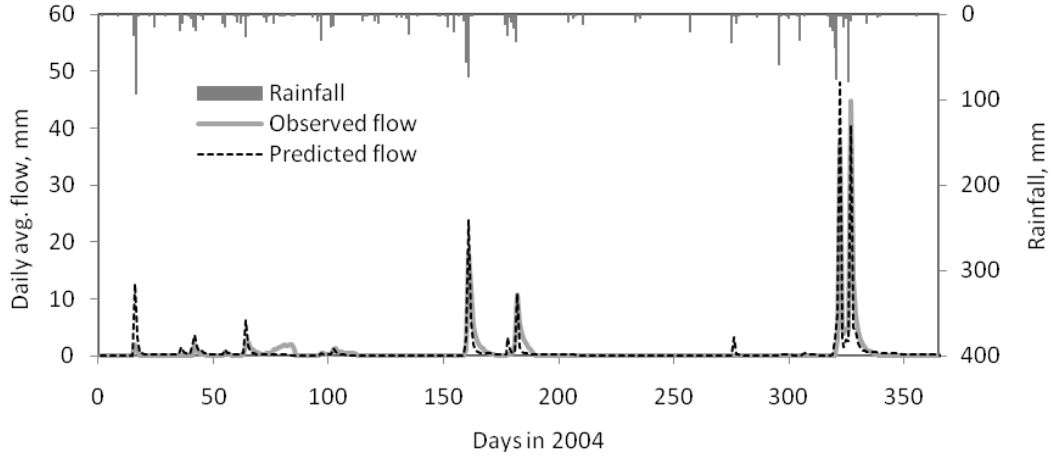
Model results at various time steps

Model output with sub-daily operational time steps (Figs. 6 and 7) was better in predicting peak flows than the daily output (Figure 8). NSE values increased appreciably when sub-daily results were aggregated to daily averages (e.g., 15min calibration: $NSE_{15min} = 0.74$ to $NSE_{15min \rightarrow 1day} = 0.93$, 1hr calibration: $NSE_{1hr} = 0.6$ to $NSE_{1hr \rightarrow 1day} = 0.86$) as summarized in Table 4. When compared with daily output, the aggregated sub-daily results were far better (e.g., $NSE_{15min \rightarrow 1day} = 0.93$ and $NSE_{1day} = 0.72$ in the calibration period). In both calibration and validation periods, the predicted stream flow with sub-daily operational time step is more reliable than daily simulation results. High resolution precipitation data (15 min and 1 hr for the respective sub-daily model runs) and subsequent calculation of rainfall intensity, infiltration/surface-runoff and routing of overland flow at sub-daily time steps could be attributed to the better performance of sub-daily model results over daily results.

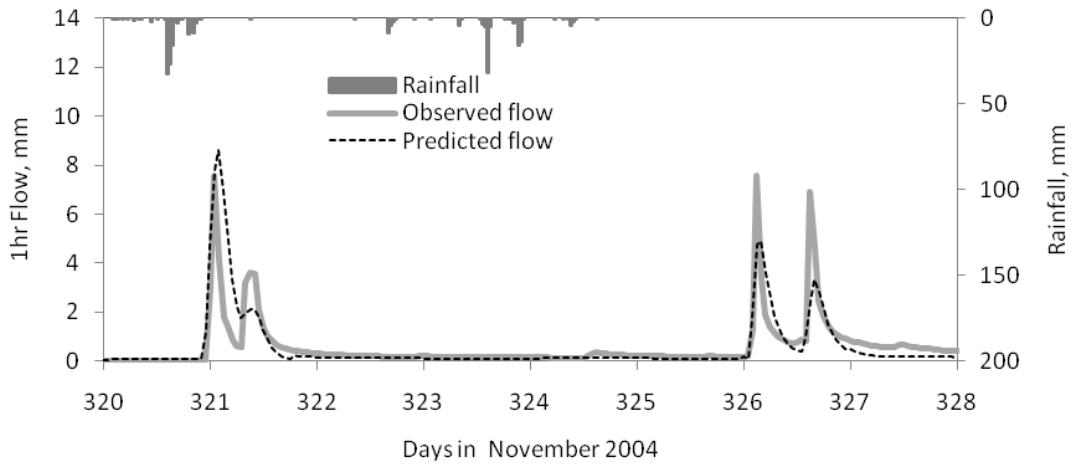
Table 4. Performance evaluation of different time intervals

Simulation Interval	Rain data resolution	Runoff generation method	Period	NSE		R^2	PBIAS (%)	RSR
				Δt	1day			
15min	15min	Green and Ampt method	Calibration	0.74	0.93	0.76	-3.84	0.51
			Validation	0.63	0.87	0.64	-12.47	0.61
1hr	1hr	Green and Ampt method	Calibration	0.60	0.86	0.67	-6.88	0.64
			Validation	0.72	0.90	0.73	-15.58	0.53
1day	1day	Curve Number method	Calibration	0.72		0.74	-6.25	0.53
			Validation	0.65		0.70	6.15	0.59

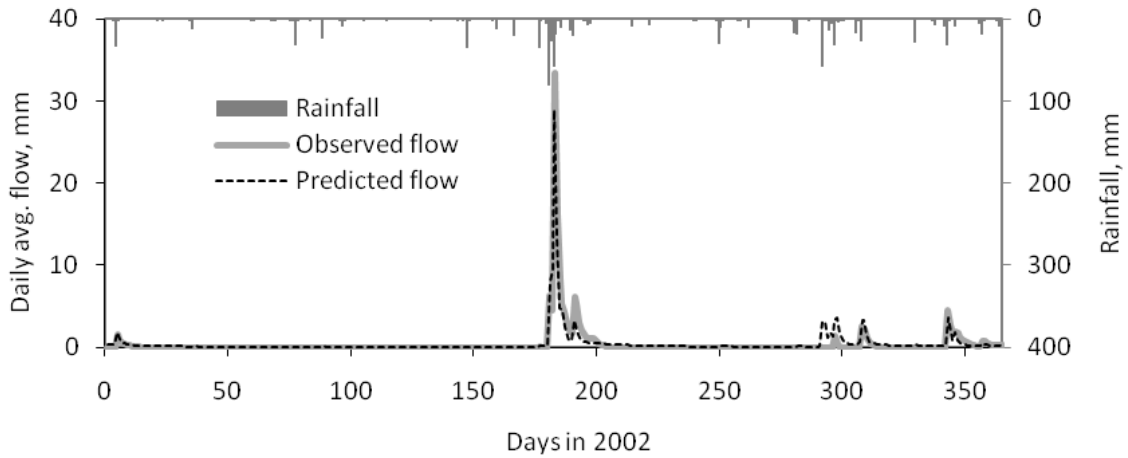
The steep slopes and short flow lengths (Time of concentration [t_c] < 2 hours) of LGA's landscape may result in flashy and spiky hydrographs as observed in figures 6 to 8. In addition, the stream flow of LGA has more than 50% of contribution from surface runoff (53% surface runoff and 47% base flow). Therefore, daily operational time step may be too sparse to adequately capture multiple sub-daily storm events. In all model runs, better performance was observed in the calibration period than in the validation period.



(a) Daily stream flow aggregated from 1hr output (calibration)



(b) 1hr stream flow (calibration). NSE_{1hr} is estimated for the entire year

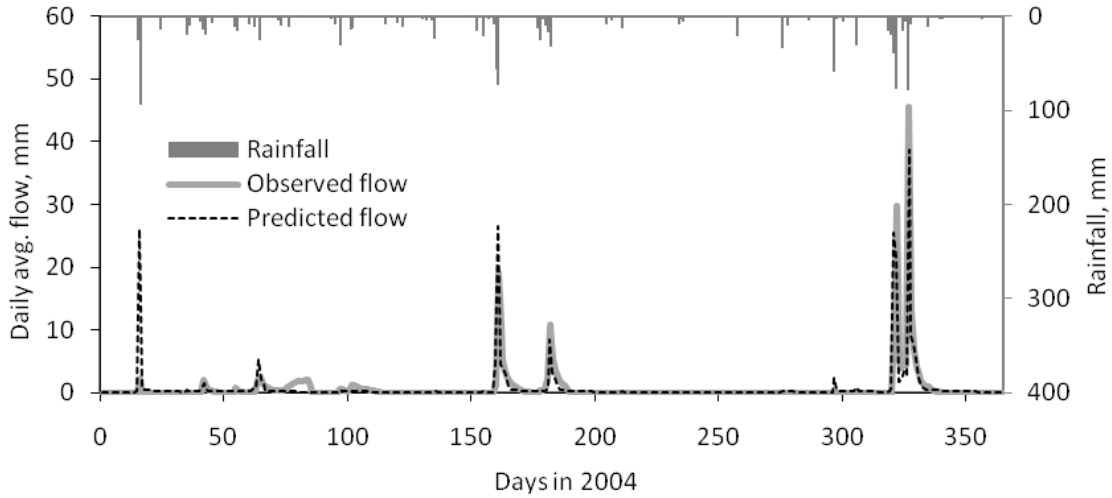


(c) Daily stream flow aggregated from 1hr output (validation)

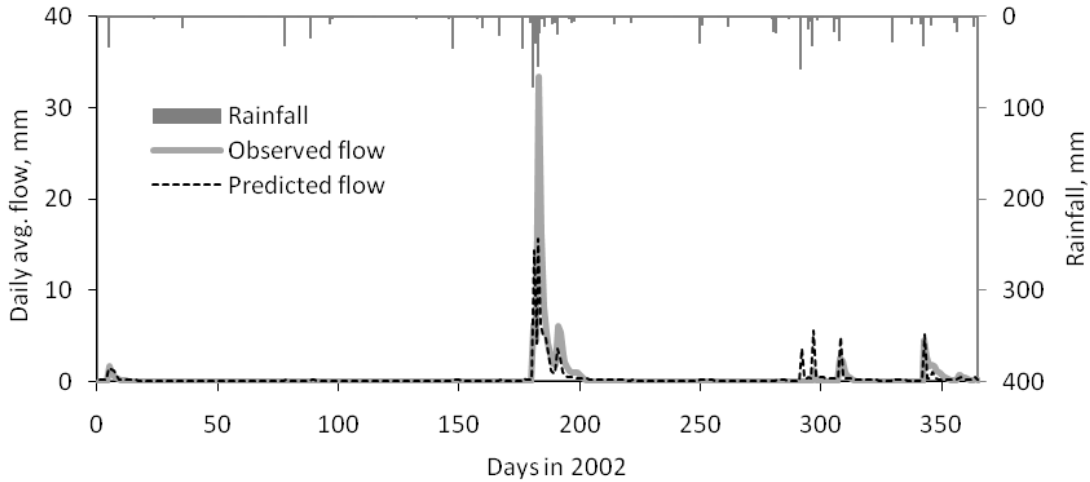
Figure 7. Stream flow hydrographs for $\Delta t = 1$ hour

High flow vs. low flow

Predicted stream flow hydrographs at sub-daily time intervals successfully captured both the timing and magnitude of peaks. Recession flows were also well simulated for high to medium storm events (Figs. 6 and 7), but the performance was marginal for small events (or low flows) as indicated by PBIAS values especially for the 1hr result (-15.58%). The daily simulation result (Figure 8) generally overestimated small to medium flows and underestimated high flows, which is similar to the findings in some of the previous studies (Eckhardt and Arnold 2001; Muleta and Nicklow 2005; Borah et al. 2007). This is further evident in the flow duration curves (FDCs) plotted with 15min, 1hr, and 1day outputs aggregated to daily time step showing the regimes for high flows (< 10% exceedance) and medium to low flows (> 10% exceedance) in Figure 9. The FDCs in Figure 9b show that sub-daily results are superior to daily results when high flows are of concern. As expected, none of the simulated results reasonably fits the observation on low flows (see Figure 9b) while sub-daily SWAT model performs very well on high flows. Since low flows are contributed mostly by base flow and there was no improvement made in the model for base flow, not much improvement is expected in the simulated sub-daily results for the regime of low flows. The clear discrepancy may be in part exaggerated by the semi-log scale used in the plotting because extreme values are generally exaggerated in semi-log plots. If plotted in normal exceedance curve, the big gaps in the medium to low flows would not be noticeable. The main reason for the model's poor performance in low flows might be attributed to the daily calculation of base flow and the equal distribution of the daily estimates to each time step. Difficulty in simulating subsurface hydrology due to high heterogeneity in the soil profile is also an important factor.



(a) Daily stream flow in the calibration period (estimated daily), $NSE_{1day}=0.72$



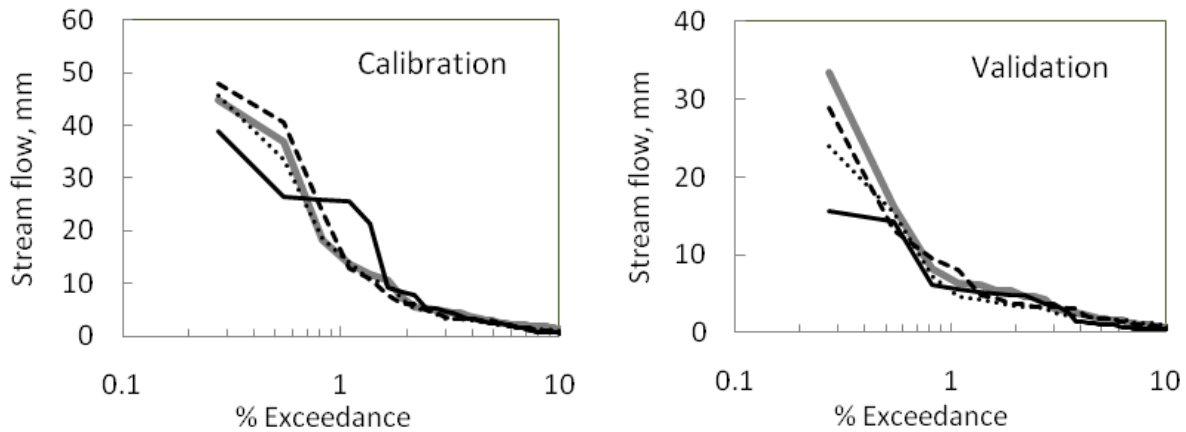
(b) Daily stream flow in the validation period (estimated daily), $NSE_{1day}=0.65$

Figure 8. Stream flow hydrographs for $\Delta t=1$ day

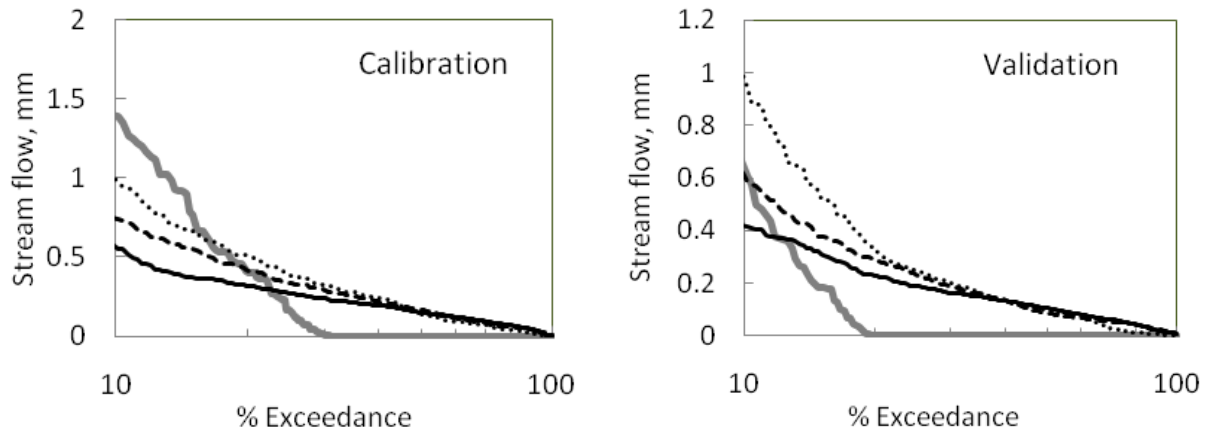
Calibration vs. validation

The statistical measures obtained from calibration and validation periods are given in Table 4. For all calibration schemes PBIAS values are less than zero meaning slight model bias toward overestimation, but all values remain within 10% in magnitude indicating “very good” ratings (Moriassi et al. 2007). In the validation period, PBIAS values for sub-daily model runs are worse than daily result. The PBIAS rank for 15min validation (-12.47%) is “good” while the rank for 1hr validation (-15.58%) is “satisfactory”. The other statistical measures (NSE , R^2 , and RSR) indicate that the model performance is very good in all cases. However, when compared to each other, the model performance is better in calibration period than in validation period. A

possible explanation for this behavior is that when data from wet conditions are used for calibration, and the model is validated for dry conditions the model needs to function just inside the range of model calibration. The data used for calibration is from the wettest year in the simulation period. Therefore, better results are expected for LGA in calibration than validation.



(a) FDC for high flow



(b) FDC for medium and low flow

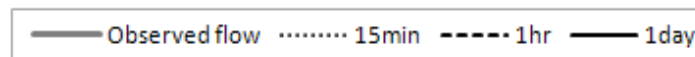


Figure 9. Flow duration curves for LGA watershed showing the impact of temporal resolution

GAML method vs. CN method

The CN method with daily precipitation was used for the daily model runs and GAML with sub-daily/sub-hourly precipitation for the sub-daily runs. In the previous sections it was established that the sub-daily model results outperform the daily results. In other words, GAML

performed better than the CN method for the LGA watershed. This could be attributed to better resolution of precipitation data (sub-daily intervals) used in the Green and Ampt method and subsequent physically based calculation of infiltration, and surface runoff and channel routing at sub-daily time steps. However, the results presented in this study differ from some of the previous studies (King et al. 1999; Kannan et al. 2007) that outlined no better results from Green and Ampt method. Quality of precipitation data and size of watershed might be the possible reasons for the difference in results.

2.5 Summary and recommendations

Sub-hourly flow simulation capability was added to the SWAT 2009 model. The new sub-hourly model components in SWAT allow simulation of runoff/infiltration, overland flow routing, reservoir/pond/wetland routing, and channel routing at any sub-daily time scale, while base flow is simulated at daily interval then distributed equally to each time step. The difference in the computational time scale between surface runoff and base flow may be a drawback of the model; however, a case study on a 1.94 Km² watershed shows significant improvement in the model output especially in the prediction of high flows compared to the daily SWAT model. The improvement in high flow predictions can benefit water quality modeling especially in the area of nonpoint sources pollution modeling as nonpoint sources are known to be a dominant environmental stressor in high flows. With the enhanced fine resolution in operation time step, the sub-hourly SWAT model is expected to successfully address hydrologic issues in urban watersheds.

Simulating sub-daily hydrological processes requires a different strategy for modelers. Using SWAT, we found that the model operational time step greatly affects the model parameters' sensitivity to the model output (see Table 2). A sensitivity analysis outlined in this study showed that the SWAT parameters related to channel routing become more influential as time interval decreases down to 15min and groundwater flow parameters get more influential as time interval increases.

A combination of automatic and manual calibrations used in this study made the calibration process very efficient. A strategy for auto-calibration was made during manual calibrations by narrowing down the range of parameters while maintaining the water balance between surface runoff and base flow in realistic ranges. Due to the complexity in hydrological processes and the formation of SWAT model, there was no unique combination of parameters that gave the best fitting to the observations whilst maintaining adequate water balance. A combination of parameters that yielded the most realistic proportion of base flow to the stream flow as well as good fitting against stream flow observations was selected after calibration of stream flow. A good knowledge on the watershed properties such as the ratio of surface runoff and base flow to the stream flow was necessary for the model calibration. Otherwise, subsequent water quality modeling can be very difficult because in-stream water quality is often very sensitive to the surface runoff.

High flows are better estimated with the sub-hourly model than the existing version of daily SWAT and therefore the developed sub-hourly model is expected to perform better in the non-point source pollution assessment studies. However, not much improvement is obtained in the low flow prediction because low flows are dominated by base flow and the model still uses soil water and ET estimation routines at daily time step. When tested for quality of flow results from CN and GAML method, our study pointed out better results from the Green and Ampt method mainly due to the high quality of precipitation data and physically based nature of infiltration/surface runoff estimation procedure.

A reasonable time interval should be selected for a sub-daily simulation based on the scale and characteristics of the watershed. Surface runoff needs be estimated at least once before it reaches the channel. Stream flow also needs to be calculated at least once before it reaches the end of channel segment. Therefore, it is recommended that the simulation time interval not to exceed the smaller of overland flow travel time and stream flow travel time. However, this does not necessarily mean that the finer the time interval always improves model performance. More capabilities are paired with the sub-hourly SWAT for simulating stormwater BMPs in urban watersheds as described in the following sections

2.6 Limitations

The enhanced SWAT model for sub-hourly flow simulation is intended for simulating short duration storms. Due to the lack of urban modules such as storm sewer network or storm water BMPs including Low Impact Development, this model may not be applicable to address hydrologic processes where pipe capacity and surcharge are factors.

2.7 References

- Abulohom MS, Shah SMS, Ghumman AR (2001) Development of a rainfall-runoff model, its calibration and validation. *Water Resour. Manag.* 15:149-163.
- Arnold JG, Allen PM, Muttiah R, Bernhardt G (1995) Automated base flow separation and recession analysis techniques. *Ground Water* 33(6): 1010-1018
- Arnold JG, Srinivasan R, Muttiah RS, Williams JR (1998) Large Area Hydrologic Modeling and Assessment Part I: Model Development. *J Am Water Resour As* 34(1): 73-89
- Aron G, White EL (1982) Fitting a Gamma Distribution Over a Synthetic Unit Hydrograph. *J Am Water Resour As* 18(1): 95-98.
- Benham BL, Baffaut C, Zeckoski RW et al. (2006) Modeling bacteria fate and transport in watersheds to support TMDLs. *Trans ASABE* 49(4): 987-1002.
- Bicknell BR, Imhoff JC, Kittle Jr JL, Donigian Jr AS, Johanson RC (1995) Hydrological Simulation Program—FORTRAN. User's Manual for Release 11

- Borah DK, Arnold JG, Bera M, Krug EC, Liang XZ (2007) Storm event and continuous hydrologic modeling for comprehensive and efficient watershed Simulations. *J Hydrol Eng* **12**(6): 605-616.
- Borah DK, Bera M (2003) Watershed-Scale Hydrologic and Nonpoint-Source Pollution Models: Review of Mathematical Bases. *Trans. ASAE* **46**(6): 1553-1556.
- Borah DK, Yagow G, Saleh A, Barnes PL, Rosenthal W, Krug EC, Hauck LM (2006) Sediment and nutrient modeling for TMDL development and implementation. *Trans ASABE* **49**(4): 967-986.
- Bracmort KS, Arabi M, Frankenberger JR, Engel BA, Arnold, JG (2006) Modeling long-term water quality impact of structural BMPs. *Trans ASABE* **49**(2): 367-374.
- Burns D, Vitvar T, McDonnell J, Hassett J, Duncan J, Kendall C (2005) Effects of suburban development on runoff generation in the Croton River basin, New York, USA. *J Hydrol*, **311**(1-4): 266-281
- Chang HJ (2007) Comparative streamflow characteristics in urbanizing basins in the Portland Metropolitan Area, Oregon, USA. *Hydrol Processes* **21**(2): 211-222.
- City of Austin (2006) Stormwater runoff quality and quantity from small watersheds in Austin, TX, City of Austin, Water Quality Report Series, COA-ERM/WQM 2006-1.
- Corbett CW, Wahl M, Porter DE, Edwards D, Moise C (1997) Nonpoint source runoff modeling - A comparison of a forested watershed and an urban watershed on the South Carolina coast. *J Exp Mar Biol Ecol* **213**(1): 133-149.
- Debele B, Srinivasan R, Parlange JY (2009) Hourly Analyses of Hydrological and Water Quality Simulations Using the ESWAT Model. *Water Resour. Manag.* **23**:303-324.
- Di Luzio M, Arnold, JG (2004) Formulation of a hybrid calibration approach for a physically based distributed model with NEXRAD data input. *J Hydrol* **298**(1-4): 136-154.
- Eckhardt K, Arnold JG (2001) Automatic calibration of a distributed catchment model. *J Hydrol* **251**(1-2): 103-109.
- Feng K, Molz FJ (1997) A 2-D, diffusion-based, wetland flow model. *J Hydrol* **196**(1-4): 230-250.
- Garen DC, Moore, DS (2005) Curve number hydrology in water quality modeling: Uses, abuses, and future directions. *J Am Water Resour As* **41**(2): 377-388.
- Gassman P, Reyes M, Green C, Arnold JG (2007) The Soil and Water Assessment Tool: Historical development, applications, and future research directions. *Trans ASABE* **50**(4): 1211-1250.
- Hantush MM, Kalin L (2006) Impact of Urbanization on the Hydrology of Pocono Creek Watershed: A Model Study, National Risk Management Research Laboratory, Office of

- Research and Development, U.S. Environmental Protection Agency, Cincinnati, Ohio 45268
- Hargreaves GL, Hargreaves GH, Riley JP (1985) Agricultural Benefits for Senegal River Basin. *J Irrig Drain Eng* 111(2): 113-124.
- Harmel RD, Rossi CG, Dybala T et al. (2008) Conservation Effects Assessment Project research in the Leon River and Riesel watersheds. *J Soil Water Conserv* 63(6): 453-460.
- Immerzeel WW, Droogers P (2008) Calibration of a distributed hydrological model based on satellite evapotranspiration. *J Hydrol* 349(3-4): 411-424.
- Jain MK, Singh VP (2005) DEM-based modelling of surface runoff using diffusion wave equation. *J Hydrol* 302(1-4): 107-126.
- Julien PY, Saghaifian B (1991) CASC2D User's Manual: A Two-dimensional Watershed Rainfall-runoff Model, Colorado State University, Center for Geosciences, Hydrologic Modeling Group.
- Kannan N, White SM, Worrall F, Whelan MJ (2007) Sensitivity analysis and identification of the best evapotranspiration and runoff options for hydrological modelling in SWAT-2000. *J Hydrol* 332(3-4): 456-466.
- Kim NW, Lee J (2009) Integration of SWAT and SWMM models, In: Proceedings of the 2009 International SWAT Conference, Boulder, CO
- King KW (2000) Response of Green-Ampt Mein-Larsen Simulated Runoff Volumes to Temporally Aggregated Precipitation. *J Am Water Resour As* 36(4): 791-797.
- King KW, Arnold JG, Bingner RL (1999) Comparison of Green-Ampt and Curve Number methods on Goodwin Creek watershed using SWAT. *Trans ASABE*, 42(4): 919-925.
- Mausbach MJ, Dedrick AR (2004) The length we go: Measuring Environmental Benefits of Conservation Practices. *J Soil Water Conserv*, 59(5): 96A-103A.
- Mein R, Larson C (1973) Modeling infiltration during a steady rain. *Water Resour Res* 9(2): 384-394.
- Moriasi D, Arnold JG, van Liew M et al. (2007) Model evaluation guidelines for systematic quantification of accuracy in watershed simulations. *Trans ASAE* 50(3): 885-900.
- Muleta MK, Nicklow JW (2005) Sensitivity and uncertainty analysis coupled with automatic calibration for a distributed watershed model. *J Hydrol* 306(1-4): 127-145.
- Nearing MA, Liu BY, Risse LM, Zhang X (1996) Curve Numbers and Green-Ampt Effective Hydraulic Conductivities. *J Am Water Resour As* 32:125-136.
- Neitsch SL, Arnold JG, Kiniry JR, Srinivasan R, Williams JR (2005b) Soil and Water Assessment Tool Input/Output File Documentation, Version 2005, Grassland, soil and water research service, Temple, TX.

- Neitsch SL, Arnold JG, Kiniry JR, Williams JR (2005a) Soil and Water Assessment Tool Theoretical Documentation, Grassland, Soil and Water Research Service, Temple, TX.
- Overton D (1966) Muskingum flood routing of upland streamflow. *J Hydrol* **4**: 185-200.
- Pitt R, Voorhees J (1995) Source loading and management model (SLAMM)
- Radcliffe DE, Lin Z, Risse LM, Romeis JJ, Jackson CR (2009) Modeling Phosphorus in the Lake Allatoona Watershed Using SWAT: I. Developing Phosphorus Parameter Values. *J Environ Qual* **38**(1): 111-120.
- Refsgaard JC, Storm B (1995) MIKE SHE. Chapter 23 in *Computer Models of Watershed Hydrology*: 809-846.
- Richardson CW, Bucks DA, Sadler EJ (2008) The Conservation Effects Assessment Project benchmark watersheds: Synthesis of preliminary findings. *J Soil Water Conserv* **63**(6): 590-604.
- Rossman L (2004) Storm water management model User's manual version 5.0. Water Supply and Water Resources Division National Risk Management Research Laboratory Cincinnati.
- Santhi C, Arnold JG, Williams JR et al. (2001) Application of a watershed model to evaluate management effects on point and nonpoint source pollution. *Trans ASAE* **44**(6): 1559-1570.
- SCS (1972) National Engineering Handbook, Section 4, Hydrology. US Department of Agriculture, SCS, Washington, DC.
- Texas Irrigation Center (2004) ET and Weather Data. <http://texaset.tamu.edu/>. Accessed 12 Dec 2010
- Tisdale TS, Yu JMHL (1999) Kinematic Wave Analysis of Sheet Flow Using Topography Fitted Coordinates. *J Hydrol Eng* **4**(4)
- van Griensven A, Meixner T (2003) LH-OAT Sensitivity Analysis Tool. Tucson, Ariz.: University of Arizona, Department of Hydrology and Water Resources. http://www.sahra.arizona.edu/software/index_main.html. Accessed 12 Dec
- van Griensven A, Meixner T, Grunwald S et al. (2006) A global sensitivity analysis tool for the parameters of multi-variable catchment models. *J Hydrol* **324**(1-4): 10-23.
- van Liew M, Veith T, Bosch D, Arnold J (2007) Suitability of SWAT for the conservation effects assessment project: Comparison on USDA agricultural research service watersheds. *J Hydrol Eng* **12**: 173.
- van Liew MW, Garbrecht J (2003) Hydrologic simulation of the little Wichita river experimental watershed using SWAT. *J Am Water Resour As* **39** (2), 413–426.

- Wang X, Youssef MA, Skaggs RW et al. (2005) Sensitivity Analyses of the Nitrogen Simulation Model, DRAINMOD-N II. *Trans ASAE* 48(6): 2205-2212.
- White M (2009) Personal conversation, USDA-ARS Grassland, Soil and Water Research Laboratory, Temple, Texas; Email: mike.white@ars.usda.gov
- Williams J (1969) Flood routing with variable travel time or variable storage coefficients. *Trans ASAE* 12(1): 100-103.
- Xiong YY, Melching CS (2005) Comparison of kinematic-wave and nonlinear reservoir routing of urban watershed runoff. *J Hydrol Eng* **10**(1): 39-49.
- Zhang WH, Cundy TW (1989) Modeling of Two-Dimensional Overland-Flow. *Water Resour Res* 25(9): 2019-2035.

3. Sub-hourly Erosion and Sediment Transport

Modeling stormwater Best Management Practices (BMPs) often requires time steps as small as minutes to realistically capture the instantaneous flow and sediment load coming from upland areas. SWAT 2009 has used the Modified Universal Soil Loss Equation (MUSLE) for modeling upland erosion and sediment load. The MUSLE model is an empirical soil loss equation, which was formulated based on field observations rather than theoretically derived relationships to predict long-term average soil loss. This paper presents modified physically-based erosion models in SWAT for seamless modeling of erosion processes with the recently developed sub-hourly flow models. In the new algorithms, splash erosion is calculated based on the kinetic energy delivered by rain drops adapted from European Soil Erosion Model, and overland flow erosion is estimated using a physically-based equation adapted from the Areal Nonpoint Source Watershed Environment Response Simulation (ANSWERS) model. The Yang model and the Brownlie model were also modified for instream sediment routing.

3.1 Introduction

In SWAT, upstream erosion and sediment yield are estimated for each hydrologic response unit (HRU) with the MUSLE equation (Williams, 1975). The MUSLE equation has a number of benefits such as good prediction accuracy, no need for a delivery ratio, and the capability of estimating sediment yield from a single storm (Neitsch et al., 2005). However, MUSLE is an empirically developed method that is typically applied for estimating long-term average erosion processes in rural watersheds and is generally not appropriate for continuous simulations with short (hourly or sub-hourly) time steps.

Therefore, our specific objective for this SWAT modification was to develop and test physically-based erosion and sediment algorithms incorporated into SWAT to run with the recently developed sub-daily flow algorithms (Jeong et al., 2010) in an effort to improve SWAT simulations of small watersheds or urban watersheds. In this paper, we present integration of a splash erosion algorithm, an overland flow erosion and sediment transport algorithm, and two in-stream sediment routing methods to create a new sub-daily SWAT structure. Sensitivity of newly added parameters was investigated using a global sensitivity method. Performance of the sub-daily erosion and sediment algorithms was tested on a small rural watershed in Texas by comparing estimated flow and sediment to observed values. The sub-daily output was also compared to the SWAT daily output for a relative evaluation.

3.2 Methods

To accomplish this objective, we evaluated the theory, data demands, modeling mechanism, and applicability of the currently available routines to determine which ones were best suited for

SWAT. Selected models were modified and inserted as algorithms, which resulted in a new structure for sub-daily erosion and sediment processes in SWAT. In the new structure, surface runoff is calculated separately for pervious and impervious areas in each HRU. The urban build-up/wash-off routine is applied to urban runoff from impervious areas, while soil erosion processes such as splash erosion apply to pervious areas. Overland flow erosion is estimated only in runoff from pervious areas. Then, the combined runoff and sediment load is routed based on the subbasin geometry (Figure 10.). The erosion and sediment transport algorithms as well as in-stream sediment routing methods adapted in the sub-daily SWAT structure are described below in detail.

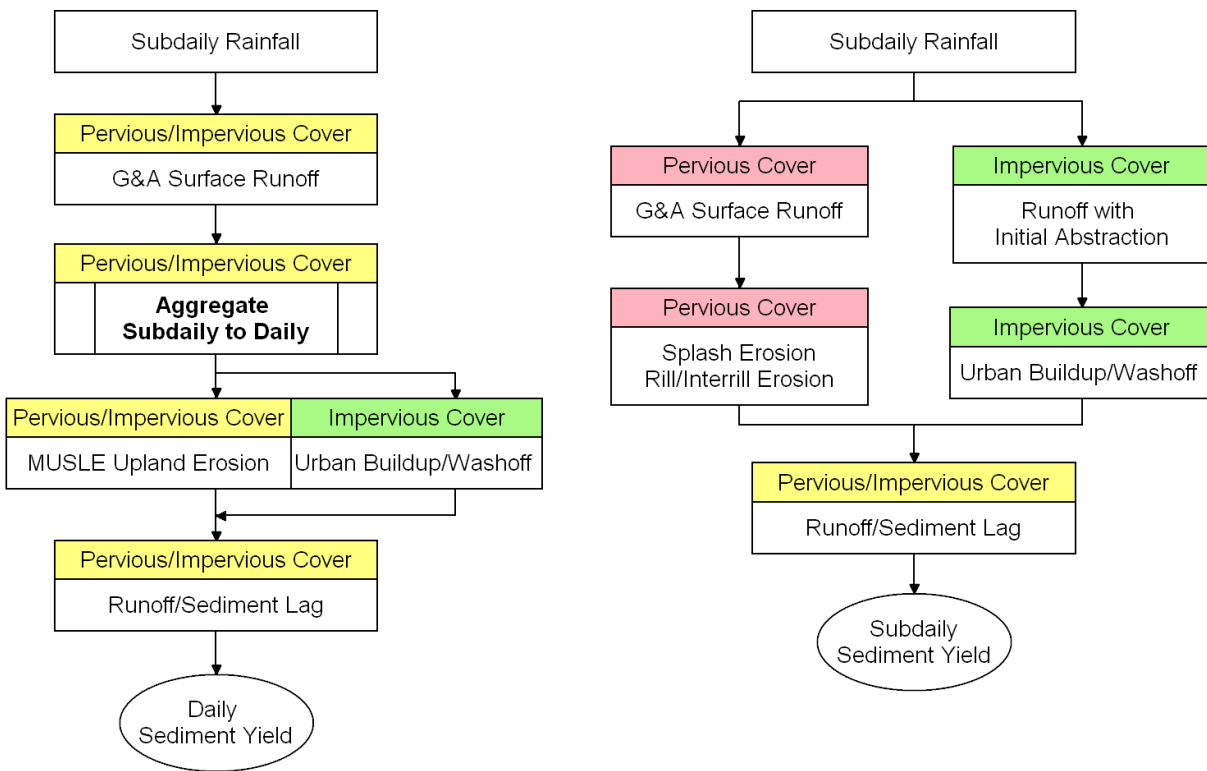


Figure 10. Schematic of sub-daily erosion processes (right) compared to daily erosion processes in SWAT2009 (left)

Erosion by rainfall (splash erosion)

Splash erosion can be a significant upland erosion mechanism in short duration, high intensity storms. Raindrops of such flashy storms often deliver high kinetic energy to the soil surface, which detaches a large amount of soil in a short time; therefore, sub-daily simulation models need to adequately represent these processes. A splash erosion model proposed by Brandt (1990) has been widely used in rainfall-runoff simulation models such as EUROSEM. Unlike

other popularly used erosion models such as WEPP that estimate splash erosion as a part of interrill erosion by parameterization, only EUROSEM estimates soil detachment by raindrop impact as a function of kinetic energy available to detach soil particles from the soil surface.

$$D_R = k \cdot KE \cdot e^{-\phi h} \quad (3-1)$$

where D_R is the soil detachment by raindrop impact ($\text{g/m}^2/\text{s}$), k is an index of the detachability of the soil (g/J), KE is the total kinetic energy of the rain (J/m^2), ϕ is an exponent varying from 0.9 to 3.1 with a representative value of 2.0 for a wide range of soil conditions (Torri et al., 1987), and h is surface runoff depth (mm).

Leaf drainage is a part of canopy interception that falls on to soil as water drops directly from leaf surface. The intercepted rainfall evaporates or becomes stem drainage and is subtracted from the total rainfall to estimate the effective rainfall. Rainfall kinetic energy is partitioned into direct through-fall and leaf drainage. The kinetic energy of leaf drainage is estimated by Brandt (1990).

$$KE_{leaf} = 15.8H_p^{0.5} - 5.87 \quad (3-2)$$

where KE_{leaf} is the kinetic energy of leaf drainage ($\text{J/m}^2\text{-mm}$) which is always equal or larger than zero, H_p is effective height of the plant canopy (m).

The kinetic energy of direct through-fall is estimated by Wischmeier and Smith (1978) which is used for rating erosivity in the Universal Soil Loss Equation (USLE).

$$KE_{direct} = 11.87 + 8.73 \log_{10} R_i \quad (3-3)$$

where KE_{direct} is the kinetic energy of direct through-fall ($\text{J/m}^2\text{-mm}$) and R_i is rainfall intensity (mm/hr). The total kinetic energy of effective rainfall is the summation of Equation (3-2) multiplied by the rainfall depth of leaf drainage and Equation (3-3) multiplied by the rainfall depth of direct through-fall.

Erosion by surface runoff

Coupled with the splash erosion model, an overland flow erosion model in ANSWERS was adapted for the sub-hourly SWAT model to estimate rill/interrill erosion. In ANSWERS overland flow erosion rate is associated with cross sectional average bed shear stress, crop management, and soil erodibility:

$$D_F = 11.02\alpha K_f C_f \tau^\beta \quad (3-4a)$$

where D_F is the flow erosion rate (kg/m²/h), K_f is the flow erodibility factor, C_f is the crop factor (Wischmeier, 1975), α and β are calibration parameters. α may vary from 0.5 to 2.0 depending on the susceptibility of rill erosion. β is by default 1.5 but can be as large as 3.0. τ is the reach-average bed shear stress (N/m²) defined in Equation 3-4b:

$$\tau = \gamma \cdot h \cdot S_f \quad (3-4b)$$

where γ is the specific weight of water, h is the depth of overland flow, and S_f is the energy slope.

Sediment yield from urban pavements

Dust, dirt, and other solids build up on urban paved surfaces during dry periods preceding a storm. The built-up solids are then washed off during storm events. Build-up is a function of time, traffic flow, dry fallout, and street sweeping (Neitsch et al., 2005). The existing buildup/washoff algorithm in SWAT, which uses the Michaelis-Menton buildup equation (Ammon, 1978) and a first order washoff equation (Huber et al., 1988), was modified for the sub-daily algorithm. Treatment of runoff and sediment from urban pavement by urban stormwater BMPs before draining to creeks can also be simulated in SWAT.

Instream sediment routing

The SWAT model uses Bagnold's (1977) stream power function for sediment routing. The transport of sediment in the channel is controlled by deposition and degradation that occur simultaneously. The net amount of sediment re-entrained is estimated based on a channel erodibility factor, the volume of water body in the channel segment, and a channel cover factor. Richardson et al. (2001) suggests that the Bagnold model works well on large rivers (width > 50 m) but the performance was less reliable on intermediate (width = 10-50 m) to small rivers (width < 10 m) in which stream bed materials are larger than 2 mm. Therefore, two new sediment routing models were added to SWAT for modeling intermediate to small rivers: Yang's

(1996) total load equations for sand and gravel and Brownlie's (1982) model. According to Richardson et al. (2001), Yang's model works the best on small rivers that have gravel or sandy bed materials, while Brownlie's model performs well on intermediate to small rivers. With the addition of the Yang model and the Brownlie model, estimation of potential sediment concentrations can be more accurately simulated over a wide spectrum of particle sizes.

The Brownlie model

The Brownlie model (1982) is a numerical model for unsteady flows in channel with sediment transport which was developed based on dimensional analysis and the best fit of a set of alluvial channel observations. The general equation for the net sediment concentration in the stream is estimated by:

$$C_{ppm} = 7115 c_F (F_g - F_{go})^{1.978} S^{0.6601} \left(\frac{R_h}{D_{50}} \right)^{-0.3301} \quad (3-5a)$$

where C_{ppm} is sediment concentration (parts per million, equivalent to mg/l), S is bed slope, R_h is hydraulic radius, D_{50} is the median particle size, and c_F is a coefficient (=1.268 for field data). The grain Froude number (F_g) is defined as:

$$F_g = \frac{v}{\sqrt{(S_g - 1) \cdot g \cdot D_{50}}} \quad (3-5b)$$

where v is flow velocity, S_g is particle specific gravity (default = 2.65 tons/m³), g is gravitational acceleration (= 9.81 m/s²). F_{go} is the critical grain Froude number defined as:

$$F_{go} = 4.596 \tau_{*o}^{0.5293} S^{-0.1405} \sigma_g^{-0.1606} \quad (3-5c)$$

where σ_g is the geometric standard deviation of particle sizes directly taken from field samples, τ_{*o} is the critical dimensionless shear stress for initiation of motion estimated by the transformed Shields curve:

$$\tau_{*o} = 0.22Y + 0.06 \cdot 10^{-7.7Y} \quad \text{where } Y = \left(\sqrt{S_g - 1} \cdot R_g \right)^{0.6} \quad (3-5c)$$

In this equation, R_g is the grain Reynolds number:

$$R_g = \frac{\sqrt{gD_{50}^3}}{\nu} \quad (3-5d)$$

The Yang model

Yang's total load equations are widely accepted in sediment routing models. There are two equations to estimate sediment concentrations for sand and gravel bed materials for each. The sand equation is used for median particle sizes less than 2.0 mm:

$$\begin{aligned} \log C_{ppm} = & 5.435 - 0.286 \log \frac{\omega D_{50}}{\nu} - 0.457 \log \frac{V_*}{\omega} \\ & + \left(1.799 - 0.409 \log \frac{\omega D_{50}}{\nu} - 0.314 \log \frac{V_*}{\omega} \right) \log \left(\frac{VS}{\omega} - \frac{V_{cr}S}{\omega} \right) \end{aligned} \quad (3-6)$$

The gravel equation is used for median particle sizes between 2.0 and 10.0 mm:

$$\begin{aligned} \log C_{ppm} = & 6.681 - 0.633 \log \frac{\omega D_{50}}{\nu} - 4.816 \log \frac{V_*}{\omega} \\ & + \left(2.874 - 0.305 \log \frac{\omega D_{50}}{\nu} - 0.282 \log \frac{V_*}{\omega} \right) \log \left(\frac{VS}{\omega} - \frac{V_{cr}S}{\omega} \right) \end{aligned} \quad (3-7)$$

In equations (3-6) and (3-7), C_{ppm} is sediment concentration in parts per million (ppm) by weight, ω is fall velocity of sediments (m/s), D_{50} is the median particle size, ν is the kinematic viscosity of water (m^2/s), V_* is shear velocity (m/s), V is stream velocity (m/s), V_{cr} is the critical velocity (m/s) to initiate erosion, and S is bed slope. In Yang's equations, the dimensionless critical velocity is given as follows.

$$\frac{V_{cr}}{\omega} = \frac{2.5}{\log \frac{V_* D_{50}}{v} - 0.06} + 0.66 \quad \text{for } 1.2 < \frac{V_* D_{50}}{v} < 70 \quad (3-8a)$$

$$\frac{V_{cr}}{\omega} = 2.05 \quad \text{for } \frac{V_* D_{50}}{v} \geq 70 \quad (3-8b)$$

Particle fall velocity is estimated by the settling velocity based on the Stokes Law.

$$\omega = \frac{9.81 D_{50}^2 (S_g - 1)}{18\nu} \quad (3-8c)$$

Evaluation of sub-daily erosion and sediment transport algorithms in SWAT

The SWAT sub-daily algorithms for erosion and sediment transport were evaluated with data from watershed Y-2 at the Agricultural Research Service (USDA-ARS) Grassland, Soil and Water Research Laboratory near Riesel, TX. The Riesel Watersheds, as they are commonly called, lie within the Brushy Creek watershed in Texas Blackland Prairie (Harmel et al., 2007). The Blackland Prairie is a stretch of fertile agricultural lands extending from San Antonio in the south to the Red River in the north. There are four sub-watersheds that comprise Y-2 (Figure 11). The dominant soils are Houston Black soils, which exhibit a strong potential for shrinking and swelling, and thus have a dramatic effect on rainfall-runoff relationships (Ponce, 1986; Ponce and Changanti, 1994). Dominant land use in the watershed is cropping and pasture systems (Arnold et al., 2005); therefore, this research focused on evaluating erosion and sediment transport algorithms on pervious areas.

The surface runoff and erosion at the Riesel Watersheds have been monitored by USDA-ARS for more than 70 years (Harmel et al., 2007). Sub-daily breakpoint data for rainfall, runoff, and sediment data were downloaded from the USDA website (<http://www.ars.usda.gov/spa/hydro-data>). 15 min interval data were prepared based on the breakpoint values.

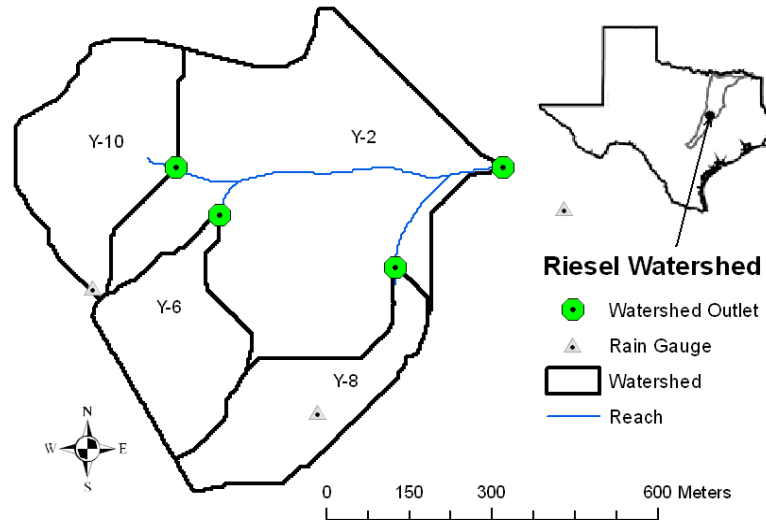


Figure 11. Experimental watersheds and rain gauges at the USDA-ARS Grassland, Soil and Water Research Laboratory near Riesel, Texas.

Flow and sediment loading at the outlet of the Y-2 watershed were calibrated to the 15 minute field data for a one year period (2001) and then validated for another one year period (2002). Infiltration and runoff were estimated by the Green and Ampt equation (King, 1999), and evapotranspiration (ET) was calculated using the Penman-Monteith model (Neitsch et al., 2005). The average annual precipitation during the 2-yr study period was 1,054 mm, and water balance components as % of precipitation determined based on calibrated model output were 34% surface runoff, 0.2% baseflow, 59% evapotranspiration, and the rest used for plant growth and increasing soil moisture content. In comparison, Allen et al. (1986) estimated that 25% of precipitation left the watershed as direct surface runoff and 11% as surface seepage (lateral subsurface return flow). Thus, a significant part of the water yield was contributed by surface runoff. The high content of expansive clay makes the soil almost impermeable when saturated and thus, only small amount of baseflow might have been generated even with excess rainfall. The rainfall-runoff relationship in the Y-2 watershed was also affected by the soil such that generated runoff was sensitive to antecedent moisture condition (Ponce, 1986; Ponce and Changanti, 1994). As the curve number is updated based on daily change in soil moisture, the response of the soil to the rainfall between storms within 24 hr could not be adequately represented by the model.

Due to the high density in data points, model performance was evaluated by comparing sub-daily, daily, and annual predicted and observed sediment yields for two 1 yr periods and for two event storms from both the calibration and validation periods. Nash and Sutcliffe efficiency (Nash and Sutcliffe, 1970) (NSE), coefficient of determination (R^2), and percent bias (PBIAS) values were calculated for statistical evaluation of model performance.

Table 5. SWAT parameters used in the sensitivity analysis

Parameter	Definition	File name	Range of values	
			Min.	Max.
CFACTOR	Cover and management factor for overland erosion	.bsn	0.001	1
CH_COV	Channel cover factor	.rte	0	1
CH_D50	Median particle diameter of channel bed (mm)	.bsn	0.001	10
CH_EROD	Channel erodibility factor	.rte	0	0.6
EROSEXPO	Exponent in the overland flow erosion equation	.bsn	1.5	3
EROS_SPL	Splash erosion coefficient	.bsn	0.9	3.1
PRF	Peak rate adjustment factor for sediment routing in the main channel	.hru	0.001	2
RILLMLT	Multiplier to USLE_K for soil susceptible to rill erosion	.bsn	0.5	2
SPCON	Linear parameter for calculating the maximum amount of sediment	.bsn	0.0001	0.001
SPEXP	Exponent parameter for calculating sediment reentrained in channel sediment routing	.bsn	1	2

Sensitivity Analysis

The erosion and sediment transport models incorporated in SWAT for sub-daily predictions are physically-based mechanistic models. Predicted output from these models depends on input parameters that represent local geophysical conditions. Sensitivity analysis was conducted to investigate the impact of input parameters to predicted sediment at 15min time interval. The sensitivity of 10 parameters related to the new erosion and sediment processes as described in Table 5 were evaluated using the Latin hypercube sampling method incorporated with One-factor-at-a-time analysis technique (LH-OAT) as described for the flow analyses.

3.3 Results and Discussion

The results of the sensitivity analysis are summarized in Table 6. The 10 parameters were ranked from 1 to 10 based on sensitivity index values for the three in-stream sediment routing methods (i.e., Bagnold, Brownlie, and Yang method). PRF and SPCON, were the most sensitive parameters when the Bagnold model was used for in-stream sediment routing. These parameters directly influence in-stream sediment calculations. Similarly, CH_D50, which is also an in-stream sediment parameter, was the most influential in the Yang model. On the other hand, CFACTOR, RILLMLT, and EROSEXPO, which are related to overland flow processes, were the most sensitive parameters in the Brownlie model.

Table 6. Sensitive sediment parameters for three routing methods as ranked by the LH-OAT method

Rank	Bagnold Model	Yang Model	Brownlie Model
1	PRF (100) ^a	CH_D50 (100)	CFACTOR (100)
2	SPCON (46.1)	CH_EROD (8.8)	RILLMLT (82.4)
3	SPEXP (13.3)	CH_COV (4.7)	EROSXPO (62.2)
4	EROSXPO (0.5)	EROSXPO (0.7)	EROS_SPL (0.04)
5	CFACTOR(0.4)	CFACTOR (0.6)	PRF (-)
6	CH_EROD (0.4)	RILLMLT (0.4)	SPCON (-)
7	CH_COV (0.3)	PRF (-)	SPEXP (-)
8	RILLMLT (0.1)	SPCON (-)	CH_COV(-)
9	EROS_SPL (-)	SPEXP (-)	CH_EROD (-)
10	CH_D50 (-)	EROS_SPL (-)	CH_D50 (-)

^a Sensitivity indices are re-scaled such that the highest sensitivity index value is set to 100

Typically, model performance is poorer for shorter time steps than for larger time steps (Moriassi et al. 2007). For example, the timing and magnitude of predicted peak flow is of great concern in subdaily flow simulation but it does not at all matter in daily or monthly runs. This observation is also found in the present analysis of sub-daily sediment modeling (Table 7). Though the sub-daily SWAT predictions were “unsatisfactory” during the calibration period (NSE = 0.49) based on the comparison of 15 min predictions and estimated measured values. It is important to note that the 15 min measured values are often in fact estimates, as many of the breakpoint data were extended to 15 min periods with no attempt to correlate flow and sediment concentration, see the flat portions of the measured sediment yields in Figure 12b. When the predictions were aggregated to a 24 hr period (daily) as are typically output by SWAT, the model performance improved to “very good” (NSE = 0.92), and the predicted sediment yield (1.46 ton/ha) was similar to the measured value (1.50 ton/ha). In fact, the sub-daily results in this case were better than produced from daily SWAT output (sediment yield = 2.89 ton/ha, NSE = 0.75). For the validation period, sub-daily SWAT predictions were “unsatisfactory” at 15 min intervals (NSE = 0.21) and when aggregated to daily values (NSE=0.16). However, daily SWAT output also produced “unsatisfactory” predictions (NSE = 0.29) for this period.

Table 7. and simulated sediment yields for annual periods and storm events

Period	SWAT (sub-daily)					SWAT (sub-daily)		SWAT	
	Observed Sediment (ton/ha)	15 min output				Aggregated to daily		Daily output	
		Sediment (ton/ha)	NSE	R ²	PBIAS (%)	Sediment (ton/ha)	NSE	Sediment (ton/ha)	NSE
Annual									
Calibration (2001)	1.50	1.46	0.49	0.37	2%	1.46	0.92	2.89	0.75
Validation (2002)	0.66	1.06	0.21	0.23	-59%	1.06	0.16	0.69	0.29
Event									
8 Mar 2001 ^a	0.10	0.21	0.28	0.80	-105%	0.21	- ^b	0.15	-
16 Dec 2001	0.56	0.45	0.59	0.61	19%	0.45	-	0.52	-
21 Oct 2002	0.04	0.05	0.57	0.70	-16%	0.05	-	0.06	-
30 Dec 2002	0.12	0.16	0.85	0.89	-36%	0.16	-	0.03	-

^a Parameter values were not calibrated for each event. Instead parameters derived from the calibration period were used unmodified.

^b NSE values are not appropriate with only one measured and predicted value for each event.

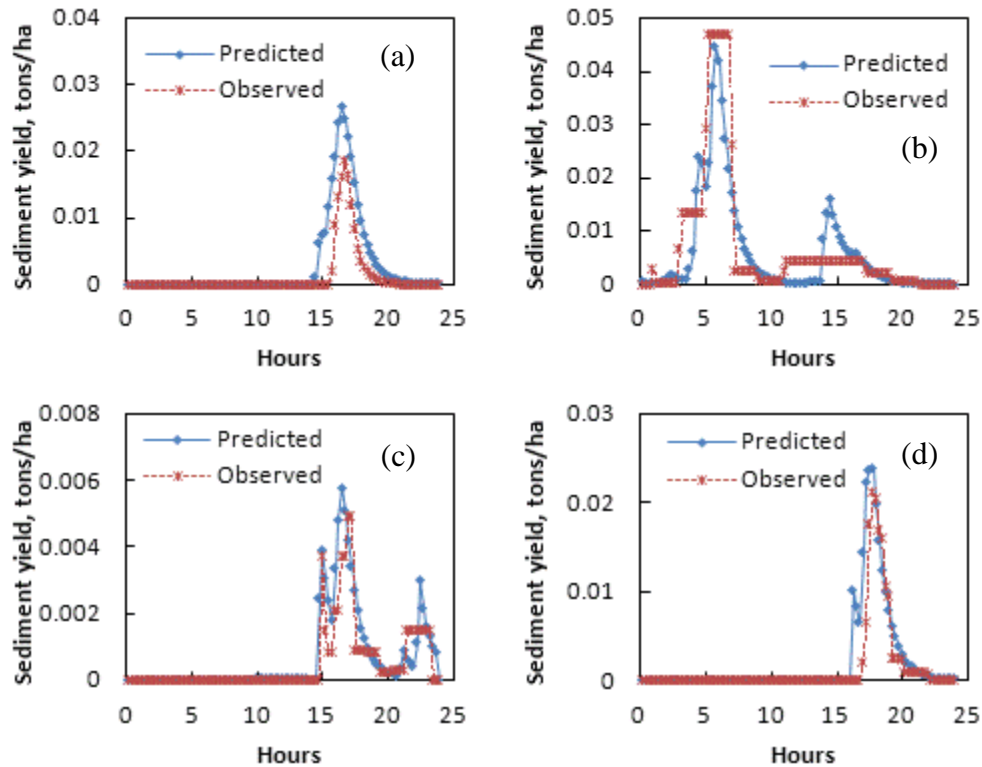


Figure 12. Calibrated sediment yield at the Y-2 outlet for events on: a) 8 Mar 2001, b) 16 Dec 2001, c) 21 Oct 2002, d) 20 Dec 2002.

For the selected storm events, the 15 min predictions from the sub-daily SWAT model ranged from “unsatisfactory” to “very good” based on NSE values; however, the timing, peak, and duration of sediment production and transport seem to have been accurately simulated (Figure 12). Even for the 8 March 2001 event, which had an “unsatisfactory” model performance rating due to a small but consistent under-prediction, sediment yield was very well represented by the sub-daily routines. In comparison, both the sub-daily SWAT results aggregated to daily and the daily SWAT predictions were reasonable in terms of the daily sediment yield, but these predictions offer no insight into the sub-daily processes that are so important in small/urban watersheds. On the other hand, as shown in Figure 13. , the simulated sediment yields for days with substantial sediment production in the 2 yr study were well predicted based on the probability of exceedance. This is important because the capability of reproducing sediment yield accurately for various storm events in the long term period is crucial for a watershed scale model. Although it was not clear in the present analysis, the differences in sediment yield for high flows may indicate a need for improvement in the sub-hourly sediment and flow routines at low flow conditions.

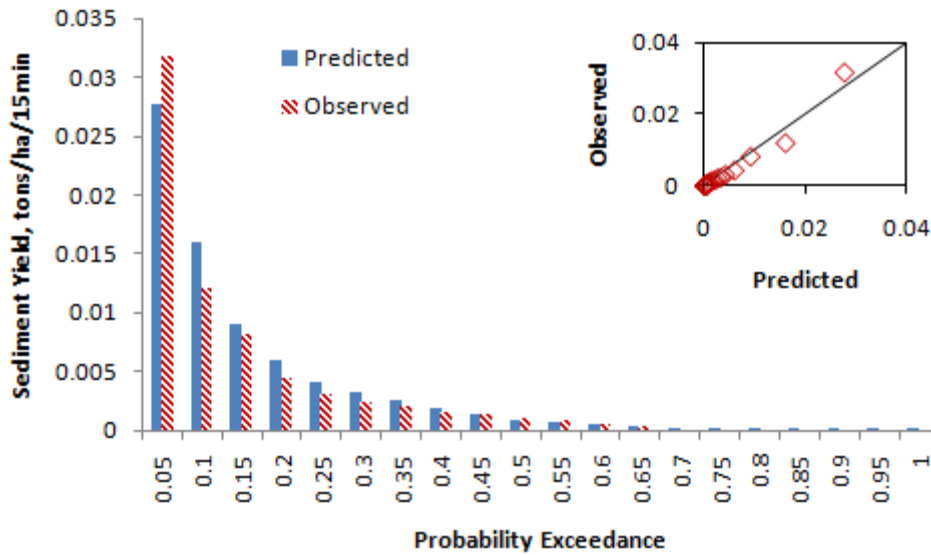


Figure 13. Exceedance probabilities for measured sediment yield data from watershed Y-2 and SWAT sub-daily predictions.

3.4 Summary and conclusion

Algorithms for representing sub-daily erosion and sediment transport processes were developed and integrated into the SWAT model. The new algorithms were modified from other watershed-scale models, which mean they were tested and validated in part before being modified for SWAT. In this new sub-daily SWAT structure, splash erosion is modeled based on the kinetic energy delivered by raindrops, and overland flow erosion is estimated by a physically-based algorithm that considers rill and interrill erosion. Options for simulating instream sediment were also added to the model specifically for simulating intermediate to small river basins. With these modified algorithms, SWAT performed well in predicting sediment loads in individual events during a long-term simulation without specific storm-by-storm calibration. Based on the results on the Riesel watershed at Y-2, it can be concluded that: (1) the new physically-based sub-daily erosion and sediment transport algorithms in SWAT may represent an important enhancement for simulations conducted at sub-daily time intervals, which are often important in projects on small/urban watersheds ; (2) in-stream parameters influence sediment output more than overland flow erosion and sediment parameters in both the Bagnold model and the Yang model, but the opposite is true in the Brownlie model; and (3) more evaluation is needed to better assess SWAT's sub-daily erosion and sediment transport predictions at various spatial and temporal scales and under other watershed conditions.

3.5 References

- Arnold J., Potter K., King K., Allen P. (2005) Estimation of soil cracking and the effect on surface runoff in a Texas Blackland Prairie watershed. *Hydrological Processes* 19:589-603.
- Bagnold R. (1977) Bed Load Transport by Natural Rivers. *Water Resources Research* 13:303-312.
- Brandt C.J. (1990) Simulation of the Size Distribution and Erosivity of Raindrops and Throughfall Drops. *Earth Surface Processes and Landforms* 15:687-698.
- Brownlie W. (1982) Prediction of flow depth and sediment discharge in open channels. Ph. D. Thesis California Inst. of Tech., Pasadena.
- Harmel R., Bonta J., Richardson C. (2007) The original USDA-ARS experimental watersheds in Texas and Ohio: Contributions from the past and visions for the future. *Transactions of the ASBAE* 50:1669-1675.
- Nash J.E., Sutcliffe J.V. (1970) River flow forecasting through conceptual models part I---A discussion of principles. *Journal of Hydrology* 10:282-290.
- Neitsch S.L., Arnold J.G., Kiniry J.R., Williams J.R. (2005) Soil and Water Assessment Tool Theoretical Documentration Grassland, soil and water research service, Temple, TX.
- Ponce V.M. (1986) DIFFUSION WAVE MODELING OF CATCHMENT DYNAMICS. *Journal of Hydraulic Engineering-Asce* 112:716-727.
- Ponce V.M., Changanti P.V. (1994) Variable-parameter Muskingum-Cunge method revisited. *Journal of Hydrology* 162:433-439. DOI: Doi: 10.1016/0022-1694(94)90241-0.
- Richardson E., Simons D., Lagasse P. (2001) River Engineering for Highway Encroachments–Highways in The River Enviroment, US Department of Transportation, Federal Highway Administration. Publication No. FHWA NHI 01-004.
- Torri D., Sfalanga M., Del Sette M. (1987) Splash Detachment: Runoff Depth and Soil Cohesion. *CATENA* 14:149-155.
- Williams J. (1975) Sediment-yield prediction with universal equation using runoff energy factor. Present and prospective technology for predicting sediment yields and sources:244-252.
- Wischmeier W. (1975) Estimating the Soil Loss Equation's Cover and Management Factor for Undisturbed Areas, USDA-ARS S-40: Present and prospective technology for predicting sediment yield and sources. Washington, USDA. pp. 118-124.
- Wischmeier W., Smith D. (1978) Predicting Rainfall Erosion Losses: A Guide to Conservation Planning Dept. of Agriculture, Science and Education Administration, pp 537.
- Yang C. (1996) Sediment Transport: Theory and Practice MCGRAW-HILL BOOK CO,(USA).

4. Urban BMPs: Sedimentation-Filtration Basins

4.1 Introduction

Sedimentation-Filtration basins are aimed at mitigating sediment bound non-point source pollution of urban creeks and rivers. It is one of the BMPs actively implemented by City of Austin in Texas to control pollution of rivers and creeks in Austin. It is composed of a sedimentation chamber hydraulically connected to a (sand) filter media. The drainage from the filter media is collected and sent to the creek/river. The BMP is typically built to receive the first half-inch of runoff from the drainage area. When the impervious cover exceeds 20 %, an additional one tenth of an inch runoff is included for every 10 % increase in impervious cover. Two different types of this BMP exist. 1. full sedimentation-filtration systems where the sedimentation chamber and filter media are separate and 2. partial systems where the sedimentation chamber is located as a part of the filter media. By-pass flow is controlled for flows exceeding the capacity via diversion structures. These BMPs are small structures typically designed for small drainage areas (a few acres). In a watershed there can be several structures. Therefore, they are modeled as distributed BMPs; this also allows the capability to simulate theoretical BMP implementation on a large scale. Algorithms are developed and integrated into Soil and Water Assessment Tool (SWAT) to simulate sedimentation-filtration systems in urban watersheds.

4.2 Water Quality Volume

City of Austin's Environmental Criteria Manual specifies design guidelines for sedimentation-filtration basins. A maximum ponding depth of 1 meter and a length to width ratio equal to 2 or larger ($L:W \geq 2$) is recommended for a typical sedimentation basin. The size of a BMP is determined based on water quality volume which is defined as the first one-half inch of runoff plus an additional one-tenth inch for each ten percent increase of gross impervious cover over twenty percent within the drainage area to the control. This can be expressed in a mathematical form as follows.

$$\text{water quality volume} = h_{wq} \times \text{total drainage area} \quad (4-1)$$

where h_{wq} is water quality depth defined by

$$h_{wq} = 0.5 + \left(\frac{\text{impervious area}}{\text{total drainage area}} - 0.2 \right) \quad (4-2)$$

For modeling purposes, these equations are useful in estimating the dimensions of the BMP structures if not provided by user and the sedimentation-filtration algorithm developed for Soil & Water Assessment Tool (SWAT) provides estimated size of the structure based on the required water quality volume (WQV) if user does not input these values.

4.3 Model configuration in SWAT

Process-based algorithms for sedimentation-filtration has been developed and integrated into SWAT model. Flow routing and sediment removal through sedimentation-filtration basins is simulated dynamically and continuously at a sub-hourly time interval as small as 1 min. Sedimentation-filtration basins are small distributed structures that can occur anywhere in the watershed. Within a watershed, the number of sedimentation-filtration basins could be hundreds or thousands depending on the size of the watershed. Therefore, for a practical purpose, sedimentation-filtration is modeled to be “distributed” in sub-watersheds, which means the model does not know the physical location of the structures in the sub-watershed. However, the user provides a percent amount of urban runoff generated in the sub-watershed that drains to each BMP structure, by specifying treated area and land uses. Therefore, the minimum knowledge that the model requires from the user is the total fraction of urban runoff treated by sedimentation-filtration basins in the sub-watershed. Each sedimentation-filtration basin may be defined individually, or several small sedimentation-filtration basins can be aggregated and modeled as one structure.

Algorithms for sedimentation basin and for filtration basin are coded separately in SWAT to allow flexible application of either full or partial type Sed-Fil. Model theory and development of algorithm are described in the following sections.

4.4 Sedimentation basin

Flow routing

A full scale sedimentation-filtration basin is comprised of a sedimentation basin serially connected to a filtration basin so that the sedimentation basin works as a pretreatment unit as well as a flow control by attenuating peak flows. The outflow from a sedimentation basin is typically controlled by orifice pipes. The maximum storage is defined by the stage of emergency spillway. Incoming stormwater bypasses to a sedimentation basin through emergency spillway if the storage of water exceeds the maximum capacity of the pond. A continuity equation is used for estimating water balance in the sedimentation basin every time step.

$$\frac{\partial V_{wtr}}{\partial t} = WQV + R - f - E - Q_{pipe} - Q_{bypass} \quad (4-3)$$

where WQV is water quality volume, R is rainfall, f is infiltration, E is evapotranspiration, Q_{pipe} is pipe flow at the outlet, and Q_{bypass} is bypass flow through spillway weir.

Sediment routing

Settling of sediment occurs if sediment concentration in the sedimentation basin exceeds a user provided equilibrium value. This model is adopted from SWAT model (Neitsch et al., 2005).

$$C_{sed,f} = (C_{sed,i} - C_{sed,eq}) \cdot \exp(-k \cdot \Delta t \cdot d_{50}) + C_{sed,eq} \quad \text{if } C_{sed,i} > C_{sed,eq} \quad (4-4a)$$

$$C_{sed,f} = C_{sed,i} \quad \text{if } C_{sed,i} \leq C_{sed,eq} \quad (4-4b)$$

where

$C_{sed,f}$ = sediment concentration in the water body at the end of the time step (mg/l)

$C_{sed,i}$ = initial sediment concentration

$C_{sed,eq}$ = equilibrium concentration

k = decay constant (1/hour)

Δt = length of the time step (hour)

d_{50} = median particle size of the inflow sediment (μm)

Assuming 99% of the 1 μm size particles settle within 25 days, k is equal to 7.667E-3. The amount of sediment (kg) transported out of the sedimentation basin during the time interval is calculated as a function of the final sedimentation concentration.

$$Sed_{out} = C_{sed,f} \cdot V_{wtr} \quad (4-5)$$

4.4 Filtration basin

A modified Green and Ampt equation is developed for unsaturated flow simulation in sand filter that takes surface ponding into account. Saturated flow is computed using Darcy's law. Surface ponding depth, soil water content, and effluent are estimated based on the mass balance equation (See Figure 14). The single isolated collector model (Yao et al., 1971) estimates TSS removal by the sand filter while clogging of filter medium due to TSS accumulation in the filter medium is simulated by relating hydraulic conductivity to volumetric deposit of TSS in the filter medium.

Mass balance

The total volume of water in the filtration basin (V_{wtr}) is estimated using a continuity equation. Stormwater runoff is the main source and through-flow and bypass flow are the main sinks. Rainfall (R) and evaporation (E) also affect the mass balance as shown in Equation 4-6.

$$\frac{\partial V_{wtr}}{\partial t} = Q_{in} + R - f - E - Q_{thru} - Q_{bypass} \quad (4-6)$$

where Q_{in} may be WQV for partial systems or outflow from sedimentation basin.

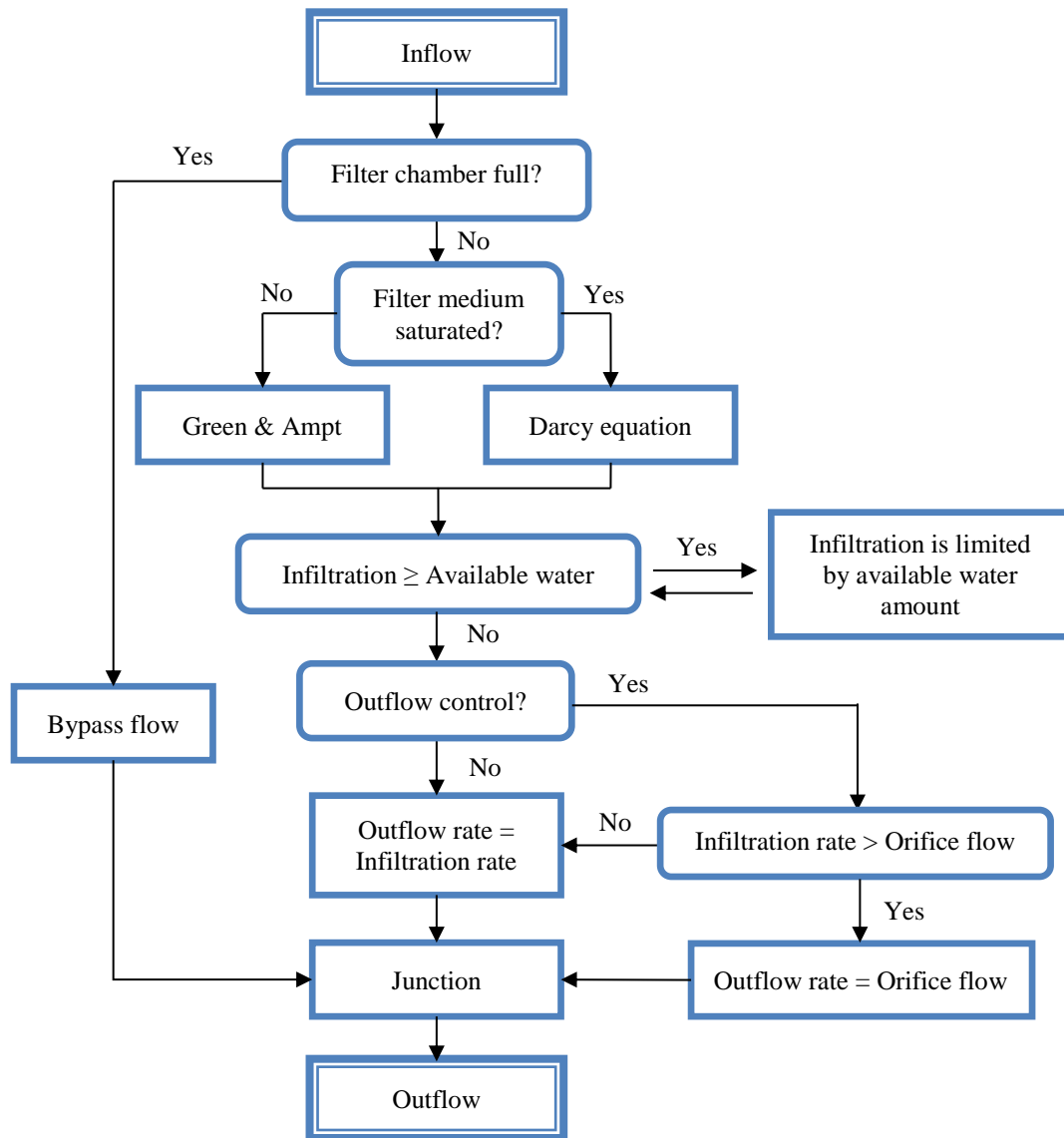


Figure 14. Schematic view of sand filter processes

Unsaturated flow

Unsaturated flow generally occurs shortly after the onset of a storm event. A series of small events may result in unsaturated flow in the filter medium as well. When a sand filter is unsaturated, capillary pressure occurring in the filter medium builds up suction head near the water front and promotes higher infiltration rate. The Green & Ampt equation is a simplified but physically based model that can be used to estimate unsaturated flow through filter medium. However, surface ponding – which may have a significant influence to the hydraulics in the filtration basin - is not considered (Chow et al., 1988). Therefore, a modified equation that counts in the surface ponding as head has been developed as follows.

Darcy's law can be used to describe the vertical flow of water through a homogeneous sand filter column. The ponding depth on the surface, length of wetted zone, and the suction head at the wetting front comprise the total head.

$$f = K \left(\frac{h + l_w + \Psi}{l_w} \right) \quad (4-7)$$

where

h = surface ponding depth

f = infiltration rate

K = hydraulic conductivity at saturation

Ψ = suction head at the wetting front

l_w = length of wetted zone, varies from >0 to filter length ($=L$)

The amount of water in the sand column increases with infiltration:

$$F = l_w \cdot \Delta\theta \quad (4-8)$$

where

F = cumulative infiltration

$\Delta\theta$ = change in water content in the sand column

This equation is valid if l_w is less than the length of the sand column and is larger than zero. Substitute l_w in eq. (4-8) into eq. (4-7), and use the relation $f=dF/dt$ to get

$$\frac{dF}{dt} = K \left(1 + \frac{(h + \Psi) \cdot \Delta\theta}{F} \right) \quad (4-9)$$

Rearrange and integrate

$$\int_{F(t-I)}^{F(t)} \left(1 - \frac{(h + \Psi) \cdot \Delta\theta}{(h + \Psi) \cdot \Delta\theta + F} \right) dF = \int_{t-I}^t K dt \quad (4-10)$$

to obtain

$$F(t) = F(t-I) + K \cdot \Delta t + (h + \Psi) \cdot \Delta\theta \cdot \ln \left(\frac{F(t) + (h + \Psi) \cdot \Delta\theta}{F(t-I) + (h + \Psi) \cdot \Delta\theta} \right) \quad (4-11)$$

Eq. (4-11) is a modified Green-Ampt equation that includes surface ponding in estimating cumulative infiltration, which can be solved numerically by successive substitution. Surface ponding promotes infiltration of water to the sand filter. As shown in Figure 15, infiltration rate can increase more than 50% when surface ponding is considered.

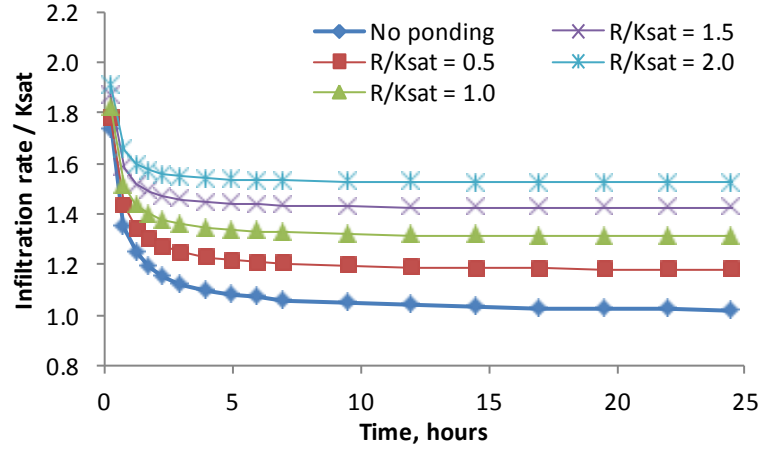


Figure 15. Infiltration rate is a function of inflow rate when ponding is considered (R = inflow rate, $K_{sat}=40\text{mm/hr}$, suction head = 50mm, porosity=0.4, $\Delta t=15\text{min}$). Baseline (no ponding) is estimated with the original Green & Ampt equation.

For large time intervals actual infiltration rate in a time step may be controlled by the rate of inflow to the filter if available inflow amount is less than the amount of potential infiltration.

$$f = q_{in} \quad \text{if } f_{GA} > q_{in} \quad (4-12a)$$

$$f = f_{GA} \quad \text{if } f_{GA} \leq q_{in} \quad (4-12b)$$

Saturated flow

Equation 4-11 is not valid for saturated condition since l_w is limited by the length of sand column. Therefore, Darcy's law applies to the saturated flow condition.

$$f = K \frac{h+L}{L} \quad (4-13)$$

where L is the thickness of sand filter. A transition from unsaturated flow to saturated flow occurs when the sand filter is fully saturated. The model evaluates the percent saturation of the filter every time step using a continuity equation and applies either modified Green & Ampt equation (Eq. 4-11) or Darcy's law (Eq. 4-13) to estimate infiltration. In Figure 16, infiltration rate decreases over time as cumulative infiltration increases, and then starts to increase semi-linearly due to saturation and linear increase in surface ponding. Finally, the infiltration rate gets steady as spillway overflow starts to occur and the ponding depth becomes constant.

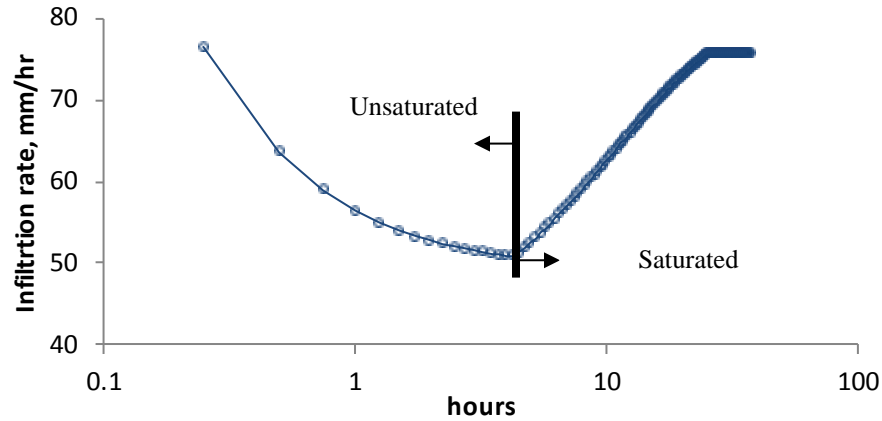


Figure 16. Infiltration rate ($K=40\text{mm/hr}$, $R=80\text{mm/hr}$) with constant inflow to the filter.

Outflow control

In practice, outflow from a sand filter is controlled by orifice pipe(s). Pipe flow is estimated by a general equation for orifice pipe flow:

$$Q_{pipe} = C_d A_{pipe} \sqrt{2gh_{head}} \quad (4-14)$$

where

Q_{pipe} = flow rate (m^3/s)

C_d = dimensionless runoff coefficient (~ 0.6)

A_{pipe} = cross sectional area of the pipe (m^2)

g = gravitational acceleration ($=9.81\text{m/s}^2$)

h_{head} = height of water table above the center of pipe (m)

The model allows outflow control from the filter with the pipe flow. If outflow is controlled by pipe flow, entire water balance is recalculated based on continuity.

Bypass flow

City of Austin's design guidelines for water quality controls require all detention units to have overflow spillway to pass high flows such as 100-year storm. A significant bypass flow over spillway weir may occur during intense flash storm events. Bypass flow rate is estimated by a general equation for horizontal rectangular weir with both ends contracted (Hwang and Houghtalen, 1996).

$$Q_{bypass} = C_{dw} \cdot (L_{weir} - 0.2h) \cdot h^{3/2} \quad (4-15)$$

where

Q_{bypass} = bypass flow rate (m^3/s)

C_{dw} = dimensionless runoff coefficient (~ 1.84 in SI units)

L_{weir} = width of weir (m)
 h = head on the weir (m)

Clogging

Hydraulic conductivity is the main variable that defines the flow characteristics of a filtration basin for which the value often remains constant in some modeling studies including the recent work by City of Austin - QUALHYMO model. However, the accumulation of solid particles near the top layer is not negligible and thus hydraulic conductivity of the filter decreases over time causing reduced treatment capacity. Urbonas (1999) suggests a power function that relates through-flow rate to cumulative TSS removed. This model provides a useful insight but limitation is that it makes a direct relationship between flow rate and TSS while hydraulic conductivity is not considered. Depth filtration theory (Mays and Hunt, 2005, Li and Davis, 2008) derived from Darcy's law relates hydraulic conductivity to volumetric specific deposit.

$$\frac{K}{K_0} = \frac{1}{(1 + \gamma\sigma_v)^2} \quad (4-16)$$

where

K = hydraulic conductivity of the filter bed

K_0 = initial hydraulic conductivity of the clean bed

γ = empirical constant

σ_v = volumetric specific deposit (the volume of deposited particles per unit filter volume)

This model has yet been tested in the Austin sand filter data, but will be adopted in the algorithm if the model gives reasonable estimates of clogging effect with varying hydraulic conductivity.

Sediment removal

The single isolated collector model by Yao et al. (1971) estimates particle removal efficiency of the filter.

$$SED_{out} = SED_{in} \left[1 - \exp \left\{ - \frac{3}{2} \left(\frac{(1 - \varepsilon)\alpha\eta}{d_c} \right) L \right\} \right] \quad (4-17)$$

where

SED_{out} = sediment mass loading to the creek from the filter (out-flow)

SED_{in} = sediment mass loading to the filter (in-flow)

ε = filter porosity

α = collision frequency (varies 0-1)

η = attachment efficiency

d_c = characteristic diameter of the filter media particles

L = filter thickness

The attachment efficiency is summation of collision efficiencies in terms of sedimentation, Brownian motion, and attractive movement occurring in the filter between TSS particles and filter media particles.

4.6 Case Study

Study area

The study area has a sand filter located in a highly urbanized area in Jollyville, Austin, TX. This site has been intensely monitored for flow, TSS and other pollutants at the inlet and outlet of the filter. The whole area of the BMP is 3176 ft² but 15% of the surface area near the inlet is concrete paved and partially separated from the filter for sedimentation of large particles. Therefore, the net surface area of the sand filter is estimated 2700ft² and urban stormwater directly drains to this BMP with no pretreatment system. A horizontal rectangular weir is placed at 4 feet height from the filter surface to allow overflow directly to the creek. The nominal depth of the filter medium is 18 inches. Through-flow drains to the creek through a 6 inch perforated under-drain pipe. The drainage area for the BMP is 2.81ha with approximately 80 feet width and 4000 feet long distance as shown in Figure 17.

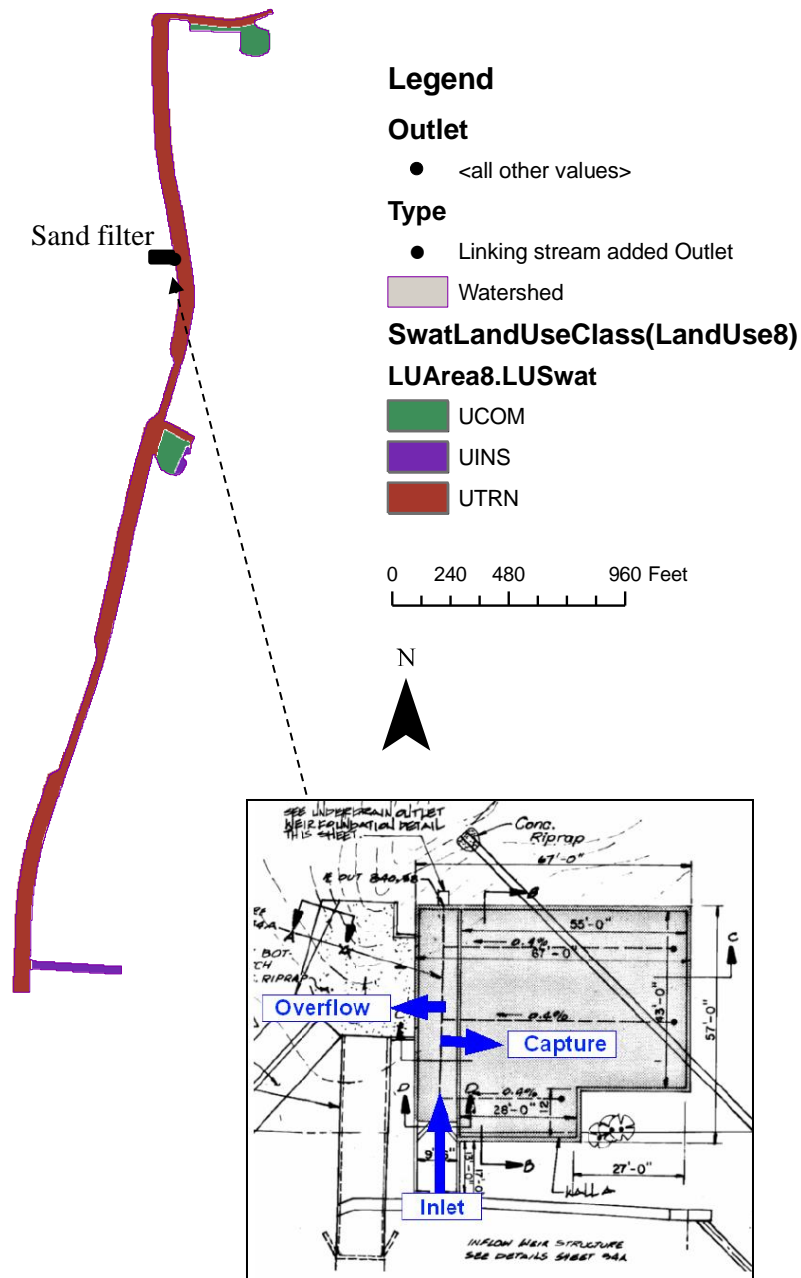


Figure 17. Jollyville Sedimentation-filtration basin and its drainage area

The entire watershed (i.e. drainage area) is urbanized and 90% of the total area is impervious that is hydraulically connected. Curb density is an important parameter to calibrate when modeling a small scale urban watershed such as Jollyville site. Because roadway comprises 84% of the drainage area and the watershed boundary follows the outside of the road, curb density and FCIMP values for A800 land type were adjusted to reasonable amounts (see Table 1).

Table 8. Property of urban land use types in the drainage area

LU Code	Description	Fraction Drainage Area (%)	FCIMP ¹ (%)	Curb Density (kg/ha)	Wash-off Coeff (mm ⁻¹)	Maximum Dirt amount (kg/curb km)	THALF ² (days)
A300	Commercial	11	64	0.28	53.67	200	1.6
A400	Office	5	47	0.4	41.29	360	3.9
A800	Transportation&Infrastructure	84	95	40.28	27.53	340	3.9

¹Fraction continuous impervious cover

²Number of days for amount of solids on impervious areas to build up from zero to half the maximum allowed

Model setup

Digital map layers for elevation, land use, and soil, were provided by City Austin. The digital elevation model (DEM) has 1ft by 1ft resolution and thus shows very detailed information of this area. One may be able to distinguish the boundary of roads from surrounding area at this resolution (see the first part of Figure 18 on the left). However, due to the fact that this area is highly urbanized with land development, ArcSWAT was not able to delineate the watershed properly so that all the flow within the watershed boundary drains to the BMP. As a way around, an artificial DEM was developed based on a desired stream lines within the boundary for the purpose of watershed delineation in ArcSWAT as shown on the right in Figure 18. The average slope between the sand filter and upstream end was retained in the new DEM for routing purpose.

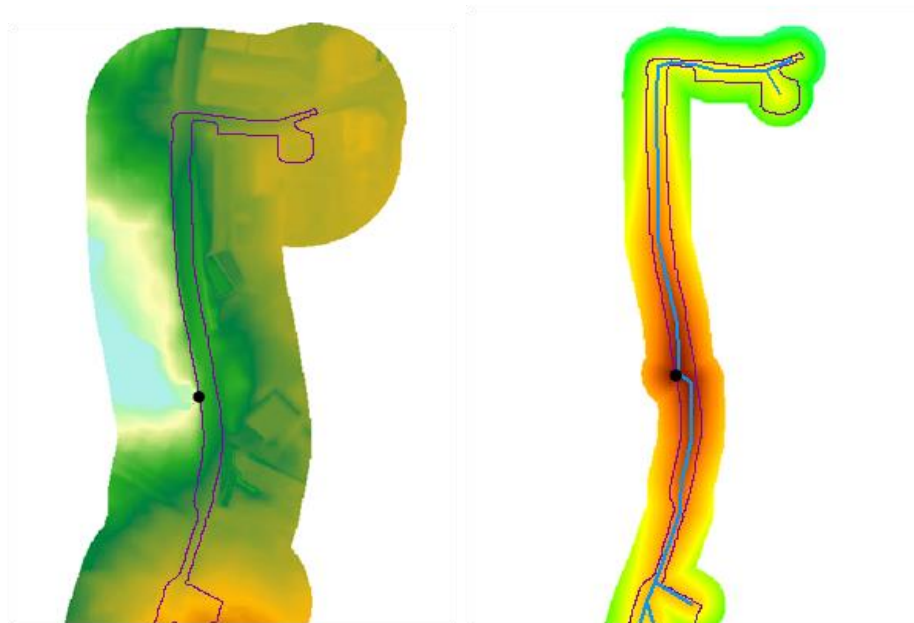


Figure 18. Original DEM for Jollyville site showing the details (left) and a hypothetical DEM generated for watershed delineation (right)

The delineated watershed model has only one subbasin with multiple HRUs for the entire watershed because SWAT algorithm for distributed BMPs is a subbasin process and is only

related to surface runoff. Therefore, subbasin outlet is identical to the watershed outlet and 100% of surface runoff generated within the watershed was assumed to enter or bypass the sand filter.

Precipitation records at 1 minute interval and daily max/min temperature were provided by City of Austin. Historical flow data recorded at 1 minute interval at the inlet and outlet of the sandfilter as well as sediment data that were grab-sampled intermittently during storm events were available for calibration.

Calibration and Validation:

The performance of the SWAT sandfilter algorithm was tested for flow routing and sediment removal at the outlet of the Jollyville sandfilter. Though the City of Austin has monitored the Jollyville sandfilter for several years, the time series field data were often not in good quality for long term calibration of the model: Total volume of outflow exceeded inflow volume in many recorded storm events. Therefore, model tests for simulating sediment clogging were not made with the long-term field data. Instead, two storm events in July 1997 were selected for the model calibration, and then a single storm event close to the calibration period (May 1997) was selected for validation.

As inflow/outflow was recorded at 1 minute interval at Jollyville site, SWAT simulation was also made at the same time interval to match the resolution of the field data. Calibration and validation were manually conducted by changing selected SWAT parameters including hydraulic conductivity of filter media, curb density, filter attachment efficiency, and the median particle diameter of sediment particles. Predicted outflow made excellent fit to the field data in both calibration and validation periods (see Figure 18). The model performance evaluation shows $R^2 = 0.92$ and Nash & Sutcliffe Efficiency (NSE) = 0.9 for the calibration period, and $R^2 = 0.94$ and NSE = 0.93 for the validation period. Overall predicted hydrograph for the through-flow matched well with observed flow in terms of timing, duration, and peak flow. Note that the predicted onset of the second storm at around 6 AM matched well and recession tails were also well predicted.

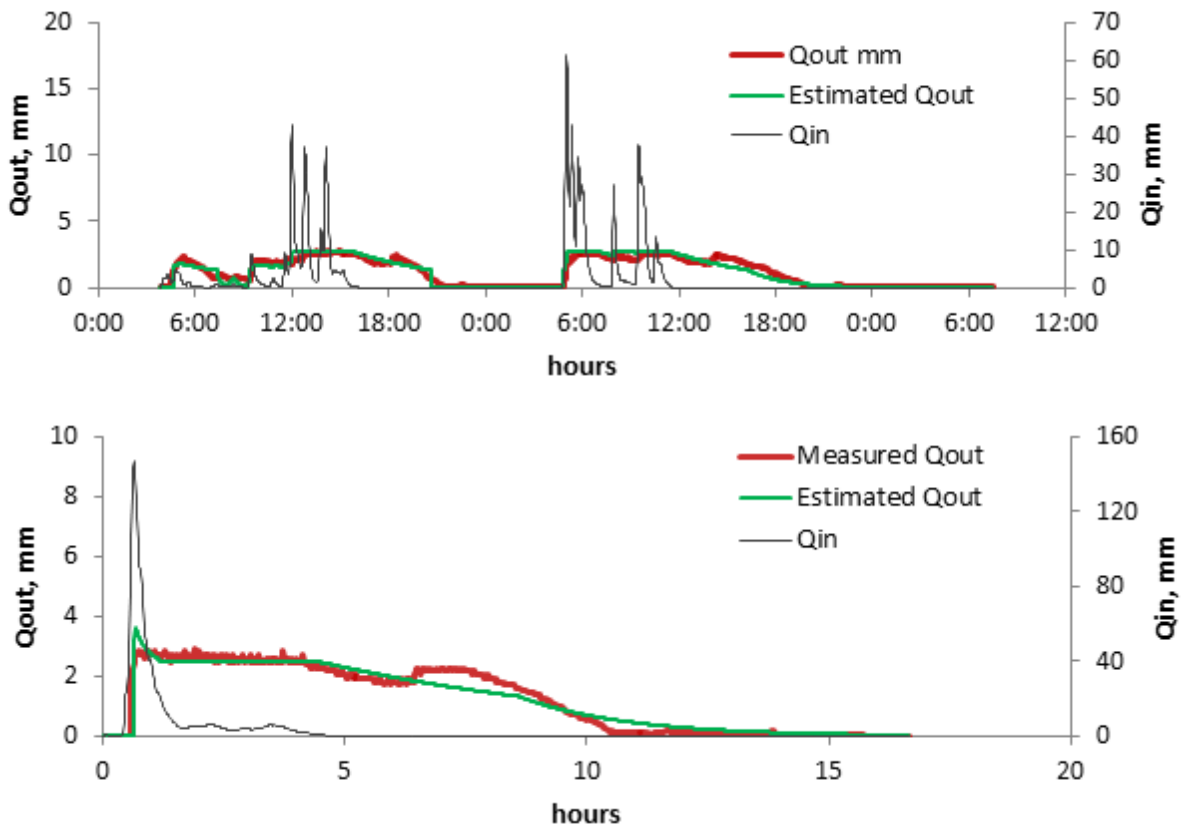


Figure 19. Through-flow at the outlet during the calibration period (top, multiple storm events on or after April 25 1997) and validation period (bottom, single storm event on May 09 1997)

Calibration of sediment was conducted at the outlet by fitting the prediction to the field data. Measured inflow sediment concentration was used as sediment input instead of letting SWAT simulate sediment inflow to the sandfilter. The use of inlet field data as input to the model allowed reducing uncertainties in the calculated outflow sediment for assessing the BMP algorithms accurately. Grab sample sediment data (<10 data points per storm event) at the inlet were linearly interpolated for each time step, and then used for predicting outflow sediment concentration.

The physically-based sediment removal algorithm showed marginal performance for the storm events during the calibration period with $R^2=0.21$ and $NSE=0.03$. The hikes in sediment pollutograph during storm events were well predicted, but overall calibration efficiency was unsatisfactory during the calibration period. Considering the high concentration at the inlet varying from 60 to 200 mg/l, the outflow sediment was over 99% treated and the temporally varying within less than 1 mg/l. Measured effluent concentrations of sediment during the validation period was observed as almost flat around 1mg/l for the entire duration of the storm event, while predicted sediment effluent profile showed a sharp decrease during the short and flashy storm event followed by a constant release of sediment with less than 0.5mg/l concentration. The statistical efficiencies were measured at $R^2 = 0$ and $NSE = -49$. Even though

these statistical measures do not interpret the performance of the model positively, it is clear that the model picks up the timing and magnitude of the peak outflow concentration very well on multiple storm events during the calibration period and overall predicted TSS concentration maintains at the same order of magnitude as observed values.

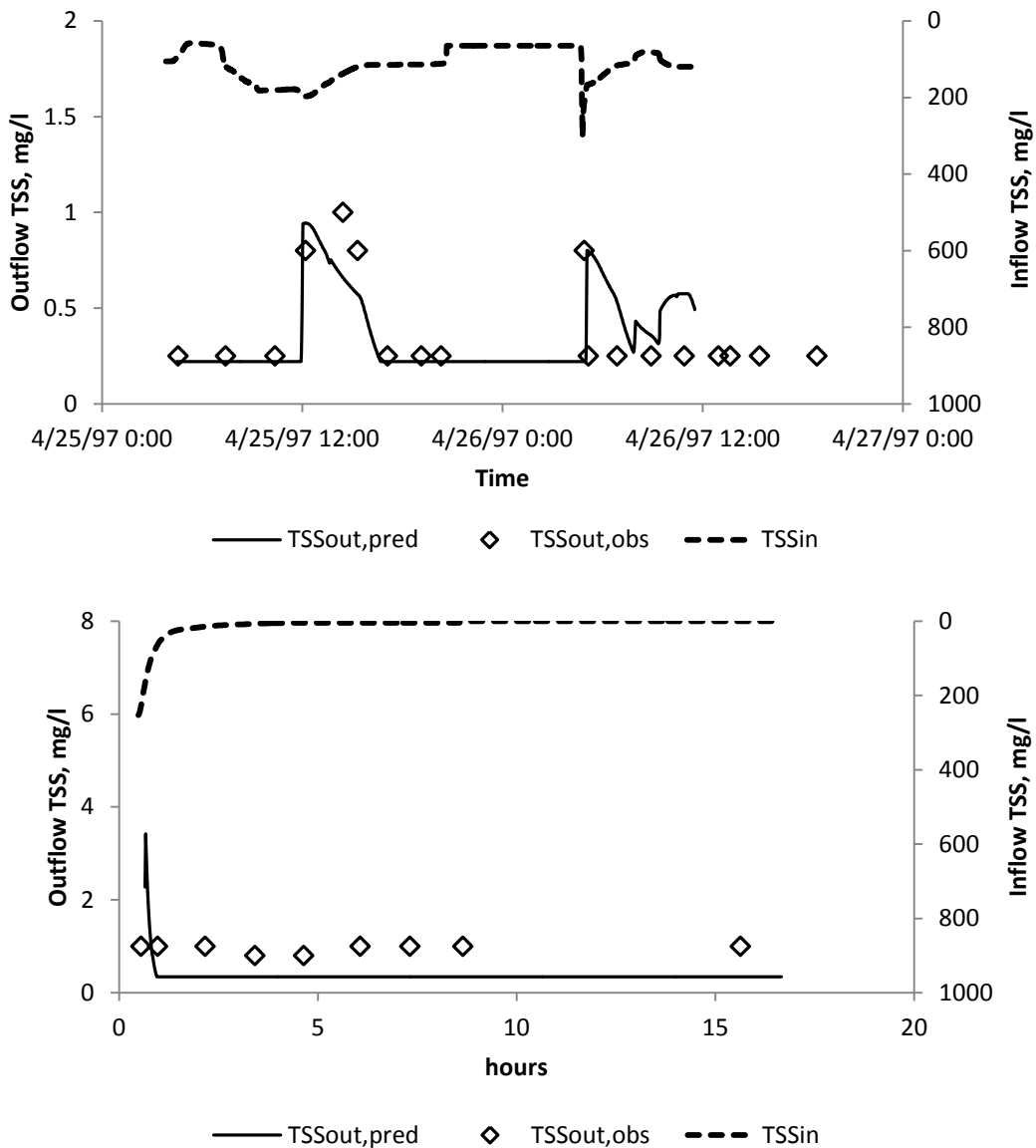


Figure 20. Sediment concentration at the outlet during the calibration period (top) and validation period (bottom, single storm event on May 09 1997)

Traditionally, the treatment efficiency of pollutants by BMPs is measured by comparing the substrate concentration before and after passing the system. Event mean concentration (EMC) is often used to calculate the removal efficiency.

$$\text{Treatment Efficiency} = \left(1 - \frac{EMC_{outlet}}{EMC_{inlet}}\right) \times 100 \quad (4-17)$$

The sediment treatment efficiency of the Jollyville sandfilter, if calculated using the traditional method, is estimated 99.7% for the calibration period and 99.3% for the validation period. The short and intense pattern of the storm during the validation period may have contributed to the slightly lower removal efficiency compared to the calibration period.

Meanwhile, the detailed water balance components available with the proposed SWAT sandfilter algorithm offer a different approach in which the removal efficiency may be considered (see Figure 20). The removal efficiency is Instead of calculating the treatment efficiency, the total mass of sediment through filter media, overflow weir, and removed by the filter was used to calculate the actual removal of sediment by the sandfilter. For estimating the removal efficiency, sediment that bypassed the filter was also counted in the calculation such that the removal efficiency is simply the ratio of what is deposited within the filter media (filtered) and what came in to the system (inflow). The sediment removal process accounts for trapping the first flush. However, subsequent inflow that tops over the bypass weir does not flow through the filter but directly enters the creek. Therefore, the removal efficiency is estimated at 45% for the storm event used in this case study. The TSS treatment efficiency may be estimated above 90% if the calculation was based on the ratio of inflow TSS concentration and through-flow TSS concentration. The decrease was mostly due to the large volume of bypass flow (>60% of total flow) and sediment in it during the test periods. The total sediment came in was estimated 248kg, which made deposit of 110kg and 137kg of bypass while only 0.33kg made through-flow. For small storms where all the flow is treated, the removal and treatment efficiencies are the same. This is why it is important for monitoring to include storms representative of the climate. Theoretically, the deposited sediment has built 0.4mm thick layer of particles in the filter media during the calibration period (assuming sediment density=1.6kg/cm³ and porosity=0.4), which seems to be a reasonable amount for two storm events.

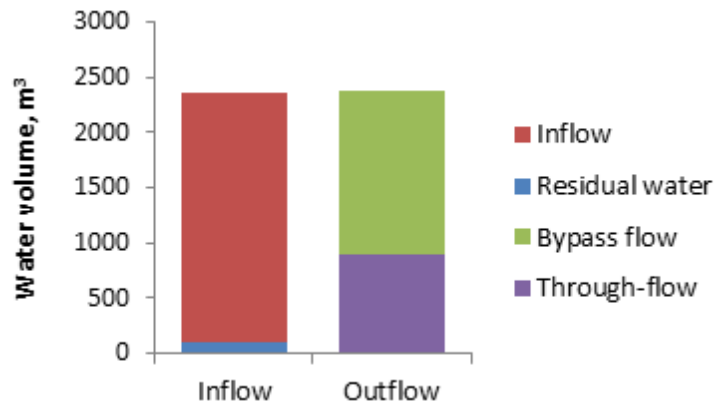


Figure 21. Water balance components during the calibration period

A long term analysis is required to further test variable K_{sat} as well as to validate calibrated parameters. It is also of interest to evaluate model performance (build up/wash off models) on predicting inflow TSS concentration over long period. The model will be useful to estimate loadings of environmental stressors to the streams in urbanized areas at large scale where conservation practices are in operation.

4.7 References

- Hwang, N., Houghtalen, R. and Akan, A., 2009. Fundamentals of hydraulic engineering systems. Prentice Hall.
- Li, H. and Davis, A., 2008. Urban particle capture in bioretention media. II: Theory and model development. *Journal of Environmental Engineering*, 134: 419.
- Mays, D. and Hunt, J., 2005. Hydrodynamic aspects of particle clogging in porous media. *Environ. Sci. Technol*, 39(2): 577-584.
- Neitsch, S.L., Arnold, J.G., Kiniry, J.R. and Williams, J.R., 2005. Soil and Water Assessment Tool Theoretical Documentration. Grassland, soil and water research service, Temple, TX.
- Urbonas, B.R., 1999. Design of a sand filter for stormwater quality enhancement. *Water Environment Research*, 71(1): 102-113.
- Yao, K., Habibian, M. and O'Melia, C., 1971. Water and waste water filtration. Concepts and applications. *Environmental Science & Technology*, 5(11): 1105-1112.

5. Urban BMPs: Retention-Irrigation Basins

5.1 Introduction

Retention-Irrigation (RI) Systems are one of the innovative urban BMPs actively implemented by the City of Austin (COA), Texas. As the name implies, a RI system is composed of a retention pond and an irrigation system. The irrigation system is comprised of a wet well, pump(s), intake riser, distribution pipes, and sprinklers. The retention pond retains stormwater runoff generated from urban areas for not more than 72 hours after the cessation of rainfall. Typically, a retention pond has no outlet because the water collected in the basin is used for irrigating vegetated areas in the vicinity. However by-pass flow is controlled for up to a 100 year storm via diversion structures. Other than water pumping for irrigation, the retention basin loses water by evaporation from the water surface and seepage loss through the bed. In the case of City of Austin, irrigation starts 12 hours after the end of a rain event. The collected water must be emptied within 72 hours since the last rainfall. An algorithm is developed and integrated into Soil and Water Assessment Tool (SWAT) to simulate RI systems in urban watersheds. This study is a part of the development of modeling tools to simulate urban stormwater BMPs with a sub-daily version of SWAT model.

5.2 Methods

Model configuration

The RI system is a distributed BMP that can occur anywhere in a sub-basin except on the stream. These systems take the stormwater drained from a portion of urban lands within a sub-basin, as specified by the user, and the location of individual systems is unknown within the sub-basin. The only source of water to a retention pond other than the direct rainfall falling on the pond is the runoff generated from its urban drainage area. The integrated SWAT-RI model allows the simulation of multiple RI systems in one subbasin and the user can provide the detailed physical characteristics for each RI system. In case the pond dimensions are not known, the SWAT-RI model can automatically estimate the basin's size based on the water quality volume as specified in COA's *Design Guidelines for Water Quality Controls*. The option for automatic calculation is especially useful if the model is used for the purpose of designing RI systems or implementing numerous hypothetical systems for a future scenario.

Specific land cover types that do not drain stormwater to the retention pond may be excluded from the drainage area. Similarly, any land cover type can be excluded from irrigation. The user has a lot of flexibility in selecting modeling options. Nevertheless, individual RI systems as distributed BMPs may not be regarded as fully physically-based systems. Each RI system is simulated individually; however, the inflow to the retention basins is proportioned (on sub-basin area) based on the drainage area of each RI system. For example, the first RI system listed in the RI input file in subbasin 1 takes 50% of urban runoff generated in the subbasin, while the second system takes 20% if the user specifies 0.5 and 0.2 as the fraction of runoff

going to each system, respectively. Then the total amount of water available for irrigation is calculated for the entire subbasin by aggregating the pumping rates from individual basins. Actual irrigation amount for each HRU is allocated in accordance with the areal proportion of the HRU over the entire irrigable area in the subbasin.

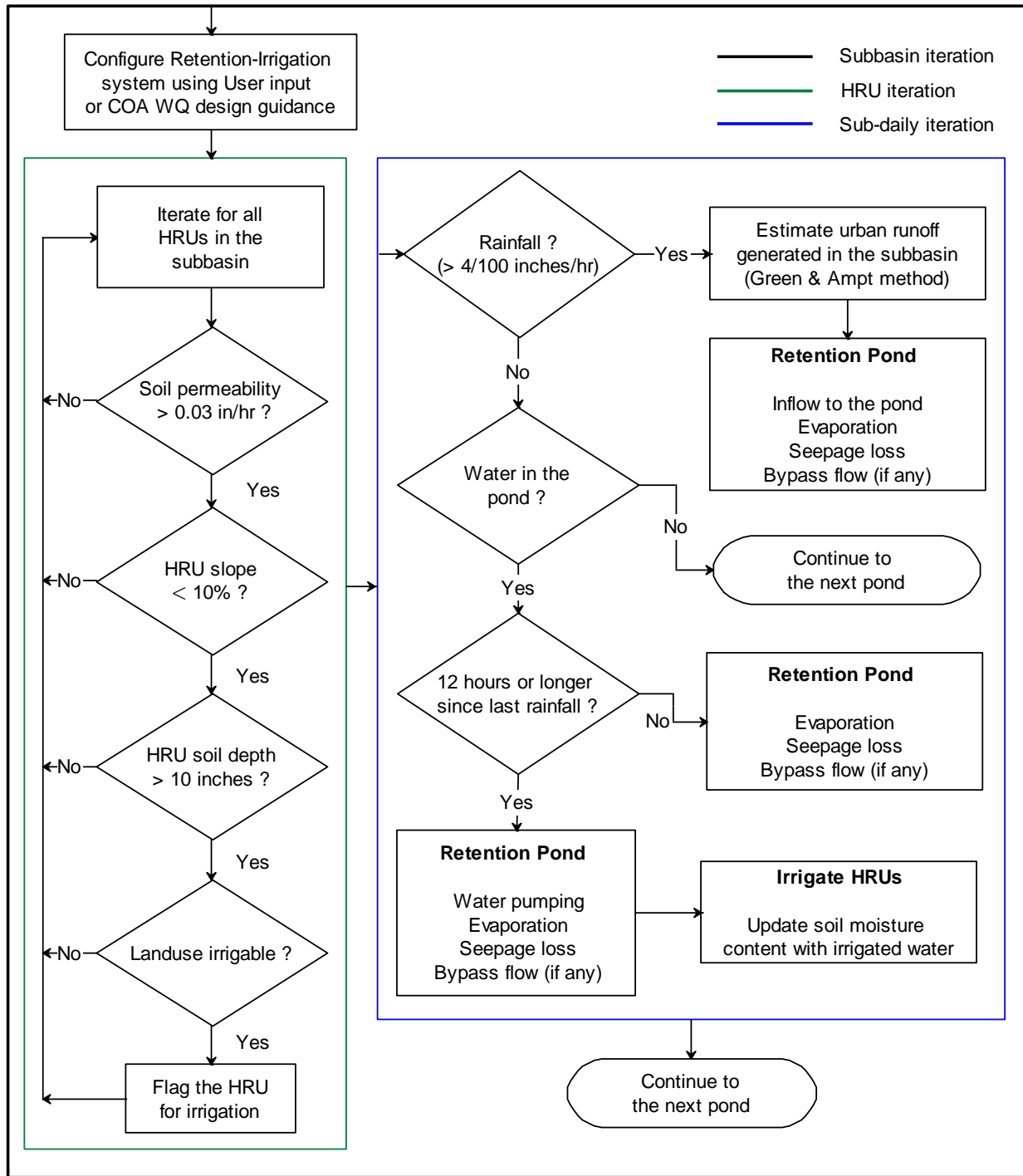


Figure 22. Flow chart of the retention-irrigation system in SWAT

The SWAT-RI module adopted some technical constraints regarding the operation of RI systems from COA's stormwater design manual (Chapter 1.6.7). These constraints include:

1. The minimum soil permeability for irrigation is 0.03 inches/hour
2. Irrigation must not occur on land with slopes greater than 10%
3. The retention pond must be emptied by pumping within 72-hours after a rain event ends.
4. Irrigation must begin no sooner than 12 hours after the end of a rainfall event
5. Retention basins are designed to capture and hold the water quality volume routed to them via diversion structures
6. Water quality volume is calculated based on COA's *Design Guidelines for Water Quality Controls* (Chapter 1.6.2)

Retention Basin

Major factors that influence the water balance in a retention basin are the inflow of urban runoff and the consumption of retained water for irrigation. The volume change in the basin is updated every time step based on the following water balance equation:

$$\left[\frac{dV_{w,i}}{dt} \right]_k = [Q_{in,i} - Q_{bypass,i} + (R_i - E_i - T_i) \cdot A_p - V_{p,i}]_k \quad (5-1)$$

where k stands for RI system ID, $V_{w,i}$ is the volume of water in the pond at time i , Q_{in} is the inflow rate, Q_{bypass} is by-pass flow rate through the diversion structure, R is rainfall, E is actual evaporation from the pond surface, T is seepage loss through the bed, A_p is the surface area of the basin, and V_p is the volume of water pumped for irrigation.

Potential evapotranspiration is estimated using Priestley-Taylor method, Penman-Monteith method, or Hargreaves method available in SWAT. Actual evaporation is then calculated based on the potential evaporation and a user entered input parameter.

$$E_i = \phi \cdot PET_i \cdot A_p \quad (5-2)$$

where ϕ is a user-defined evaporation coefficient (a calibration parameter) varying from 0 to 1, PET is the potential evaporation (mm) during the time step i . SWAT estimates PET on a daily basis. Therefore, the daily amount is evenly divided for each time interval to compute the actual evaporation. Seepage loss is a function of saturated hydraulic conductivity (K_{sat}) of the basin's bed material.

$$T_i = K_{sat} \cdot A_p \quad (5-3)$$

Other constraints include 1) no irrigation until 12 hours since the last rainfall, 2) inflow by-passes if the retention pond is full, and 3) no evaporation or seepage loss occurs if the basin is empty.

Irrigation

In practice, the water pumped from the retention basin is irrigated through sprinklers that have full or partial circle rotor pop-up heads. Irrigation is stipulated by the permeability, soil depth and slope constraints. Therefore, theoretically, there should not be any runoff caused by the irrigation. To ensure this in the model, the above-mention constraints were imposed on each irrigable HRU. In addition, irrigated water is first added to the soil moisture of the first soil layer, and subsequently to the bottom layers. The amount of irrigation water for a HRU is calculated by

$$V_{irr,i,j} = \sum_k V_{p,i,k} \cdot \left[\frac{A_j}{\sum_j A_j} \right] \quad (5-4)$$

where V_{irr} is the volume of water irrigated on j^{th} HRU at i^{th} time step, A_j is the pervious area of the j^{th} HRU. The bracketed term represents the fractional area of j^{th} HRU in the subbasin.

5.3 Case study

Study area

There is no monitored data for RI systems for Austin watersheds that can be used for validating the SWAT-RI algorithm. Therefore, the SWAT-RI model was tested by simulating artificial RI systems in the Lost Creek Golf Course (LGA) watershed which was previously used for testing the sub-hourly rainfall-runoff processes developed as a part of this study. Located in Austin, Texas, the LGA watershed is a small (1.94 Km²) and mostly undeveloped watershed that has low density residential areas in several subbasins.

A Digital Elevation Model (DEM) with 0.3 meter (1 foot) resolution was prepared by City of Austin for watershed delineation. Soil data was obtained from Natural Resources Conservation Service (NRCS) Soil SURvey GeOgraphic (SSURGO) database. A land cover map of the study area for the year 2003 was prepared by City of Austin through aerial survey. Rainfall data at 1 minute interval recorded at a weather station near the watershed outlet was collected,

and then aggregated to 15 minute interval. The watershed was divided into 4 subbasins based on the delineated stream network, and 36 HRUs based on land use, soil and slope combinations. The dominant soils are fine textured (proportion of clay+silt > 65 %) shallow soils underlain by karstic rocks. Most of the soils are classified as hydrologic soil groups C and D. The dominant land cover is undeveloped (70 %), which includes small residential structures and roads. Golf course/pasture (18 %) and residential (12 %) are other dominant land covers in the watershed. The main channel in the LGA watershed is highly ephemeral, having no stream flow for more than 70% - 80% of time during the test period.

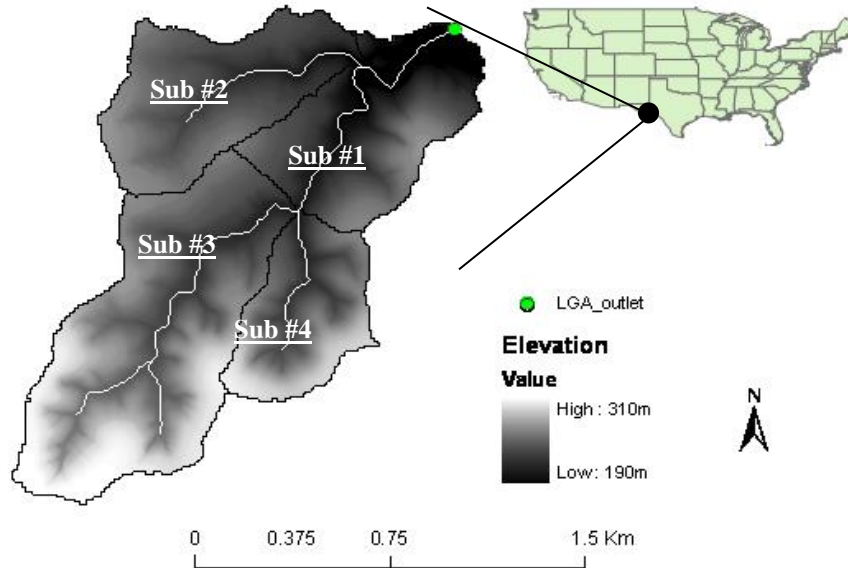


Figure 23. LGA watershed

Model setup

Subbasin 1 of the LGA watershed has 5.9 hectares urban residential areas contributing to runoff, which accounts for 14% of the total subbasin area (43.2 hectares). The ideal size of a retention basin was estimated as 655 m³ based on the COA-water quality volume guidelines. With this basic information, two scenarios were modeled for a hypothetical RI system in Subbasin 1. The two scenarios are: 1) a retention basin of 500m³ of the total volume (RI-500) and 2) a RI system with 1000m³ (RI-1000). Base-line scenario was made for no RI system. Pond depth was assumed 1.0 m for all scenarios. The hydraulic conductivity of the basin bed was assumed as 2.5 mm/hr and the actual evaporation coefficient was 0.6. The draw-down time was 72 hours after the last rainfall. The land cover types that do not typically drain to urban BMPs were excluded from the contributing land covers to the retention basin. These land cover types include Large Lot Single Family (A160), Mining (A560), Landfill/Salvage (A570), Cemetery (A670), Parks and Recreation (A710), Golf Course (A720), Camp Grounds (A730), Protected Open Space (A750), Undeveloped (A900), Agriculture (A910), and Water (A940). Several HRUs in Subbasin 1 were classified as ‘Undeveloped’ and thus excluded from the drainage area of the

retention basin. The model allows users to exclude any urban land use types from the areas that are irrigated by the RI system. However, no land cover types were excluded in this case study. A subdaily SWAT simulation ($\Delta t=15\text{min}$) was conducted for 3 years (2002-2004) and a detailed analysis was made for the year 2004. The sub-hourly flow calibration parameters for this watershed which were previously determined were used in this model.

Results

With the RI systems simulated for Subbasin 1, the total annual cumulative runoff that reached the channel in 2004 decreased by 40% with RI-500 and by 60% with RI-1000 (Figure 24). The surface runoffs for the two scenarios represent cumulative bypass flow from the basin as the retention basins do not have flow outlets. From the two scenarios on retention irrigation, it appears that only a few floods resulted in flow bypassing the RI system. Note that the urban runoff presented in Figure 24 accounts for approximately one third of the total surface runoff (not plotted in the graph) generated from the subbasin.

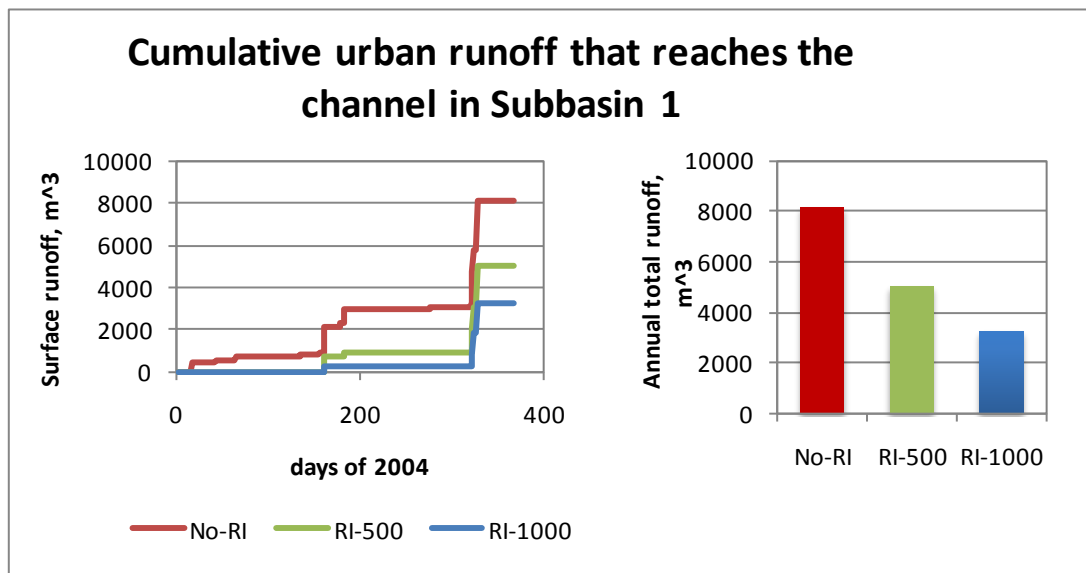


Figure 24. Influences of the two simulated RI systems are apparent in the amount of runoffs that actually reach the channel

The retention basin is filled with stormwater during wet weather conditions, and then the retained water is pumped for irrigation after 12 hours to empty the basin in less than 72 hours. Two flooding events are presented in Figure 25 for a demonstration of the dynamic response of the retention basin. The first storm event that occurred on day 161 generated a large amount of urban runoff that exceeded the maximum capacity of both RI-500 and RI-100 systems and the water volume retained in the pond hit the maximum capacity in both scenarios. This storm event

is highlighted in a box and shown in detail on the right in Figure 25. Once the water level hits the maximum capacity, any additional inflow bypasses through a diversion structure to prevent from flooding over the bank. Therefore, the retained water volume does not exceed the maximum capacity of the basin. The slow decrease in the retained water shown on the right side in Figure 25 during the first 12 hours since the last rainfall represents losses by evaporation and seepage loss. The down slope gets steeper as irrigation begins after 12 hours. The retention basin was emptied within 72 hours as scheduled.

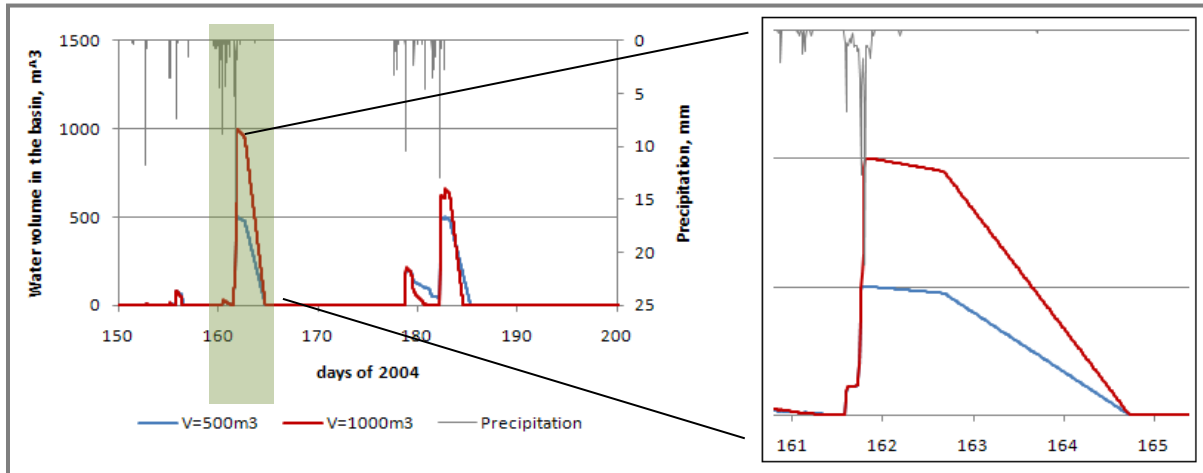


Figure 25. Profile of water volume in the retention pond

The pumping rate of RI-500 was estimated as $2.1 \text{ m}^3/15\text{min}$. This rate is calculated such that the basin fully filled with water is emptied in 72 hours with initial 12 hours no-pumping ($500\text{m}^3 / (60\text{hours} * 4\text{time-steps/hr} * 15\text{min/time-step}) = 2.1\text{m}^3/15\text{min}$). Similarly, the pumping rate was $4.2 \text{ m}^3/15\text{min}$ for RI-1000, twice of RI-500 system as the basin volume is doubled. About 56% of total inflow bypassed RI-500 system while 34% bypassed RI-1000 system. The ratio of irrigated water over the volume of retention basin was 5 for RI-500 and 3.8 for RI-1000 which implies that RI-500 system was more efficient than RI-1000 system in terms of utilizing more stormwater for irrigation. This is mainly because more transmission losses are associated with a bigger RI system ($2,379\text{m}^3$ for RI-1000 vs. $1,406 \text{ m}^3$ for RI-500). Therefore, it appears that the size of the retention basin is critical in controlling high floods, but the pond surface area and bed lining that affect transmission losses are more important than the pond size when it comes to utilizing stormwater for irrigation.

Table 9. Annual water budget for retention ponds

Scenarios	Basin volume (m^3)	Inflow+Direct rainfall (m^3)	Bypass flow (m^3)	Irrigated water (m^3)	Transmission losses ¹ (m^3)	Pumping rate ($\text{m}^3/15\text{min}$)
-----------	-------------------------------	---	------------------------------	----------------------------------	---	--

RI-500	500	8,913	4,998	2,509	1,406	2.1
RI-1000	1,000	9,472	3,247	3,846	2,379	4.2

¹ Transmission losses include evaporation and seepage loss

5.4 Conclusion

A retention-irrigation system algorithm was developed and integrated in SWAT model as a part of the effort to develop urban BMP modeling tools in SWAT. The integrated algorithm was tested with a case study using LGA watershed in Austin, Texas. For LGA there is no monitored data for RI systems. However, two different hypothetical RI systems that differ in the retention capacity were modeled and the results were analyzed. From the results it can be concluded that retention irrigation systems capture an appreciable amount of urban runoff and therefore mitigate flood peaks in urban creeks. The model's functionality and the simulated results were analyzed in several different aspects to check the algorithm for possible duplication, programming errors, or other bugs in the code, none were found to date.

6. Urban BMPs: Detention Ponds

6.1 Introduction

A detention basin is a stormwater BMP aimed to protect against flooding. It uses a controlled outflow structure to limit the outflow for large volumes of inflow. That is why they are also referred to as “holding pond” or dry detention pond. The outflow structure can be a weir or orifice depending on the need. Detention ponds are typically built across creeks or rivers (on-line structure) near new land development projects to mitigate flooding and subsequent erosion as a result of that new development. The outflow from detention pond is passed to the same river or creek from where it received the inflow. Sometimes they are built primarily to control extreme events such as a 100 year storm event. They are typically designed to empty within 6 to 12 hours after the storm. Detention ponds are widely used in many parts of the country (especially Texas and California) to mitigate flood peaks and magnitude. An algorithm is developed and integrated into the SWAT model to simulate detention pond.

6.2 Methods

Model Configuration

A detention pond is an online structure. There is no exclusion of specific land cover for runoff to the pond, it drains water from all upstream areas. Therefore, in terms of configuration it is analogous to a reservoir. The detention pond can be configured to become operational in the middle of a simulation period (e.g. in a simulation of 1981-2000 we can have detention pond from 1995) to reflect construction dates. The user can enter physical characteristics of the pond or, if not, the algorithm developed will use model default values based on City of Austin Environmental Criteria manual. The pond can receive direct precipitation, seep water through the bed and evaporate water from its surface. Two methods are available for computation of outflow namely 1. a semi-parabolic wedge equation for computation of water back-up and outflow and 2. a stage-discharge relationship (user entered). Apart from this user-entered outflow data can also be read into the model. Presently rectangular weir and orifice are included for outlet structures (Figure 26). The outlet can be in multiple stages (vertically) for control of different storm events. More details on the modeling of detention pond are given below.

A detention pond is a controlled release structure. Therefore, for a large volume of water inflow there will be back-up on the upstream side. If we compute, the shape and size of water backup, we can compute the water balance at any time step given the inflow. The inflow will be computed by the model depending on the contributing drainage area. The water backup can be

assumed to be a semi parabolic wedge or trough (Figure 26). The steps in computation of volume and surface area are as follows.



(a) Detention Pond-Type 1 with stepped rectangular weir for flow control



(b) Detention Pond-Type 2 with multi-stage circular weir for flow control

Figure 26. A regional detention pond in Austin

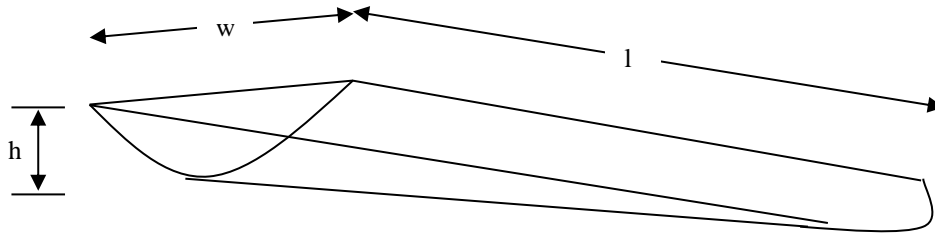


Figure 27. Parabolic Wedge (Shape of water backup)

Assumption: Water backup behind the detention pond weir will have a parabolic wedge shape.

Volume of parabolic wedge is

$$V = \frac{h \times w \times l}{3} \quad (6-1)$$

where, V is volume of parabolic wedge (volume of water back up),

l is length of water backup , d is depth and w is width

$$S = \frac{h}{l} \quad (6-2)$$

where, S is slope of the creek

User enters a value for length width ratio (l/w)

$$R = \frac{l}{w} \quad (6-3)$$

where, R is the ratio of length to width of water back up

substituting equations (6-2) and (6-3) in equation (6-1) we have,

$$V = \frac{h^3}{3 \times R \times S^2} \quad (6-4)$$

or

$$h = \sqrt[3]{3 \times R \times V \times S^2} \quad (6-5)$$

once l is known, w and other required parameters can be computed from the above set of equations

Surface Area Computation

Seepage surface area (see Figure 27) = (wetted perimeter of parabolic channel x channel length)/2

$$SSA = \frac{P \times l}{2} \quad (6-6)$$

where, SA is seepage surface area

$$P = \left(w + \frac{8 \times h^2}{3 \times w} \right) \quad (6-7)$$

Substituting 6-3 and 6-7 in equation 6-6, we have

$$SSA = \left(\frac{l}{R} + \frac{4 \times R \times h^2}{3} \right) \quad (6-8)$$

Evaporative surface area (ESA) = Area of parabola with channel length (l) as height and water backup width as width (w)

$$ESA = \frac{2 \times w \times l}{3} \quad (6-9)$$

Substituting 6-3 in equation 6-9, we have

$$ESA = \frac{2 \times l^2}{3 \times R} \quad (6-10)$$

Stage-Discharge relationship

Apart from the physically based algorithm developed for routing flow through detention pond, stage-discharge relationship can also be used. It is provided as one of the options to the users. For using stage-discharge method, the users are expected to provide the relationship between inflow and outflow of the detention pond in question. The relationship can be linear (described by a coefficient and an intercept), logarithmic (a coefficient and an intercept), polynomial (one or more depending on the degree of polynomial and an intercept [e.g. two coefficients and an intercept are required for a second degree polynomial]), exponential (a coefficient and an exponent) and power (a coefficient and an exponent). The users are expected to use the relationship that most closely fits the outflow hydrograph for a given inflow

hydrograph for the study area. Some more information on the stage-discharge relationships are provided in Table 16.

Table 10. Annual water budget for retention ponds

Relationship	Form	Expected data from the users		
		Coefficient	Intercept	Exponent
Linear	$Y=AX+B$	A	B	
Logarithmic	$Y=A \ln(X)+B$	A	B	
Exponential	$A e^{BX}$	A		B
Polynomial	$Y=AX^2+BX+C$	A,B	C	
Power	$Y=A X^B$	A		B

Y=Outflow from the detention pond

X=Inflow to the detention pond

Sequence of calculations

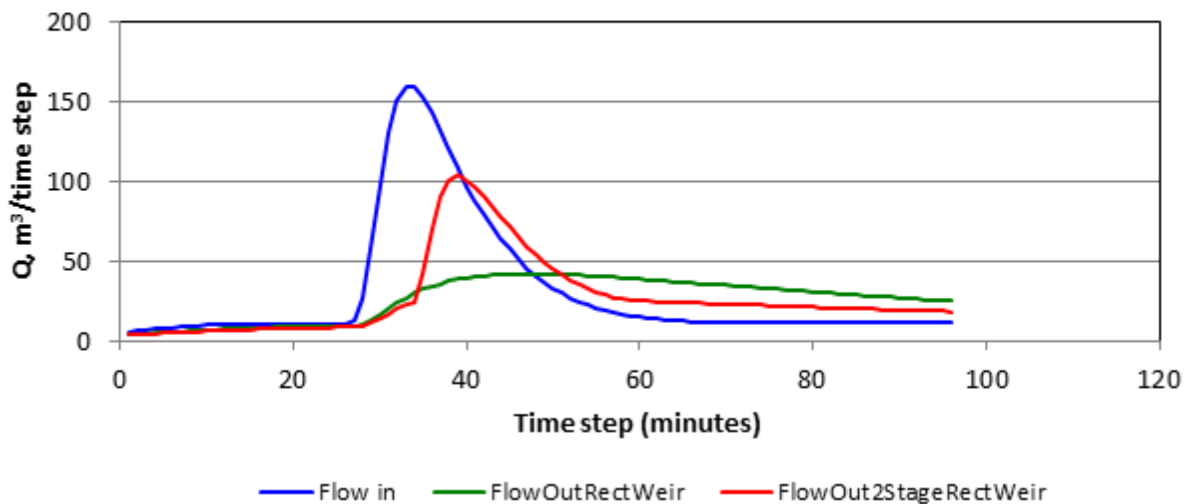
- 1) Read input from detention pond input file
- 2) Set default values when user-entered values are not available/zero
- 3) If not entered by the user, estimate flow rate/volumes for each emergency spillway based on precipitation, drainage area and standard discharge coefficient (0.5 hardwired in the model)
- 4) If not entered by the user, estimate the weir dimensions for rectangular or circular weir depending on the case
- 5) Get inflow coming to the BMP (estimated by SWAT)
- 6) Add inflow to the water volume already backed up
- 7) Estimate water depth based on semi parabolic wedge equation
- 8) Compare calculated water depth with the total depth of weir and compute discharge appropriately using one or multiple weir levels
- 9) Estimate surface area of water backed up
- 10) Estimate evaporation and seepage losses based on surface area
- 11) Calculate outflow and do water balance
- 12) Calculate water backup (inflow-outflow-evaporation-seepage)

6.3 Results and Discussion

Monitored outflow data from a detention pond is not available to validate the developed algorithm. Instead the flow calibrated LGA watershed (outlined in previous sections of this

report) was used as a hypothetical case study to validate the detention pond algorithm. Flow results from the outlet of LGA watershed were assumed to flow through a detention pond with two different outlet structures namely a stepped rectangular weir and circular weir (or orifice) (Figure 28). The outflow from each case corresponding to inflow was plotted to analyze the behavior of the detention pond algorithm and to check whether the algorithm is performing similar to what is expected. From the analysis, we see that the detention pond algorithm is mitigating the hydrograph peaks and delay the recession which is expected from the functionality of the BMP in reality. Also it makes sense from the results that the detention pond algorithm describing multiple outlets (weirs with 2 or more stages) pass more water through the structure at a given time than single stage weir outlet. Therefore, it appears that the developed algorithm for the detention pond is working well.

Flow through a stormwater detention pond-modeled results



Flow through stormwater detention pond with circular weir

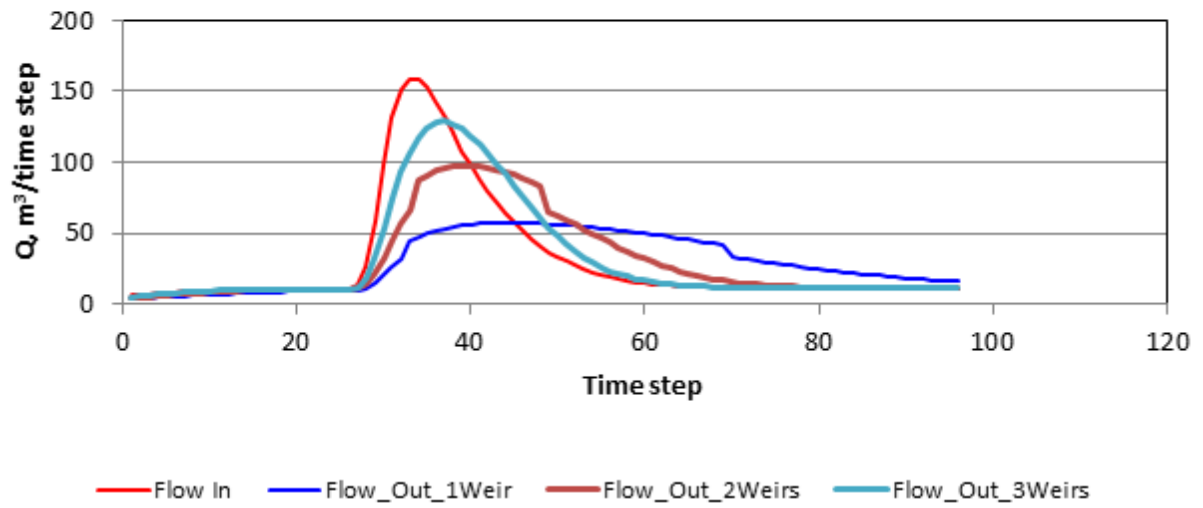


Figure 28. Flow through stormwater detention pond

7. Urban BMPs: Wet ponds

7.1 Introduction

A wet pond is a stormwater BMP aimed at removing pollutants from stormwater before it joins the creek or receiving water by both sedimentation and vegetative uptake of nutrients. In many cases it is coupled with a provision to store additional water and control flooding. As the name implies it is a 'wet pond' meaning there will be a permanent storage of water. Similar to a reservoir, the pond typically has two storage levels namely 1. Permanent pool and 2. Emergency spillway (with flood control option). Typically the pond has an inverted pipe from the bottom of the pond as the principal water quality volume spillway to facilitate removal of old stored water with new incoming stormwater. The removal of old water with new incoming stormwater creates long retention times and results in better pollutant removal rates. Because the water is stored in pond the pollutants associated with sediment can settle down. Another important feature of wet pond is the presence of plants (called aquatic bench) on the banks which help to remove significant amount of soluble pollutants. Usually native plants that live longer are chosen for aquatic bench. The longer the residence time of water, the better is the pollutant removal. Minimum recommended residence time is 1 day (24 hours) for better pollutant removal. For a 14 day residence time, field studies show that a wet pond behaves like a sedimentation filtration basin in removing pollutants. The size of a wet pond also matters when it comes to pollutant removal. In general, the larger the size, the better is the pollutant removal. For aesthetic purposes, the pond can be designed to any regular or irregular shape. Essentially the pond has two portions 1. Forebay (or sediment forebay) and 2. Main pool. The function of forebay is to capture debris and sediment from incoming stormwater and therefore avoid frequent maintenance of the main pool. The forebay and main pool are separated in terms of location but they are hydraulically connected by means of a pipe, weir or some other type of overflow structure. A typical wet pond is shown in Figure 29. Wet ponds are widely used in many parts of the country (especially Texas and California) to capture pollutants in stormwater and control flooding. An algorithm developed and integrated into SWAT model to simulate wet pond is described here. Additional storage for flood waters is controlled with a weir overflow structure.



Emergency spillway

Figure 29. A Wet Pond in Austin

7.2 Methods

Model configuration

A wet pond is an online structure located across a creek/river. It collects water from all upstream areas. Therefore, in terms of configuration in SWAT, it is analogous to a reservoir. Similar to the definition of reservoirs in SWAT, only one wet pond may be defined in a subbasin. Multiple wet ponds within a subbasin may be aggregated in terms of capacity, and then simulated as single system. The wet pond can be configured to become operational in the middle of simulation (e.g. in a simulation of 1981-2000 we can have wet pond from 1995). The user can enter physical characteristics of the pond. If not, the algorithm developed will use model default values based on City of Austin Environmental Criteria manual. The pond can receive direct precipitation, seep water through the bed and evaporate water from surface and release excess water through the outlet structure. The inflow to the pond is computed by SWAT depending on the contributing drainage area. The outflow from the pond is computed based on a physically based approach using hydraulic equations. More details on flow and sediment routing through wet pond are described below.

Design capture volume

The permanent pool is designed to maintain water level at or nearly at the full capacity and treat urban stormwater through settling and biological uptake. The SWAT wet pond algorithm is capable of sizing a wet pond at any subbasin in the watershed for design purposes by using the drainage area of the upstream subbasins. The City of Austin's design guidelines for wet ponds specify that the permanent pool volume should be calculated such that the minimum residence time of 14 days should be achieved for the amount of runoff from 0.72 inches of rainfall using the following equation.

$$V = 0.162 \cdot R_f \cdot A_{drain} \quad (7-1)$$

where R_f is the annual runoff coefficient (Figure 31), A_{drain} is the drainage area. The extended detention volume for wet ponds is determined using the one-year, three-hour storm event (Figure 30) to allow 72 hour drawdown period.

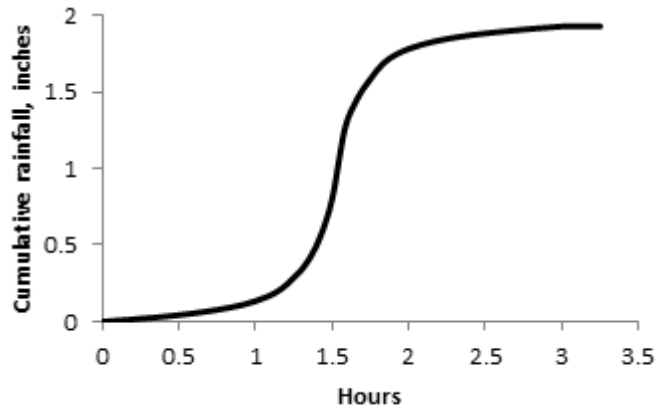


Figure 30. Cumulative rainfall of the 1-year 3-hour design storm (City of Austin)

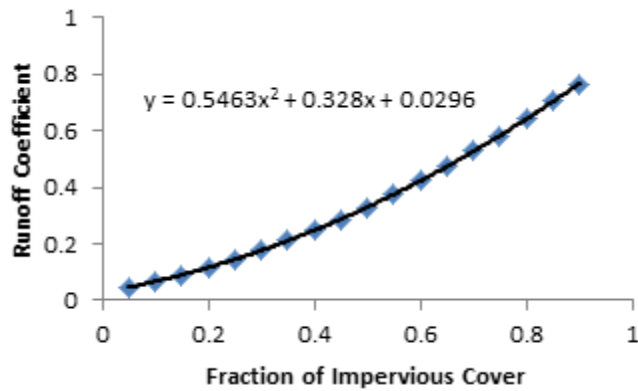


Figure 31. Annual runoff coefficient used to estimate the permanent pool volume (City of Austin)

Wet pond geometry

Wet ponds are designed such that stormwater runoff enters the forebay where preliminary screening and settling occur, then goes to the permanent pool for physical and biological treatment with extended residence time. The shape of the forebay and the main pond is generally designed arbitrary to mimic natural landscape. For modeling purpose, however, the pond geometry is simplified to a trapezoidal shape with rectangular bottom and top. Distinction between the forebay and the main pool is neglected in the model, as the primary function of the forebay is to ease maintenance and removal of accumulated sediment, and thus the total storage volume includes both the forebay and the main pool (see Figure 32).

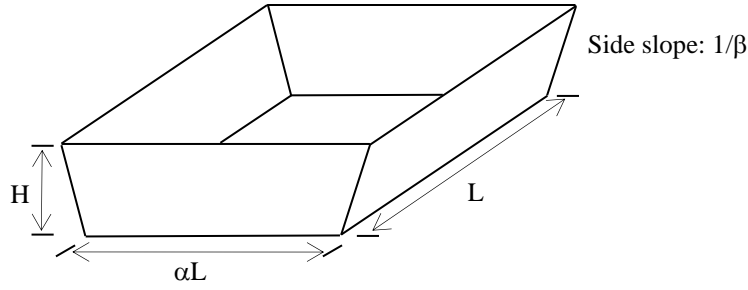


Figure 32. Simplified trapezoidal shape of wet ponds

The model uses Equation (7-1) to estimate the permanent pool volume if the model is used for design purposes or for hypothetical future scenarios. To simulate existing wet ponds that are in operation, the user needs to provide the following information: the total volume of the permanent pool (V_{PT}), depth of the permanent pool (H_p), bank slope ($1/\beta$), and the ratio of the longitudinal and lateral lengths (α). The length of the wet pond bed is then calculated using the geometry of trapezoids.

$$L = \frac{-3\beta H_p(\alpha + 1) + \sqrt{9\beta^2 H_p^2(\alpha + 1)^2 + 12\alpha \left(\frac{3V_{PT}}{H_p} - 4\beta^2 H_p^2 \right)}}{6\alpha} \quad (7-2)$$

The amount of water in the pond varies over time as stormwater comes in and discharges downstream. Total volume of water is updated every time step using a mass balance equation, and then the pond depth (stage) is estimated by the following equation using the Newton's method.

$$V_{p,i} = \alpha L^2 h_i + \beta L(1 + \alpha) h_i^2 + \frac{4}{3} \beta^2 h_i^3 \quad (7-3)$$

Two other time dependent variables are the wetted area and the water surface area. These are updated every time step for estimation of seepage and evaporation.

$$A_{wet,i} = \alpha L^2 + 2(\alpha + 1)L h_i \sqrt{\beta^2 + 1} + 5.64 h_i^2 \beta (\beta^2 + 1) \quad (7-4a)$$

$$A_{surf,i} = \alpha L^2 + (1 + \alpha)L\Phi + \Phi^2 \quad \text{where} \quad \Phi = 2.82 h_i \beta \sqrt{\beta^2 + 1} \quad (7-4b)$$

where $A_{wet,i}$ is the wetted area of the pond at time step i , through which seepage occurs, $A_{surf,i}$ is the water surface area at time step i , where evaporation occurs. These values vary as a function of water depth.

Flow routing

Change in water volume in the pond is estimated every time step by a mass balance equation. Stormwater runoff entering the pond (Q_{in}) and the direct rainfall on the pond surface (R) contribute to the increase of water in the pond. Water in the extended detention discharges downstream through an inverted orifice pipe (Q_{ext}). Any inflow beyond the maximum capacity of the pond makes outflow through an emergency spillway weir (Q_{weir}). Evaporation (E) and seepage (SP) are continuous processes through which water is lost. Permanent pool does not make discharge to downstream by any means, but may lose water through evaporation and seepage over time.

$$\frac{dV}{dt} = Q_{in} + R - Q_{ext} - Q_{weir} - E - SP \quad (7-5)$$

The volume of water lost to evaporation on a given time step is calculated by:

$$E_i = \frac{\phi_{res} \cdot PET \cdot A_{surf,i}}{N} \quad (7-6)$$

where ϕ_{res} is an evaporation coefficient, PET is the potential evapotranspiration for a given day, $A_{surf,i}$ is the wetted area of the pond at time step i , and N is the total number of time steps during the day. The volume of water lost by seepage through the bottom of the pond is calculated by:

$$SP_i = \frac{0.024 \cdot K_{sat} \cdot A_{wet,i}}{N} \quad (7-7)$$

K_{sat} is the effective saturated hydraulic conductivity of the pond bottom, $A_{wet,i}$ is the wetted area of the pond, and N is the total number of time steps during the day. The water in the extended detention makes outflow controlled by an inverted orifice pipe. Pipe outflow is calculated as a function of water depth in the extended detention, friction loss, and minor losses.

$$Q_{ext} = A_{pipe} \sqrt{\frac{2gh_{ext}}{1+k_f+k_{minor}}} \quad \text{where} \quad k_f = \frac{29L_{pipe}n^2}{R^{1.33}} \quad (7-8)$$

where A_{pipe} is the cross sectional area of the pipe, g is the gravitational acceleration (9.81m/s^2), k_f is friction loss of the pipe, k_{minor} is minor losses including bending loss, entrance loss, and exit loss, L_{pipe} is the effective length of the pipe, n is the manning's roughness coefficient of the pipe, R is hydraulic radius of the pipe flow.

Sediment routing

The transport of sediment into and out of wet ponds is estimated by a simple mass balance equation. SWAT assumes the pond is instantaneously and completely mixed throughout the volume as sediment enters the water body. The mass balance equation for sediment is:

$$SED_i = SED_{i-1} + SED_{in,i} - SED_{stl} - SED_{out} \quad (7-9)$$

where SED_i is the amount of sediment in the water body at the end of the time step i , $SED_{in,i}$ is the amount of sediment in the water body at the beginning of the time step, SED_{stl} is the amount of sediment removed from the water by settling, SED_{out} is the amount of sediment transported out of the water body with outflow.

It is difficult to achieve the full hydraulic efficiency for wet ponds by simulating plug-flow conditions, mostly due to the turbulence and non-ideal routing behavior caused by physical configuration of real ponds. Water Environment Research Foundation (WERF) (2009) suggests that a hydraulic efficiency factor be considered in estimating sediment removal for wet ponds as suggested by Fair and Geyer (1954):

$$C_{sed,stl} = C_{sed,ini} \cdot \left[1 - \left(1 + \frac{u_c}{Nu_s} \right)^{-N} \right] \quad (7-10)$$

where $C_{sed,stl}$ is the sediment concentration after the settling, $C_{sed,ini}$ is the sediment concentration at the beginning of the time step, u_c is the surface overflow rate ($=Q/A$), u_s is the settling velocity calculated by Stokes' law, and N is the hydraulic efficiency factor representing the number of continuously stirred tanks (CSTRs) in series (1~10). Equation 7-10 is applied only when the

water level is above the permanent pool. During the period when water level is below the top of permanent pool, sediment settling is calculated using the SWAT sediment equation (8:2.2.2 in SWAT documentation).

$$C_{sed,sl} = (C_{sed,ini} - C_{sed,eq}) \cdot e^{-k_s \cdot \Delta t \cdot d_{50}} + C_{sed,eq} \quad (7-11)$$

where $C_{sed,eq}$ is the equilibrium concentration of sediment in the water body, k_s is the decay constant(1/day), d_{50} is the median particle size. Assuming 99% of the 1 μ m size particles settle out of solution within 25 days, k_s is equal to 0.184

Sequence of computations

1. Read wet pond input file
2. Estimate pond dimensions (size of bottom, top and sides) based on user entered or model default using City of Austin-Environmental criteria manual
3. If not entered by the user, compute volume of main pool and extended detention
4. If not entered by the user, compute dimensions of outlet pipe and emergency spillway weir
5. Compute volume of water in pond at present time step
6. Estimate evaporation and seepage using respective surface areas
7. Calculate water outflow from pond for each time step using water balance equation
8. Compute sediment concentration in pond outflow based on sediment mass balance equation

7.3 Results and Discussion

Input and output processes as well as simulation with theoretical values has been tested to eliminate code errors. Validation of the wet pond algorithm against observed pond data is underway using monitoring data from the Ceylon Tea wet pond in Austin, Texas.

7. Summary

Sub-hourly flow simulation capability was added to the SWAT 2009 model. The new sub-hourly model components in SWAT allow simulation of runoff/infiltration, overland flow routing, reservoir/pond/wetland routing, and channel routing at any sub-daily time scale, while base flow is simulated at daily interval then distributed equally to each time step. With the enhanced fine resolution in operation time step, the sub-hourly SWAT model is expected to successfully address hydrologic issues in urban watersheds.

Algorithms for representing sub-daily erosion and sediment transport processes were developed and integrated into the SWAT model. The new algorithms were modified from other watershed-scale models, which mean that they were tested and validated in part before being modified for SWAT. In this new sub-daily SWAT structure, splash erosion is modeled based on the kinetic energy delivered by raindrops, and overland flow erosion is estimated by a physically-based algorithm that considers rill and interrill erosion. With these modified algorithms, SWAT performed well in predicting sediment loads in individual events during a long-term simulation without specific storm-by-storm calibration.

SWAT algorithms for stormwater BMPs including sedimentation-filtration, retention-irrigation, detention, and wet ponds were developed and integrated into the SWAT model. These water quality control structures are commonly used in urban Austin areas. The test results show that the physically based algorithms work reasonably at 15 minute time interval within the framework of the SWAT model. The performance of wet pond routine needs further validation using field.

The integration of this suite of additional capabilities into SWAT provides the City of Austin with a tool which allows long-term continuous modeling which simulates watershed processes on a small-time step to capture the impacts of flow regime alterations as well as the benefits of control structures put in place to reduce those impacts. This basic suite of BMPs is a toolbox of not only the most frequently used regional and development water quality controls, but begins the process of incorporating process-based algorithms for sediment capture in the structures, allowing both design estimates based on water quality control volume required, but simulation of existing structures and the ease of using required design default values to evaluate future scenarios. The ability of SWAT to simulate watershed surface processes, particularly relating to vegetation and soils, not only makes this process-based modeling easily adapted to other regions, but also lends itself to further BMP implementation for green infrastructure controls that seek to use these landscape processes to mitigate effects of urbanization.